JUSTUS-LIEBIG-
UNIVERSITÄT
GIESSEN

Differential Effects of Silibinin on Cardiovascular and Leukocyte Differentiation of Mouse Embryonic Stem Cells

Inaugural dissertation submitted to the Faculty of Medicine
in partial fulfillment of the doctoral degree in human biology at
Justus Liebig University Giessen

Submitted by

Enas Hussein Ali

from

Baghdad, Iraq

Giessen 2018

From the Institute of Physiology
Director of the Institute: Prof. Dr. Rainer Schulz
Faculty of Medicine of the Justus Liebig University Giessen

First Supervisor and Committee Member: **Prof. Dr. Heinrich Sauer**
Second Reviewer and Committee Member: **Prof. Dr. Thomas Linn**

Date of Doctoral Defense: **10. 12. 2018**

Dedication

To my parents, the reason of my existence in this life, my success was a result of your pray & qualitative support. I spent hard moments without you, I ask God to bless you and I hope that I will be the daughter that you will be proud of.

Enas

Table of Contents

1. Introduction

1.1. The medical plant milk thistle (*Silybum marianum* (L.) Gaertn.)

Milk thistle belongs to the family Asteraceae, genus Silybum and species *Silybum marianum*. According to an ancient legend the virgin Mary lost some drops of milk during breast feeding of her new-born child which caused the white spots on the white-veined leaves of the plant (Siegel and Stebbing, 2013) (figure 1.1). Milk thistle is grown in the Mediterranean region as a native home, but is cultivated in Asia and Europe for centuries. The active compound is called silymarin and is composed of seven flavonolignans (Silibinin (Silybin) A, Silibinin (Silybin) B, Isosilybin A, Isosilybin B, Silychristin, Isosilychristin and Silydianin) and one flavonoid (Taxifolin). Silymarin represents about 65%-80% of milk thistle extracts. Flavonoids are natural occurring substances that have a polyphenolic structure. They belong to secondary metabolites and are found in fruits, vegetables, grains, bark, flowers, roots, stems, tea and wine. Flavonoids are responsible for the pigment of flowers and exert anti-oxidative and anti-inflammatory properties (Panche et al., 2016).

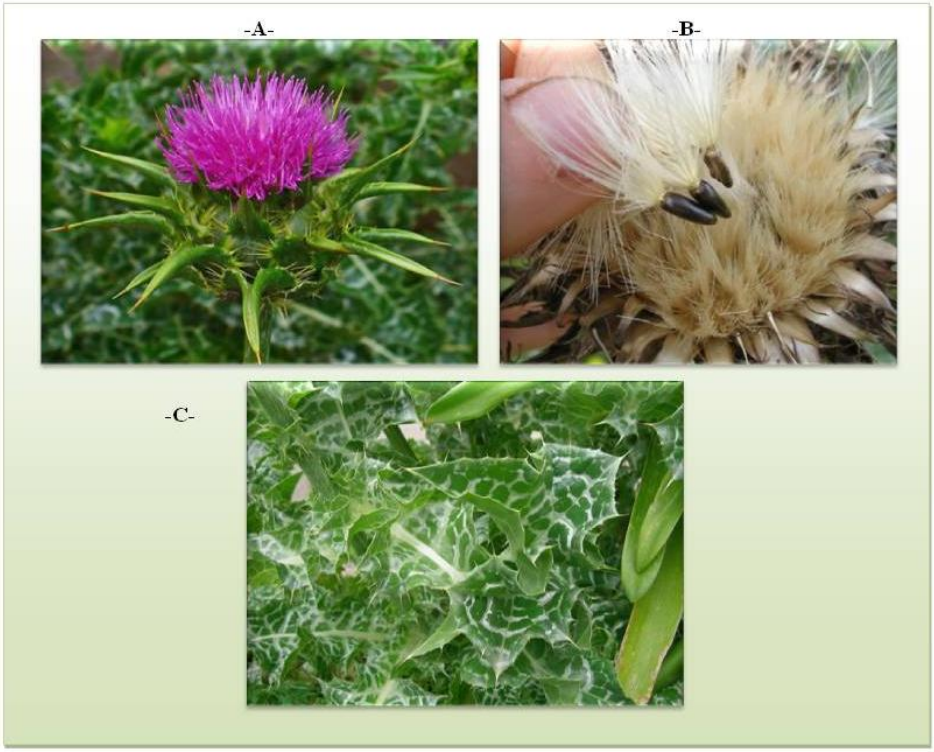

Figure 1.1: Silibinin (A) Milk thistle flower (http:/doctormurray.com/the-positive-estrogenic-effect-of milk-thistle-extract). **(B)** Milk thistle seeds (https://www.saltspringseeds.com/products/milk-thistle-silybum-marianum-1). **(C)** Leaves of milk thistle.

Silymarin has been utilized for more than 2000 years as a general medical herb. Since the sixteenth century, it is used for hepatoprotection in humans, because of its strong anti-hepatotoxic activity against different types of liver damage and toxicity (Dehmlow et al., 1996; Schuppan et al., 1999; Wellington and Jarvis, 2001; Polyak et al., 2013). In the early 1990s, various reports described the use of milk thistle as a potential chemopreventive agent against cancer diseases (Kroll et al., 2007; Gufford et al., 2015). Furthermore, Silybin appears an encouraging medication for chronic liver disease due to hepatitis C virus (HCV) infection (Loguercio and Festi, 2011).

1.2. Silibinin

Silibinin is the major active compound of Silymarin, comprising 50-70% of it. Silibinin is largely water-insoluble, and it is slowly absorbed in the intestine, needing about 3-6 hours to be completely absorbed. To increase resorption and bioavailability, a water soluble derivative of Silibinin, i.e. a mixture of Silibinin A and B dihydrogen disodium succinate, which is sold under the trade name Legalon® SIL, was synthetised (Mengs et al., 2012) (figure 1.2).

In Germany, Legalon Sil is used intravenously for the treatment of toxic mushroom poisoning. In addition, Silibinin was demonstrated to exert considerable anti-viral action against HCV (Ferenci et al., 2008; Wagoner et al., 2011; DebRoy et al., 2016).

Figure 1.2: Legalon® SIL for intravenous treatment.

1.3. Differences between Silibinin and Legalon SIL

1.3.1. Chemical structure

Silibinin, consists of a 1:1 mixture of two diastereoisomers, Silibinin A and Silibinin B. Moreover, Silibinin was presented as isosilybin, consisting of isosilybin A and isosilybin B, as ratio 1:1 mixture of two diastereoisomeric compounds (Lee et al., 2007; Loguercio and Festi, 2011; Samanta et al., 2016). Legalon SIL consists of a 1:1 mixture of disodium disuccinyl Silibinin A and disodium disuccinyl Silibinin B. Silibinin is dissolved in dimethylsulfoxide (DMSO), while Silibinin-C-2',3-dihydrogen succinate, disodium salt (Legalon SIL), which has been developed by Dr. Ulrich Mengs and Ralf T. Pohl (Rottapharm/Madaus), is dissolved in water (Wagoner et al., 2011; Mengs et al., 2012) (figure 1.3).

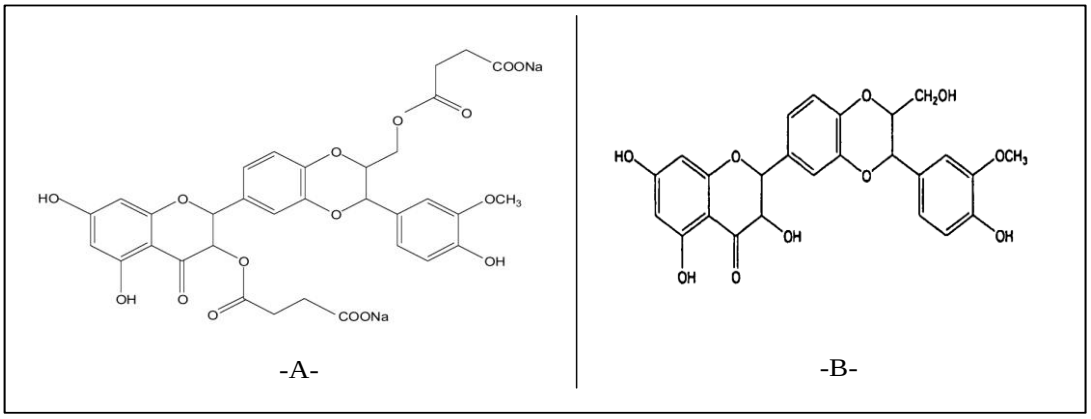

Figure 1.3: Chemical structures of Silibinin (A) Silibinin-C-2', 3-dihydrogen succinate, disodium salt. (Legalon SIL) (Mengs et al., 2012), **(B)** Silibinin (Wu et al., 2008).

1.4. Biological activity of Silibinin

Silibinin is the main active biological ingredient of the milk thistle, it has several biological activities. It is anti-inflammatory, anti-oxidant, anti-proliferative, anti-fibrotic, anti-neoplastic, immunomodulatory and anti-viral (Agarwal et al., 2006; Polyak et al., 2007; Polyak et al., 2010; DebRoy et al., 2016).

1.5. Medical benefit of Silibinin

Currently Silibinin it is applied as hepatoprotective as well as anti-viral agent against HCV in humans (Polyak et al., 2013). It exerts proven anti-hepatotoxic activity against different types of liver damage and toxicity (Dehmlow et al., 1996; Wellington and Jarvis, 2001; Payer et al., 2010; Federico et al., 2017).

Many studies confirmed the benefits of Silibinin and Legalon SIL in the treatment of liver disorders such as hepatitis and alcoholic liver cirrhosis as well as mushroom poisoning with *Amanita phalloides* toxin (Varghese et al., 2005; Cheung et al., 2010; Mengs et al., 2012).

In addition to its hepatoprotective effects, Silibinin has recently been shown to possess bone-forming and osteoprotective effects *in vitro* (Kim et al., 2012; Kim et al., 2013). Moreover, it has been suggested to act as an inhibitor of Aβ amyloid aggregation, thus reducing memory impairment *in vivo*. Therefore Silibinin may be a potential therapeutic agent for the treatment of Alzheimer's disease (Yin et al., 2011; Tota et al., 2011).

Furthermore, Silibinin has anti-hyperglycemic properties, due to its capacitiy to enhance the glycemic control in Type 2 diabetic mellitus patients (Lirussi et al., 2002; Voroneanu et al., 2016). Not least, Silibinin has cosmeceutical properties and has been shown to support effective wound healing (Singh and Agarwal, 2009; Samanta et al., 2016).

1.6. Anti-cancer activity of Silibinin

Silibinin was applied as a chemopreventive agent in a variety of *in vitro* and *in vivo* cancer models of epithelial cancer such as skin cancer (Cheung et al., 2010; Singh et al., 2014), lung cancer (Singh et al., 2006; Mateen et al., 2013), bladder cancer (Tyagi et al., 2004; Singh et al., 2008; Zeng et al., 2011), as well as cancers of colon, breast, prostate and kidney (Cheung et al., 2010; Özten-Kandaş and Bosland, 2011; Kim et al., 2011; Zheng et al., 2017).

1.7. Action of Silibinin as an antagonist of angiotensin II (Ang II) signaling

Research on the Renin-Angiotensin System (RAS) has revealed the primordial impact of Ang II in cardiovascular diseases and blood pressure control (Benigni et al., 2010). In the heart, the pharmacological activity of Silibinin is so far not investigated. Recently it was suggested that Silibinin may act as an antagonist of the angiotensin receptor 1 (AT1) since

Silibinin abolished Ang II-mediated Ca^{2+} signals in Chinese hamster ovary (CHO) cells over-expressing the AT1 receptor (Bahem et al., 2015). Cardiomyocytes express the AT1 as well as the AT2 receptor (Busche et al., 2000). In the cardiac conduction system increased Ang II may induce cardiomyocyte apoptosis (Vongvatcharanon et al., 2004). It has role in cardiac hypertrophy (Zhu et al., 2003; Chen et al., 2017), depending on the experimental conditions and the expression pattern of AT receptor subtypes. In ES cells Ang II has been shown to regulate glucose uptake (Han et al., 2005), supporting the notion that Ang II may play a role in the energy metabolism during embryogenesis. Notably Ang II has been demonstrated to stimulate cardiomyogenesis of ES cells (Wu et al., 2013). In differentiating ES cell-derived EBs the AT1 receptor is expressed already at very early stages of cardiac cell commitment. Components of the RAS are highly expressed in many tissues during embryonic development. AT1 receptor expression is downregulated shortly after birth, whereas the AT2 receptor is upregulated, suggesting a potential role of AT1 in cell/tissue differentiation processes during embryogenesis and AT2 in adult organ function (Gao et al., 2012). In fetal ovine cardiomyocytes Ang II stimulates hyperplastic growth (Sundgren et al., 2003), indicating that Ang II is involved in fetal heart growth. Moreover, besides insulin-like growth factor (IGF) receptors, AT1 receptor expression has been shown to be present in human cardiac stem cells (D'Amario et al., 2011), thus outlining an impact of Ang II signaling in cardiac progenitor cell differentiation and/or proliferation.

1.8. Stem cells

Stem cells are undifferentiated cells which can develop to different cell types of all tissues of the body. They can originate from the embryo, fetus and grown-up to adult (Passier and Mummery, 2003; Li and Ikehara, 2013). One of most important features of stem cells is their self-renewing capacity. This implies that following the division of a mother cell, one daughter cell remains a stem cell, thus sustaining the stem cell pool, whereas the other daughter cell is entering differentiation pathways to give rise to multiple types of cells and tissues (Bjornson et al., 1999; Toma et al., 2001). The self-renewing capacity of stem cells implies that they can be kept under appropriate conditions in culture for prolonged times and cell division cycles. Notably, stem cells retain their karyotype even after multiple passages in cell culture (Bradley et al., 1984; Vats et al., 2005; Jin et al., 2016). According

to the differentiation potency of stem cells they are classified as: totipotent, pluripotent, multipotent/oligopotent and unipotent (figure 1.4).

Totipotent stem cells

Totipotent stem cells are cells with the capacity to form an entire, independent organism. In mammalian organisms, embryonic cells are considered totipotent until the 8-16 cell stage of embryonic development (Johnson and Ziomek, 1981; Marikawa and Alarcón, 2009; Gonzalez et al., 2016).

Pluripotent stem cells

Pluripotent stem cells derive from totipotent stem cells and have the capacity of self-renewal and differentiation into all cell types within the organism. Pluripotent stem cells comprise of ES cells, embryonic germ (EG) cells and embryonic carcinoma (EC) cells (Beddington and Robertson, 1989; Boheler et al., 2002; Lensch et al., 2006).

Multipotent/oligopotent stem cells

Multipotent stem cells possess the ability to differentiate into all cell types within one specific lineage. Since multipotent stem cells are present in adult organisms, they may play important roles in tissue repair and protection. Moreover, they can be used in cell therapies of, e.g. spinal cord injury, bone fractures, autoimmune diseases, rheumatoid joint inflammation, hematopoietic defects, and fertility preservation (Sobhani et al., 2017).

Unipotent stem cells

Unipotent cells have a very limited differentiation potential and differentiate just into one cell type. Examples are: satellite cells of skeletal muscle or hematopoietic progenitor cells which give rise to only one specific type of blood cells (e.g. erythroblasts) (Dulak et al., 2015).

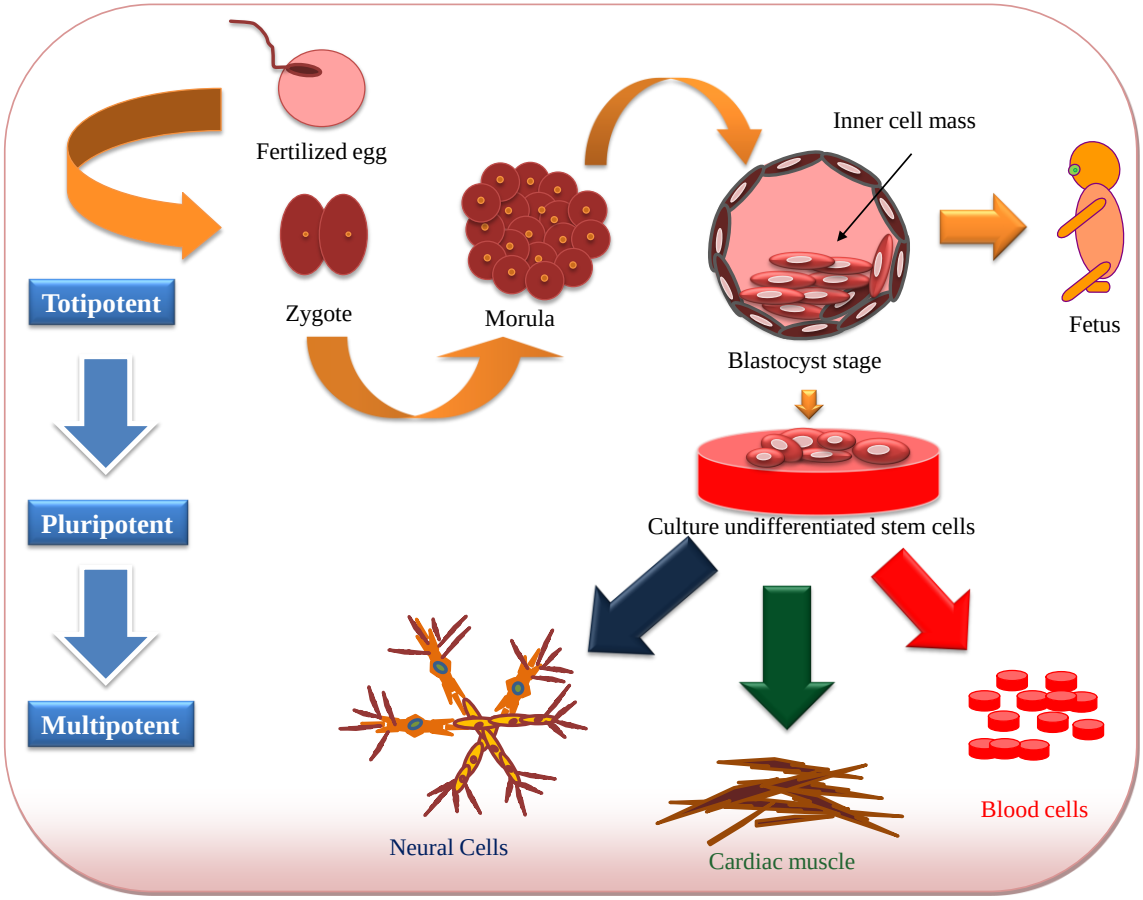

Figure 1.4: Extraction and culture of ES cells.

1.9. Embryonic stem (ES) cells

ES cells are derived from the inner cell mass of blastocysts. Their stemness is regulated by stemness genes which express the core pluripotency factors: Nanog, Oct4, Sox2, and other factors: Klf2, Klf4, Tfcp2l1, Esrrb, Gbx2, and Sall4 (Bourillot et al., 2009; Aksoy et al., 2014; Qiu et al., 2015). The signal transduction pathways elicited by LIF, bone morphogenetic protein (BMP) and Wnt support self-renewal and pluripotency of ES cells through upregulation of the transcription factor Nanog. Furthermore, intrinsic transcription factors such as FoxD3, P53 and Oct4 have a role in regulating Nanog expression to maintain mouse ES cell properties (Pan and Thomson, 2007).

Mouse ES cells were isolated and grown *in vitro* for more than 20 years (Martin, 1981; Evans and Kaufman, 1981). The pluripotency of mouse ES cells can be maintained if the culture contains the cytokine LIF. Upon removal of LIF, mouse ES cells are going to differentiate spontaneously to form EBs *in vitro* (Stewart et al., 1992; Burdon et al., 2002; Wobus and Boheler, 2005). LIF is a member of the interleukin-6 (IL-6) family of cytokines and promotes self-renewal by activating janus kinase/signal transducers and activator of transcriptions (JAK/STAT), mitogen activated protein kinase (MAPK) and PI3K signaling cascades (Nicola and Babon, 2015).

Human ES cell (hESC) lines were firstly derived from human embryos in 1998 by Thomson et al., 1998, and have since then been proven as un-restricted source of cells for regenerative medicine (Wobus and Boheler, 2005). hESCs were derived from blastocysts obtained after *in vitro* fertilization (Pera et al., 2000). hESCs share basic qualities with mouse ES cells, such as the maintenance of stemness by the transcription factors Oct-4, Sox-2 and Nanog as well as the capacity to form three germ layers (ectoderm, endoderm and mesoderm) (Richards et al., 2002; Boyer et al., 2005). However, in hESCs, LIF is imperfect to suppress the differentiation process (Pera et al., 2000).

1.10. Cardiomyogenesis

Cardiomyogenesis is defined as the differentiation of pluripotent stem cells to specialized cell types of the heart, such as atrial-like, ventricular-like and sinus nodal–like cells. During the differentiation process, cardiac-specific genes, receptors, ion channels and proteins are expressed (Wobus, 2001; Boheler et al., 2002). In early stages of differentiation, cardiomyocytes inside EBs are small and round with single nuclei. The early myofibrils are sparse and irregularly organized, while others contain parallel bands of myofibrils that show A and I bands. However, with maturation, these cells are going to be distinctly lengthened and develop regular myofibrils and sarcomeres. Beating cells are principally mononucleated, rod-shaped and they contain cell-cell junctions with developing cells in the heart (Westfall et al., 1997; Tajsharghi, 2008).

There are several of transcription factors which have important roles in cardiomyocyte differentiation, such as Nkx2.5, GATA and MEF2. Nkx2.5 is required for heart

development, and is regulating the expression of myocardin which is important for cardiomyogenesis (Jamali et al., 2001; Ueyama et al., 2003).

Sarcomeric proteins of cardiomyocytes are established in the following order: titin (Z disk), myomesin, α-actinin, titin (M band), myosin heavy chain (MHC), α-actin, cardiac troponin T and M protein (Skwarek-Maruszewska et al., 2013; White et al., 2014). The GATA family of transcription factors plays a role in cardiac development that leads to heart muscle differentiation (Brewer and Pizzey, 2006). Studies of cis-regulatory elements have confirmed the important role of GATA factors (particularly GATA-4) in promoting the expression of many myocardial genes, including α- and β-myosin heavy chain (α- and β-MHC) and cardiac troponin C (Zeisberg et al., 2005; Hewitt et al., 2016).

1.11. Calcium (Ca^{2+}) signaling

The Ca^{2+} ion is the main ion in cell signaling. Ca^{2+} has regulatory functions in gene transcription, cell motility and exocytosis (Bonny and Bochud, 2014). In addition, Ca^{2+} is an important secondary messenger in cell signaling and regulates physiological functions including contraction of cardiac-, smooth- and- skeletal muscle and release of hormones and neurotransmitters. Moreover, Ca^{2+} drives stem cells towards cardiac cell differentiation through regulation of cardiac transcriptional cascades, secretion of cardiogenic factors and in turn gene expression and myofibrillogenesis (Pucéat and Jaconi, 2005). Dysregulation of intracellular Ca^{2+} can lead to loss of physiological function and pathological changes in cell growth (Zhang et al., 2004).

In mature cardiomyocytes Ca^{2+} sparks occur which are activated by voltage-dependent L-type Ca^{2+} channel (LTCC) mediated Ca^{2+} influx. Ca^{2+} sparks are the basic unit of heart excitation-contraction (E-C) coupling in the adult. Ca^{2+} sparks occur during E-C coupling when Ca^{2+} enters the cells through LTCCs and activates the ryanodine receptor (RyR) on the sarcoplasmic reticulum (SR) to release Ca^{2+} from intracellular stores. This process is named Ca^{2+} -induced Ca^{2+} release (CICR) (Zhang et al., 2004; Pucéat and Jaconi, 2005). E-C coupling is ended by removal of intracellular Ca^{2+} from the cytoplasm which is accomplished by the sarcoplasmic reticulum (SR) Ca^{2+} ATPase (SERCA) and

phospholamban (PLB). In the heart the SERCA isoform SERCA2a is expressed. The activity of SERCA2a is controlled by the phosphorylation state of PLB (figure 1.5).

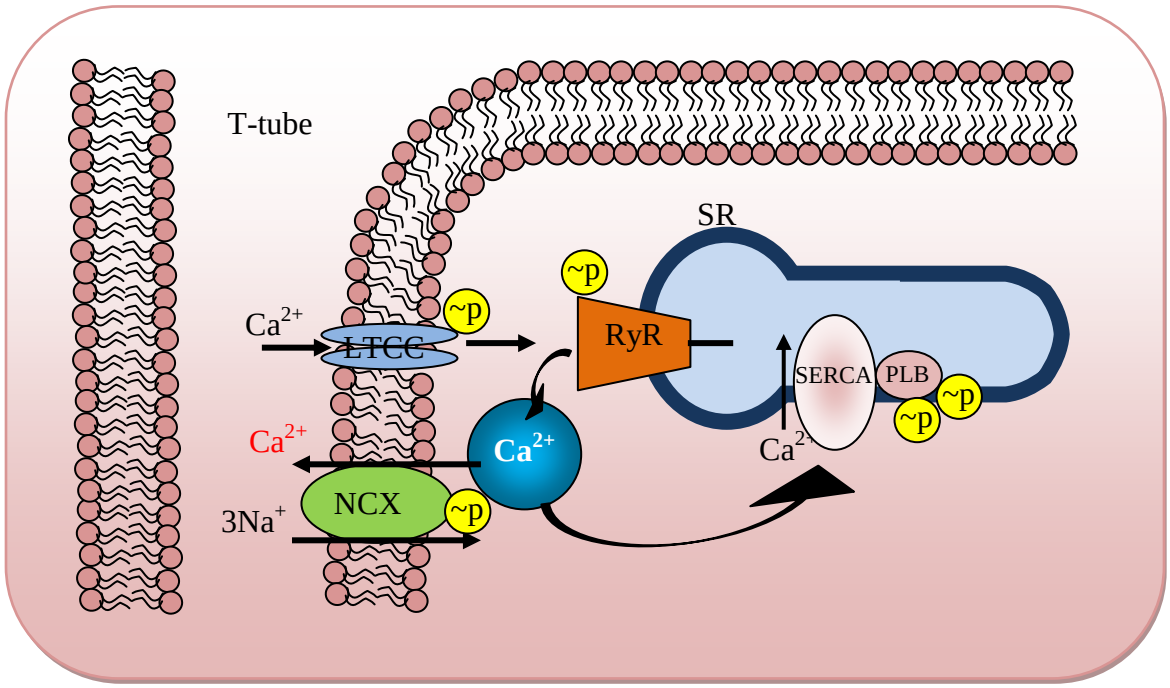

Figure 1.5: Schematic figure explaining Ca^{2+} regulation in cardiac cells. Influx of Ca^{2+} through LTCCs releases Ca^{2+} through RyRs. Ca^{2+} is pumped back into the SR through SERCA which is controlled by PLB. In addition, the Na^{+}/ Ca^{2+} exchanger (NCX) removes Ca^{2+} from the intracellular compartment. ~p = phosphorylation.

1.12. Vasculogenesis from ES cells

During embryonic development a vascular network is formed to provide the growing embryo with oxygen and nutrients. The process of blood vessel formation can be divided in two processes, namely vasculogenesis and angiogenesis (Geudens and Gerhardt, 2011). The initial process of blood vessel formation from vascular progenitor cells is termed vasculogenesis (Geudens and Gerhardt, 2011; Rakocevic et al., 2017). It happens when angioblasts, i.e. vascular endothelial cell precursors (precursor cells) are differentiated, expand and adhere to form endothelial cells which multiply inside a former vascular tissue to generate a primitive capillary plexus (Risau and Flamme, 1995). The different steps of vasculogenesis from ES cells can be monitored by immunohistochemical analysis of PECAM-1 - positive areas in EBs (Bekhite et al., 2016). PECAM-1 (or CD31) is expressed

in the cell junctions between endothelial cells and plays important roles in cell adhesion and signal transduction (Newman et al., 1990; Müller et al., 2002).

Outgrowing blood vessels contain two different types of cells: tip cells and vessel elements. Tip cells migrate depending on the mechanical forces induced by neighboring vessel elements and the local tissue (Perfahl et al., 2017). During angiogenesis, new blood vessels arise from pre-existing vessels (figure 1.6). These vessels can be formed by two mechanisms: sprouting angiogenesis and intussusception.

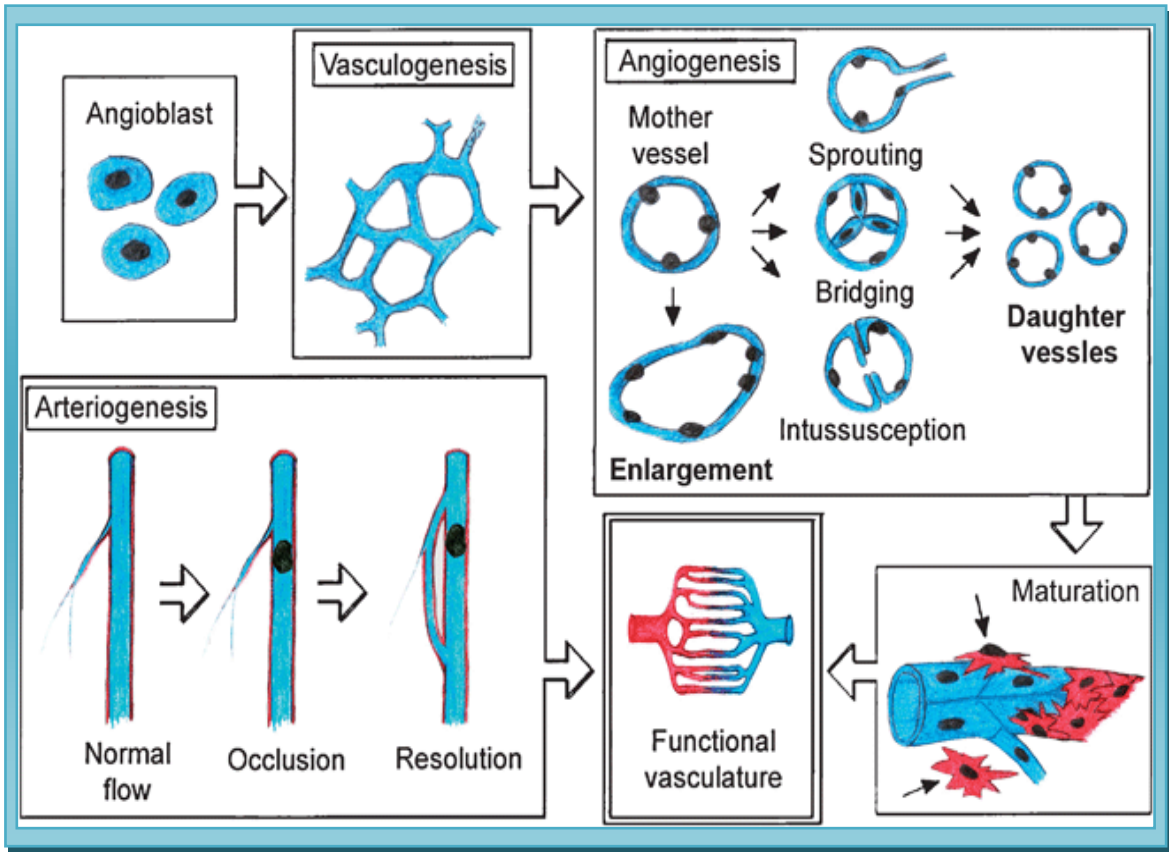

Figure 1.6: Schematic representation of vasculogenesis and angiogenesis (Korpisalo and Ylä-Herttuala, 2010)**.**

Blood vessels may originate from endothelial cells, while tissue columns are embedded inside existing vessels to split the vessels. As a result, the development of these segments and their adjustment leads to division of the vessel and remodeling of the neighboring cells

of blood vessels (Risau, 1997; Patel-Hett and D' Amore, 2011). Vasculogenesis and angiogenesis are regulated by hypoxia through hypoxia inducible factor-1α (HIF-1α) which regulates the expression of vascular endothelial growth factor (VEGF) (Sauer et al., 2001a).

1.13. Factors involved in vasculogenesis and angiogenesis

VEGF is the essential angiogenic growth factor that modifies angiogenesis through receptor tyrosine kinase VEGF receptors (VEGFRs). The VEGF family comprises of various members: VEGF-A, VEGF-B, VEGF-C and VEGF-D which are interacting with VEGF receptors such as VEGFR1, VEGFR2 and VEGFR3 (Lohela et al., 2009). The process of angiogenesis is mainly regulated by the VEGFA/VEGFR-2 system. VEGF contributes to the angiogenic response by enhancing microvascular permeability, improving endothelial cell proliferation, migration, survival and secretion of matrix metalloproteinases (MMPs) (Brychtova et al., 2008; Abhinand et al., 2016).

VEGF-A is the basic regulator for vasculogenesis and regulates angiogenic sprouting (figure 1.7). It has been demonstrated that VEGF-A stimulated the migration of tip cells, while it induced proliferation in stalk cells (Gerhardt et al., 2003).

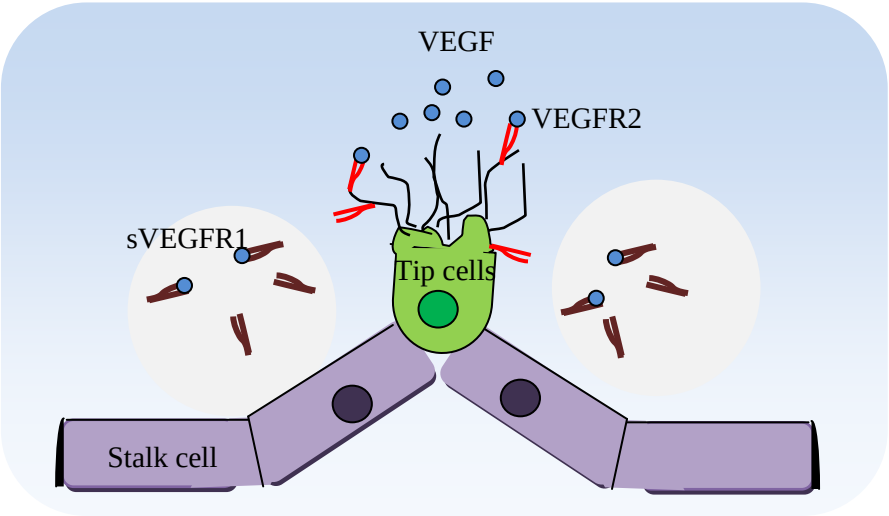

Figure 1.7: VEGF signaling during sprouting. Brown color: soluble VEGFR1, red color: VEGFR2 and blue color: VEGF (Geudens and Gerhardt, 2011).

Activation of VEGFR2 regulates major signaling pathways involved in vasculogenesis and angiogenesis. The binding of VEGF to VEGFR results in phosphorylation of a specific tyrosine in VEGFR2. VEGFR2 in the mouse is named fetal liver kinase-1 (Flk-1) while the

human VEGFR2 is referred to as kinase insert domain receptor (KDR) (Fuh et al. 1998; Shinkai et al., 1998).

Vascular endothelial cadherin (VE-Cadherin) is the most important endothelial adhesion molecule which is located between endothelial cells at cell junctions. VE-Cadherin is essential for preservation of vascular system integrity and leukocyte extravasation (Vestweber, 2008).
Endothelial cell-to-cell junctions do not just preserve intercellular adhesion, but additionally exchange intracellular signals that regulate cell differentiation (Dejana et al., 2009). Other studies mentioned that VE-Cadherin is necessary for development of the cardiovascular system during embryo development as it controls vascular permeability and represses excessive vascular cell proliferation and branch formation (Breier et al., 1996; Crosby et al., 2005; Giannotta et al., 2013).

HIF-1α is an oxygen sensing transcription factor which plays important roles in angiogenesis during mammalian embryonic and adult angiogenesis as well as in tumor angiogenesis. The activity of HIF-1α is regulated by different post-translational modifications (Lee et al., 2004). Growth factors increase HIF-1α protein translation so that HIF-1α contributes to the control of growth factor-induced glucose digestion even without hypoxia (Lum et al., 2007).

1.14. Nitric oxide (NO)

NO is a soluble gas synthesized enzymatically from the amino acid L-arginine in endothelial cells (Cannon, 1998; Kampoli et al., 2012). Many functions such as blood pressure, vascular tone and oxidant-sensitive mechanisms can be regulated by NO (Ignarro and Napoli, 2004). NO is reacting with oxygen, superoxide or metals, nucleic acids and proteins. During the cellular metabolism of NO, nitrate and nitrite can be formed by oxidation processes, and - especially under hypoxic conditions - can be recycled to form NO (Thomas et al., 2008; Lundberg and Weitzberg, 2009) (figure 1.8). The biological chemistry of NO is either direct or indirect, depending on its concentration in cells and tissues (Wink et al., 1996). In low concentrations NO is directly activating NO-sensitive signal cascades which regulate physiological cell functions. In high concentrations NO is

reacting with superoxide ($O_2^{\cdot-}$) or oxygen (Wink and Mitchell, 1998) to form peroxynitrite, which is a very reactive molecule and exerts severe oxidative stress under pathophysiological conditions. NO is generated by three different enzymes, namely inducible NO synthase (iNOS, NOSII), endothelial NO synthase (eNOS, NOSIII) and neuronal NO synthase (nNOS, NOSI) (Rochette et al., 2013).

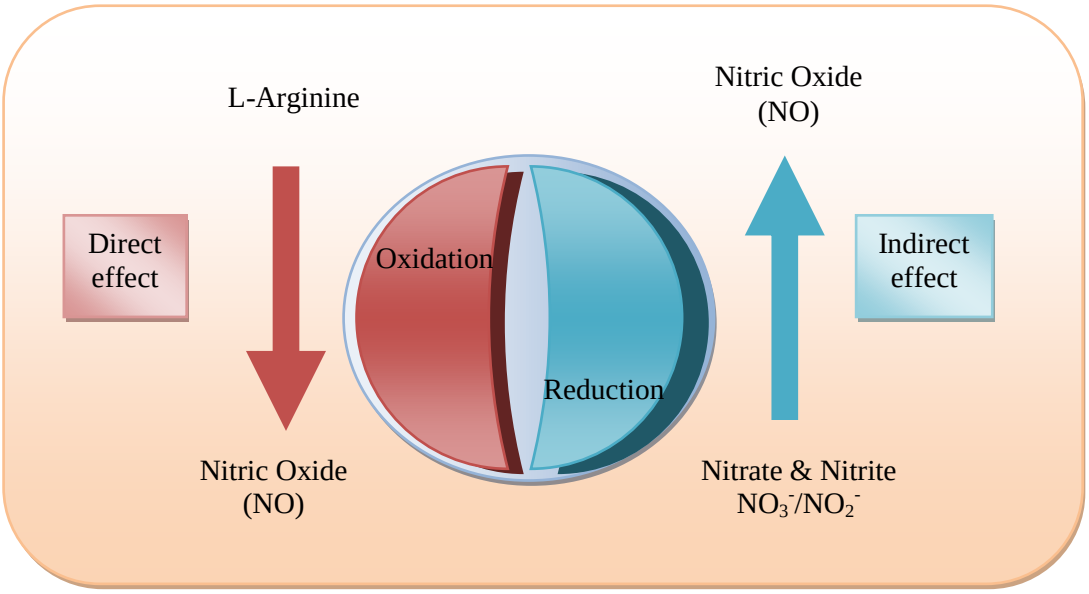

Figure 1.8: Schematic view of NO generation. Direct effect: NO can originate from L-arginine and oxygen by NO synthases; indirect effect: Nitrate and Nitrite are reduced to make NO.

1.15. Signaling pathways involved in differentiation of ES cells

1.15.1. Endothelial NO synthase (eNOS)

eNOS is responsible for NO generation in the vascular system and has essential vasoprotective roles (Dimmeler et al., 1999; Jones et al., 2004; Edgar et al., 2017).

eNOS derived NO keeps veins expanded, controls blood pressure and has various anti-atherosclerotic impacts. Numerous cardiovascular risk factors induce oxidative stress by eNOS uncoupling, thus causing endothelial dysfunction in the vasculature (Förstermann and Sessa, 2012). The phosphorylation of eNOS (p-eNOS) occurs on serine (Ser1177) and threonine (Thr495) residues, and is fundamental for the activity of eNOS (Fleming and

Busse, 2003). eNOS has been shown to be inhibited by N^G -nitro-L-argininemethyl-ester (L-NAME) (Pfeiffer et al., 1996; Isenberg, 2003; Lu et al., 2015), which depressed the inflammatory reaction exerted by pro-inflammatory cytokines (Isenberg, 2003).

1.15.2. AKT signaling pathway

AKT (protein kinase B) kinase acts downstream of PI3K, AKT kinase controls cellular processes such as cell proliferation, survival, cell size, response to nutrient availability, tissue invasion and angiogenesis (Scheid and Woodgett, 2003; Bellacosa et al., 2005). *In vitro,* AKT activation is important for the survival and propagation of vascular progenitor cells generated from mouse ES cells. *In vivo,* AKT maintained endothelial cell identity in embryonic vessels that anastomose with vessels of the host (Israely et al., 2014). The phosophorylation of AKT (p-AKT) occurs at Ser473, and AKT inhibitor VIII specifically inhibited the AKT pathway, as well as down-regulated active AKT (Alessi et al., 1996; Bayascas and Alessi, 2005; Peng et al., 2010).

1.15.3. Signal transducer and activator of transcription 3 (STAT3) signaling pathway

The transcription factor STAT3 is initiated by numerous cytokines and growth factors and plays a key function in cell survival, proliferation and differentiation (Wang et al., 2011). During infection, released IL-6 participates in induction of STAT3 kinase. Other studies suggested that STAT3 kinase exerts a substantial role in early developmental stages of embryogenesis (Levy and Lee, 2002). STAT3 is an important key in transcriptional determination of mouse ES cell self-renewal. Moreover, the development of many organs needs the activation of STAT3 (Xie et al., 2009).

1.15.4. Phosphatidylinositol-3-kinase (PI3K) signaling pathway

PI3K has an important role in cell stimulation to initiate cell growth, cell cycle, cell migration, cell survival cascades, cell metabolism and the control of gene expression. PI3K

induced NO production in endothelial cells (Cantley, 2002; Isenović et al., 2002). Furthermore, PI3K has a fundamental role in the treatment of obesity (Beretta et al., 2015), since PI3K-mediated cell survival was activated by unregulated signaling of the AKT pathway (Shiojima and Walsh, 2002). PI3K comprises of four classes (IA, IB, II and III) dependent on their structural characteristics; all types of PI3K contain a C2 domain and a catalytic domain that is not found in protein kinases but is present in lipid kinases (Koyasu, 2003). The PI3K subunit p110α plays an important role in VEGF-regulated vascular differentiation and the control of cell polarity and migration (Bekhite et al., 2016). *In vitro*, the PI3K/AKT pathway is crucial for hypoxia-induced proliferation of bone marrow-derived mesenchymal stem cell, their differentiation into endothelial cells and paracrine functions (Sheng et al., 2017).

1.16. Leukocyte differentiation (Leukopoiesis) from ES cells

In the adult, the hematopoietic system arises from bone marrow hematopoietic stem cells. It consists of erythrocytes, leukocytes (neutrophils, basophils, eosinophils, lymphocytes, monocytes, macrophages) and platelets (Dzierzak and Speck, 2008). Leukocytes belong to the cellular immune system and participate in the defense against infection, allergy and inflammation. In addition, leukocytes are involved in advancement and determination of inflammation, elimination of apoptotic cells, support of cell proliferation and tissue rebuilding following damage (Koh and DiPietro, 2011).

During embryogenesis, hematopoietic and endothelial cell lineages develop from a common precursor which contains intermediate stages between mesodermal cells and committed precursors for hematopoietic and endothelial cell lineages (Ogawa et al., 2001). There are two types of hematopoietic cell lineages which are different in origin, one of them derives from hemangioblasts and is called primitive hematopoietic lineage. The other originates from endothelial cells, and is called definitive hematopoietic lineage (Ogawa et al., 2001).

In vitro, ES cells differentiate towards hematopoietic progenitors which can be used for basic and clinical research applications. Recently, it has been demonstrated that pluripotent ES cells are able to differentiate to the endothelial cell lineage as well as into hematopoietic

lineages such as leukocytes (monocytes/macrophages) (Choi et al., 2005; Shen and Qu, 2008). Hematopoietic progenitors derived from EBs express high numbers of $CD45^+$ cells and - when cultured in presence of cytokines - are capable to differentiate to macrophages. (Subramanian et al., 2009), T lymphocytes (T-cell), neutrophil cells, natural killer (NK) cells and dendritic cells (Liang et al., 2013; Lieber et al., 2003; Luevano et al., 2012; Tseng et al., 2009). A previous study of our group has demonstrated that ES cells differentiated vascular cells as well as leukocytes, including monocytes/macrophages and neutrophils (Hannig et al., 2010; Sharifpanah et al., 2015). Leukopoiesis from ES cells follows vasculogenesis in a time-controlled manner and can be inhibited if vasculogenesis is blunted by antagonists of the VEGFR2 signaling pathway (Hannig et al., 2010, Sharifpanah et al., 2015).

Aims of study:

The milk thistle compound Silibinin is stimulating regenerative processes which may involve the activation of stem cells. The present study undertakes to investigate the effect of Silibinin (Silibinin-C-2', 3-dihydrogen succinate, disodium salt) on cardiovascular differentiation as well as leukopoiesis of mouse ES cells.

Specifically the following goals were pursued:

1- To study the effect of Silibinin on cardiomyogenesis of ES cells and cardiac cell function.

2- To unravel the effect of Silibinin on the stimulation of cardiomyogenesis and cardiac cell function by Ang II.

3- To investigate the effect of Silibinin on vasculogenesis of ES cells.

4- To decipher NO-mediated signaling pathways underlying the stimulation of vasculogenesis by Silibinin.

5- To assess, whether Silibinin stimulates leukopoiesis from ES cells.

2. Materials and methods

2.1. Materials

2.1.1. General materials

Table 1: Materials

Materials	Supporting Company
24 well cell culture plate	Sarstedt, Nümbrecht, Germany
6 well cell culture plate	Sarstedt, Nümbrecht, Germany
96 well flat bottom tissue plate	Sarstedt, Nümbrecht, Germany
Bacterial culture dish	Sarstedt, Nümbrecht, Germany
Cellspin	Integra Biosciences, Chur, Switzerland
Conical flasks	Fischer Scientific GmbH, Schwerte, Germany
Conical tubes 15ml, 50ml	Greiner Bio-One GmbH, Frickenhausen, Germany
Cover slips	Deckgläser, Menzel-Gläser, Darmstadt, Germany
Eppendorf tubes	Sarstedt, Nümbrecht, Germany
Filter paper for blotting	Universal, Biotech Fischer, Reiskirchen, Germany
Glass pasteur pipettes	Brand GmbH, Wertheim, Germany
Glass slides	R. Langenbrinck GmbH, Emmendingen,

	Germany
Gloves	Paul Hartmann AG, Heidenheim, Germany
Gloves Micro-Touch (Nitra-Tex)	Ansell, Brussels, Belgium
Immersion oil	Leica Microsystems, Wetzlar, Germany
Optical microscope TELAVAL 31	Carl Zeiss, Jena, Germany
PAGEr EX mini-Gels	Lonza, Rockland, USA
Parafilm	Bemis Flexible Packaging, Neenah, USA
Pipette filter tips	Biozym Scientific, Hessisch Oldendorf, Germany
Pipette tips	Sarstedt, Nümbrecht, Germany
PVDF millipore transfer membrane	Merck Millipore, Darmstadt, Germany
Serological glass pipettes	ISO Lab, Wertheim, Germany
Serological glass pipettes, wide tip	Corning, New York, USA
Serological plastic pipettes	Greiner Bio-One GmbH, Frickenhausen, Germany
Spinner flask (250ml)	Integra Biosciences, Fernwald, Germany

Sponge Pad for blotting	Invitrogen by Thermo Fisher Scientific, Darmstadt, Germany
Tissue culture plate (60mm, 150 mm)	Sarstedt, Nümbrecht, Germany

2.1.2. Instruments

Table 2: Instruments

Instruments	Supporting Company
-20ºC freezer	Thermo Fisher Scientific, Darmstadt, Germany
-80ºC freezer	Heraeus, Hanau, Germany
4ºC refrigerator	Siemens, Munich, Germany
Autoclave	Holzner GmbH, Nussloch, Germany
Blotting chamber, Xcell II Blot module	Life Technologies, Darmstadt, Germany
Cell culture incubator (Heracell)	Heraeus, Hanau, Germany
Centrifuge (Eppendorf 5417C)	Eppendorf AG, Hamburg, Germany
Centrifuge (Multifuge 1S-R)	Heraeus, Hanau, Germany
Chemiluminescence imaging system	PeQLab Bitechnologie GmbH, Chemi-Capt-50001, Erlangen, Germany
Confocal laser scanning microscope SP2,	Leica, Wetzlar, Germany

AOBS	
Electrophoresis chamber (Xcell SureLock Mini-Cell)	Invitrogen by Thermo Fisher Scientific, Darmstadt, Germany
FireBoy portable safety Bunsen burner	Integra Biosciences, Fernwald, Germany
Gel electrophoresis high voltage power supply	Invitrogen by Thermo Fisher Scientific, Darmstadt, Germany
Gel electrophoresis power station	Invitrogen by Thermo Fisher Scientific, Darmstadt, Germany
Heating block or TB2 Thermoblock,	Biometra, Göttingen Germany
Homogenizer	Sigma-Aldrich, Taufkirchen, Germany
Ice machine (Icematic F200)	Castel MAC, Castelfranco Veneto, Italy
Laminar flow cabinet, class II biological safety	Heraeus, Hanau, Germany
Light microscope	Zeiss, Jena, Germany
Liquid nitrogen and cryopreservation storage tank	Air Liquide Global E&C, Vitry-sur-Seine, France
Magnetic stirrer	IKA RH-KT/C, Staufen, Germany
Magnetic stirrer for spinner flask (Cellspin)	Integra Biosciences, Fernwald, Germany
Microplate ELISA reader, Infinite M200	Tecan Austria GmbH Model, Männedorf, Switzerland

Microscope heating stage TRZ 3700	Labexchange, Burladingen,Germany
Milli-Q Advantage A10 System	Merck Millipore, Darmstadt, Germany
pH-meter	Hanna Instruments, Kehl am Rhein, Germany
Shakers	Heidolph Elektro GmbH, Schwabach, Germany
Tube roller mixer	Stuart, London, UK
Vacuum pump	HLC BioTech, Bovenden Germany
Vortex (Vortex genie 2)	VWR, Darmstadt, Germany
Water bath	Lauda, Lauda-Königshofen, Germany
Weighing machines (TE153S, AB265S)	Sartorius AG, Göttingen, Germany Meltter toledo, Columbus, USA

2.1.3. Solutions and chemical materials

Table 3: Solutions and chemical materials

Materials	**Supporting Company**
Acetic acid	Sigma-Aldrich, Taufkirchen, Germany
Copper sulfate	Sigma-Aldrich, Taufkirchen, Germany
DAF-FM diacetate	Invitrogen by Life Technologies, Darmstadt, Germany

Dimethyl sulfoxide (DMSO)	Merck Millipore, Darmstadt, Germany
Di-Sodium hydrogen phosphate dihydrate	Carl Roth, Karlsruhe, Germany
Dulbecco's PBS without Ca^{2+} & Mg^{2+}	PAA, Cölbe, Germany
EDTA	Carl Roth, Karlsruhe, Germany
Ethanol	Carl Roth, Karlsruhe, Germany
Fluo-4-AM	Invitrogen by Life Technologies, Darmstadt, Germany
Fluoromount-G	Southern Biotech, Birmingham, USA
Hydrogen peroxide solution (30%)	Sigma-Aldrich, Taufkirchen, Germany
Luminol	Sigma-Aldrich, Taufkirchen, Germany
Methanol	Carl Roth, Karlsruhe, Germany
Novex Sharp pre-stained protein standard	Life Technologies, Darmstadt, Germany
NuPAGE antioxidant	Invitrogen, Thermo Fisher Scientific, Darmstadt, Germany
NuPAGE LDS sample buffer (4X)	Invitrogen, Thermo Fisher Scientific, Darmstadt, Germany
NuPAGE reducing agent (10X)	Invitrogen, Thermo Fisher Scientific, Darmstadt, Germany
Paraformaldehyde (PFA)	Carl Roth, Karlsruhe, Germany

P-coumaric acid	Sigma-Aldrich, Taufkirchen, Germany
Phosphatase inhibitor cocktail 3	Sigma-Aldrich, Taufkirchen, Germany
Ponceau S	AppliChem, Darmstadt, Germany
Potassium chloride	Carl Roth, Karlsruhe, Germany
Potassium dihydrogen phosphate	Carl Roth, Karlsruhe, Germany
ProSieve EX running buffer	Lonza, Rockland, USA
ProSieve EX transfer buffer	Lonza, Rockland, USA
Protease inhibitor cocktail	BioVision, Milpitas, USA
Restore PLUS western blot Stripping Buffer	Thermo Fisher Scientific, Darmstadt, Germany
Sigmacote	Sigma-Aldrich, Taufkirchen, Germany
Sodium carbonate	Carl Roth, Karlsruhe, Germany
Sodium chloride	Carl Roth, Karlsruhe, Germany
Sodium potassium tartrate	Merck Millipore, Darmstadt, Germany
Sterile distilled water	Braun Melsungen AG, Melsungen, Germany
Tris base	Sigma-Aldrich, Taufkirchen, Germany
Triton X-100	Sigma-Aldrich, Taufkirchen, Germany

Tween-20	Sigma-Aldrich, Taufkirchen, Germany

2.1.4. Cell lines

CCE S103 cell line, mouse ES cell line isolated from embryos mouse strain129/sv (Robertson et al., 1986).

2.1.5. Cell culture media components and substances

Table 4: Cell culture media components and substances

Substances	Supporting Company
β-Mercaptoethanol	Sigma-Aldrich, Taufkirchen, Germany
Ang II	Sigma-Aldrich, Taufkirchen, Germany
Collagenase B	Roche, Mannheim, Germany
Dulbecco´s modified Eagle medium (DMEM)	Biochrom, Berlin, Germany
EmbryoMax 0.1% gelatin solution	Merck Millipore, Darmstadt, Germany
ESGRO mouse LIF medium	Chemicon, Hampshire, UK
Fetal bovine serum	Sigma-Aldrich, Taufkirchen, Germany
Iscove's Modified Dulbecco's Medium (IMDM)	Biochrom, Berlin, Germany
L-Glutamine 200mM (100X)	Biochrom, Berlin, Germany

Mitomycin-C	Merck Millipore, Darmstadt, Germany
NEA-non-essential amino acids (100X)	Biochrom, Berlin, Germany
Non-fat dried milk powder	AppliChem GmbH, Darmstadt, Germany
Penicillin/Streptomycin (100X)	Biochrom, Berlin, Germany
Plasmocin prophylactic	InvivoGen, California, USA
Silibinin (Silibinin-C-2', 3-dihydrogen succinate, disodium salt (Legalon Sil))	Meda Pharma, Bad Homburg, Germany
Trypsin EDTA 1X	Life Technologies, Darmstadt, Germany

2.1.6. Inhibitors

Table 5: Inhibitors

Inhibitors	Final concentration	Dissolve in	Supporting Company
AKT inhibitor VIII	5µM	DMSO	STEMCELL Technologies, Vancouver, Canada. Cat. No. 72942
L-NAME (eNOS inhibitor)	100µM	water	Sigma-Aldrich, Deisenhofen, Germany. Cat. No. 51298-62.5
LY294002 (PI3K inhibitor)	5µM	DMSO	InvivoGen, San Diego, CA, USA Cat. No. tlrl-ly29
Stattic (STAT3 inhibitor)	7µM	DMSO	TOCRIS Biosciences, Bristol, UK. Cat. No. 19983-44-9

2.2. Media and buffers

2.2.1. Media

2.2.1.1. CCE Complete medium

-	IMDM high glucose medium	1X
-	Heat inactivated fetal calf serum	16%
-	β- mercaptoethanol	0.1mM
-	Sodium pyruvate (100mM)	1.0mM
-	L- Glutamine (200mM)	2.0mM
-	Non-essential amino acids (100mM)	0.1mM
-	Penicillin/Streptomycin (10000U/ml)	50U/ml

2.2.1.2. EMFI medium

-	DMEM high glucose medium	1X
-	Heat inactivated fetal calf serum	10%
-	β- mercaptoethanol	0.1mM
-	Sodium pyruvate (100mM)	1.0mM
-	L- Glutamine (200mM)	2.0mM
-	Non-essential amino acids (100mM)	0.1mM
-	Penicillin/Streptomycin (10000U/ml)	50U/ml

2.2.1.3. LIF medium

-	IMDM high glucose medium	1X
-	Heat inactivated fetal calf serum	16%
-	β- mercaptoethanol	0.1mM
-	Sodium pyruvate (100mM)	1.0mM
-	L- Glutamine (200mM)	2.0mM
-	Non-essential amino acids (100mM)	0.1mM
-	ESGRO LIF	1000U/ml

2.2.1.4. LIF pLpro medium

-	LIF medium	50ml
-	Plasmocin prophylactic	2.5µg/ml

2.2.1.5. Medium for feeder cell freezing

-	EMFI medium	50%
-	Heat inactivated fetal calf serum	40%
-	DMSO	10%

2.2.2. Buffers and other solutions

1x PBS

-	KCl	2.7mM
-	KH_2PO_4	1.8mM
-	NaCl	137mM
-	$Na_2HPO_4\,2H_2O$	10mM
	adjust pH to 7.4	

1% PBST

-	1x PBS	100ml
-	Triton X-100	1ml

0.01% PBST

-	1x PBS	100ml
-	Triton X-100	10µl

0.01% PBST Tween-20

-	1x PBS	100ml
-	Tween-20	10µl

1x TBS

-	Tris base	50mM
-	NaCl	150mM
	adjust pH to 7.6	

0.1% TBST

-	1x TBS	100ml
-	Tween-20	100µl

β- mercaptoethanol solution (10mM)

-	1x PBS	50ml
-	β- mercaptoethanol (stock 14mM)	35µl

Lowry Solution (stock concentration)

-	Lowry Solution 1 Na-K-Tartrate	117mM
-	Lowry Solution 2 Cu_2CO_4	50mM
-	Lowry Solution 3 Na_2CO_3	2.4M

Lowry Solution 4

-	NaOH	1M

Lowry Solution 5

-	Folin-Ciocalteu's phenolreagent (Merck 9001)	~ 0.5N

RIPA buffer

-	Tris, pH 7.4	50mM
-	NaCl	150mM
-	Nonidet P-40	1%
-	Sodium dodecyl sulfate (SDS)	0.1%
	Deoxycholate (excluded in phospho-protein assays)	0.5%

Lysis solution for protein extraction

-	RIPA buffer	1x
-	Protease inhibitor cocktail	1x

Lysis solution for phospho-protein extraction

-	RIPA buffer	1x
-	Protease inhibitor cocktail	1x
-	Phosphatase inhibitor cocktail	1x
-	Glycerophosphate	1mM
-	EDTA, pH 8	1mM

Ponceau staining solution

-	Ponceau S	0.1% (w/v)
-	Acetic acid	1% (v/v)

Paraformaldehyde fixing solution (4% PFA)

-	1x PBS	1 Liter
-	PFA	40g
	adjust pH to 6.9 with 1N NaOH	

Blocking solution

10% milk

-	Non-fat dried milk powder	10g
-	0.01% PBST	100ml

5% milk

-	Non-fat dried milk powder	5g
-	0.01% TBST	100ml

Enhanced Chemi-Luminescence (ECL) detection solution

-	Tris–HCl , pH 8.5	100mM
-	Hydrogen peroxide solution (30%) (v/v)	3mM
-	Luminol	1.25mM
-	Cumaric acid	225µM

2.2.3. Antibodies

Table 6: A- Antibodies for immunohistochemistry

Primary antibody		
Antibodies	**Company**	**Cat. No.**
Mouse anti-mouse α-actinin	Abcam, Cambridge, UK	ab9465
Rat anti-mouse CD31	Merck Millipore, Darmstadt, Germany	LV1815894
Leukocyte markers		
Rat anti-mouse CD18	Biolegend, Koblenz, Germany	101409
Rat anti-mouse CD45	Merck, Darmstadt, Germany	2395751
Rat anti-mouse CD68	Bio Rad (AbD Serotec), Düsseldorf, Germany	0713
Secondary antibody		
Alexa Fluor 488 donkey anti-rat IgG	Life Technologies, Darmstadt, Germany	A-21208
DyLight 650 goat anti-rat IgG	Abcam, Cambridge, UK	ab98408
Cy5-conjugated goat anti-rat IgG	Jackson ImmunoResearch, West Grove, PS, USA	712-176
Alexa Fluor 647 sheep anti-mouse IgG	Jackson ImmunoResearch, West Grove, PS, USA	515-605-072
Nuclear staining		
DRAQ5	Cell Signaling Technology, Danvers, USA	4084

Table 7: B- Antibodies for western blot

Primary antibody			
Antibodies	**Company**	**Cat. No.**	**Weight (KDa)**
Endothelial cell markers			
Rat anti-mouse VE-Cadherin (CD144)	BD Biosciences GmbH, Heidelberg, Germany	555289	115
Progenitor marker			
Rabbit anti-mouse Flk-1 (VEGFR2)	Cell signaling Technology, Danvers, USA	8324	230
Rabbit anti-mouse Flk-1 (VEGFR2)	Biorbyt, Biozol, Eching, Germany	Orb11556	147
Hypoxia marker			
Mouse anti- HIF-1α (H1α 67)	Santa Cruz Biotechnology, Heidelberg, Germany	D1913	120
House-keeping proteins			
Mouse anti-Vinculin	Sigma-Aldrich, Taufkirchen, Germany	V9131	110
Rabbit anti-GAPDH	Abcam, Cambridge, UK	ab22555	36
Rabbit anti β-actin	Biolegend, Koblenz, Germany	622102	45

Leukocyte markers			
Rat anti-mouse CD18	Biolegend, Koblenz, Germany	101409	95
Rat anti-mouse CD45	Novus Biologicals, Wiesbaden Nordenstadt, Germany	15811	147
Rat anti-mouse CD68	Bio Rad (AbD Serotec), Düsseldorf, Germany	MCA1957 GA	110
Phosphoproteins			
Mouse anti-p-STAT3 (Ser722)	Cell signaling Technology, Danvers, USA	9136S	86
Rabbit anti-p-AKT (Ser473)	Biolegend, Koblenz, Germany	649002	60
Rabbit anti-p-eNOS (Ser1177)	Cell signaling Technology, Danvers, USA	9571S	140
Rabbit anti-p-ERK1/2 (Thr202/Tyr204)	Cell signaling Technology, Danvers, USA	9101	42, 44
Rabbit anti-p-JNK (Thr183/Tyr185)	Cell signaling Technology, Danvers, USA	9251S	46, 54
Rabbit anti-p-p38 MAP Kinase (Thr180/Tyr182)	Cell signaling Technology, Danvers, USA	9211	43
Rabbit anti-p-PI3K p85 (Tyr458)/p55 (Tyr199)	Thermo Fisher Scientific, Darmstadt, Germany	PA5-17387	60, 85

Rabbit anti-p-VEGFR2 (p-Tyr951)	Biorbyt, Biozol, Eching, Germany	Orb106137	152
Total protein markers			
Rabbit anti-eNOS	Sigma-Aldrich, Taufkirchen, Germany	N3893	135
Rabbit anti-PI3K	Cell signaling Technology, Danvers, USA	4292S	85
Secondary antibody			
HRP-linked donkey anti-goat IgG	Abnova, Heidelberg, Germany	PAB10570	
HRP-linked goat anti-rabbit IgG	Cell signaling Technology, Danvers, USA	7074	
HRP-linked donkey anti-rabbit IgG	Abcam, Cambridge, UK	ab205722	
HRP-linked goat anti-rat IgG	Cell signaling Technology, Danvers, USA	7077	
HRP-linked donkey anti-rat IgG	Abcam, Cambridge, UK	ab102265	
HRP-linked horse anti-mouse IgG	Cell signaling Technology, Danvers, USA	7076	
HRP-linked donkey anti-mouse IgG	Abcam, Cambridge, UK	ab20524	

2.2.4. Fluorescence substances

2.2.4.1. DAF-FM

DAF-FM diacetate (4-amino-5-methylamino-2',7'- difluorofluorescein diacetate) is a reagent which is used for the detection of NO. It is non-fluorescent, but when reacting with NO, becomes a fluorescent benzotriazole, and can be detected by fluorescent microplate readers, fluorescence microscopy and flow cytometers (Itoh el al., 2000). Maximum excitation wavelengths of the oxidized form is at 495nm and fluorescence emission is detected at wavelengths > 515nm. DAF–FM is dissolved in DMSO.

2.2.4.2. Fluo-4-AM

Fluo-4 is utilized to quantify Ca^{2+} inside living cells. It is regularly utilized as the non-fluorescent acetoxymethyl ester (Fluo-4-AM) which is cleaved inside the cell by cellular esterases to give a free, fluorescent Fluo-4. Fluo-4 is excited at 488nm, and emission is recorded at > 515nm.

2.2.4.3. DRAQ5

DRAQ5 (1, 5-bis{[2-(di-methylamino)ethyl] amino}-4, 8-dihydroxyanthracene-9, 10-Dione) is a cell permeable far-red fluorescent DNA dye that can be applied in fixed or non-fixed/ live cells. DRAQ5 is excited at 633nm, and emission is rercorded at > 655nm.

2.3. Methods

2.3.1. Cell culture

2.3.1.1. Thawing mouse embryonic fibroblasts (MEFs)

MEFs are used as feeding layer for proliferating ES cells, since they secrete LIF which inhibits ES cell differentiation**.** First of all LIF plasmocin prophylactic medium was warmed in 37°C water bath, and 5ml medium was distributed in 60mm cell culture plates and incubated in a (37°C and 5% CO_2) incubator**.**

Vials of MEFs frozen in a liquid nitrogen tank (-196°C) were thawed in water bath at 37°C. Subsequently MEFs cells were transferred into a 50ml conical tube containing 20ml of warmed EMFI medium and centrifuged for 5 min at 209*g* at RT. The supernatant was removed, and the pellets were resuspended in equal volumes of warmed EMFI medium and seeded in 60mm cell culture plates which were transferred to a CO_2 incubator.

The mitotic inactivation of MEFs is started by the replacement of the growth medium with 3ml medium containing mitomycin C in a concentration of 10µg/ml and incubation for 3h (Verweij and Pinedo, 1990). To stop the inactivation process, the mitomycin containing medium was aspirated, cells were washed 3 times with EMFI medium, and were incubated in 5ml of fresh EMFI medium (figure 2.1).

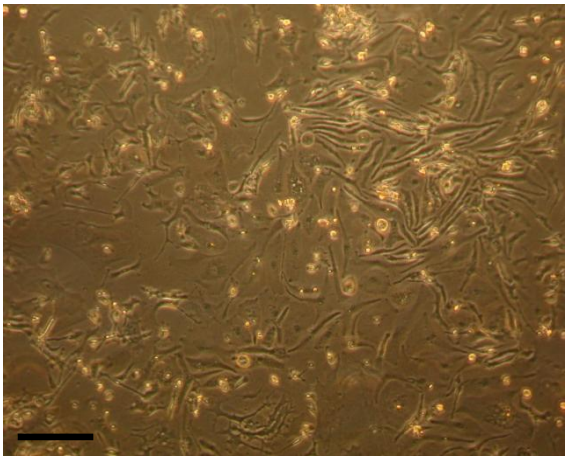

Figure 2.1: Transmission image of confluent MEFs, The bar represents 100µm.

2.3.1.2. Thawing of ES cells

Vials of ES cells frozen in liquid nitrogen were rapidly thawed in water bath at 37°C. The cell suspension was transferred to a 50ml conical tube containing 20ml pre-warmed CCE-

medium and centrifuged for 5 min at 209*g* at RT. Subsequently the supernatant was removed and the cell pellet resuspended with 200µl of pre-warmed CCE-medium. The thawed ES cells were seeded at a density of 9 x 10^4 cells/ml onto confluent, mitomycin C-inactivated MEFs in 60mm cell culture dishes and further incubated in a CO_2 (5%) incubator at 37°C (Kent, 2009).

2.3.1.3. Passaging of ES cells

ES cells were grown on inactivated MEFs until 70% sub-confluency. The medium containing LIF was changed every 24h. Every 2 days, the cells were passaged by enzymatic dissociation. Briefly, the cell culture medium was removed and ES cell cultures were washed with 2ml pre-warmed trypsin-containing dissociation medium. After aspiration, 2ml warm trypsin-containing dissociation medium was added, and the cells were further incubated at 37°C and 5% CO_2. Subsequently ES cell colonies were further dissociated by gently pulling up and down with a 1ml pipette to obtain single cells suspension. A number of 9 x 10^4 ES cells/ml was added to each MEF plate and further incubated in the CO_2 incubator (figure 2.2) (Tamm et al., 2013).

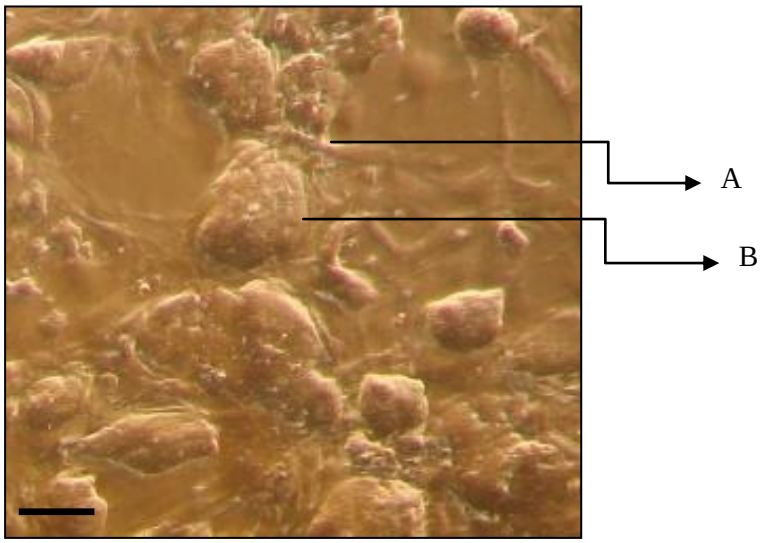

Figure 2.2: Colonies of mouse ES cells growing on mitotically inactivated MEFs, A- Feeder layer of MEFs, B- Colonies of undifferentiated mouse ES cells. The bar represents 100µm.

2.3.1.4. Preparation of spinner flask (cleaning and siliconizing)

Spinner flasks were washed with distilled water and subsequently filled with 250ml of 70% ethanol for 30 min. Then, 5N NaOH was added for 8 to 12h; the flasks were washed with water, and left for drying.

The purpose of silicon coating is, to prevent the cells from adhesion to the interior glass wall prior to the formation of EBs. The spinner flask and magnetic stirring bars were coated by silicon solution (Sigmacote). The silicon coated spinner flask should be dried in the oven at 60°C for 1h. Finally, the spinner flask was washed three times with distilled water before autoclaving.

2.3.1.5. Generation of embryoid bodies (EBs)

In suspension culture and absence of LIF, ES cells aggregate together and form three-dimensional (3D) tissues, named EBs (Bratt-Leal et al., 2009). After coating and autoclaving, spinner flasks were washed with pre-warmed cell culture medium, filled with a volume of 125ml medium, and placed on a magnetic stirring plate in the incubator as shown in (figure 2.3-A). ES cells grown on MEFs were enzymatically dissociated as described and seeded in the spinner flask at a cell density of 3 x 10^6 cells/ml. On the following day another 125ml medium was added to the spinner flask to give a final volume of 250ml. The speed of the magnetic stirrer system was set to 25 r.p.m. The spinning direction was changed every 1440°. In general, 3-day-old EBs cultivated in spinner flasks (figure 2.3-B) were used for the experiments.

2.3.1.6. Freezing of ES cells

For freezing purposes, confluent mouse ES cell culture plates (60mm) were washed and incubated with 2ml of trypsin for 2 min in the incubator. The dissociated cell suspension was transferred into 20ml of pre-warmed medium to stop enzymatic digestion, and was centrifuged for 5 min at 209*g*. The supernatant was aspirated and cell pellets cooled on ice. Finally, 1ml of cell freezing medium (4°C) was slowly added to the pellets, gently mixed, immediately transferred to 1.8ml labeled cryopure vials and frozen in a -80°C freezer prior to long term storage in liquid nitrogen tank.

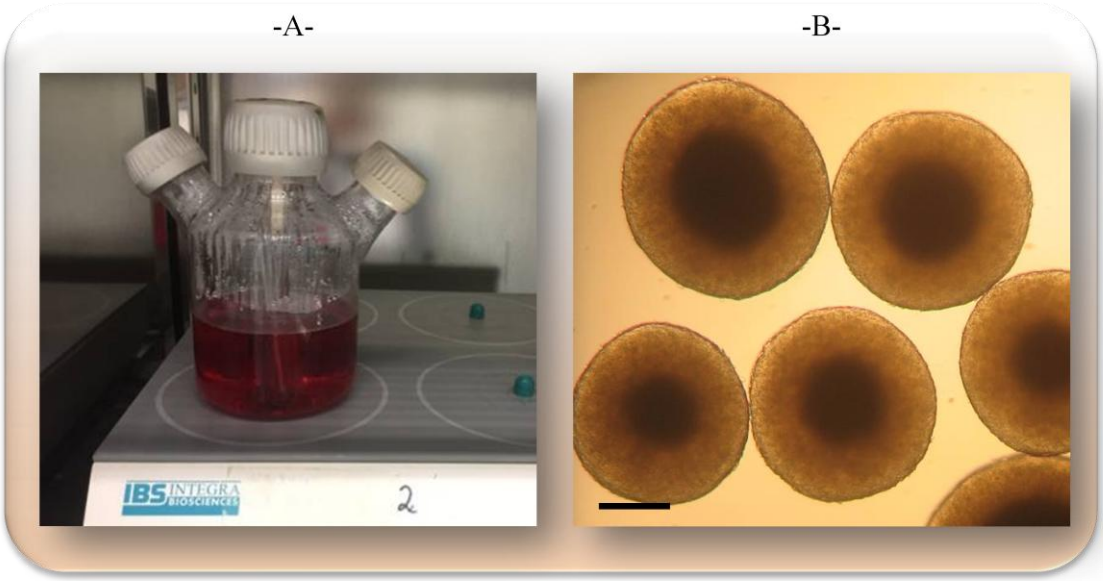

Figure 2.3: Spinner flask and EBs (A) Spinner flask on top of a magnetic stirring plate. Two glass pendula are rotating with a speed of 25 r.p.m. The spinning direction is changed every 1440°. **(B)** Transmission image of EBs at day 3 of cell culture. The bar represents 100μm.

2.3.2. Treatment protocol for Silibinin

To explore the effect of Silibinin on mouse ES cells, EBs were removed from spinner flasks at day 3 of cell culture and 25-30 EBs were transferred in either 60mm bacterial culture plates or tissue culture plates containing 5ml medium. Treatment with Silibinin at different concentrations ranging from 1-50μM was performed from day 3 to day 10 of differentiation to investigate the effect of Silibinin on vasculogenesis and cardiomyogenesis. For the investigation of leukopoiesis, EBs were treated with Silibinin from day 3 to day 14 of cell culture. Cell culture medium containing Silibinin was exchanged every 24h. After the incubation period, EBs for vasculogenesis and cardiomyogenesis were either fixed in ice-cold methanol to perform immunohistochemistry, while for the investigation of leukopoiesis EBs were fixed in 4% PFA or protein was extracted for western blot experiments (figure 2.4).

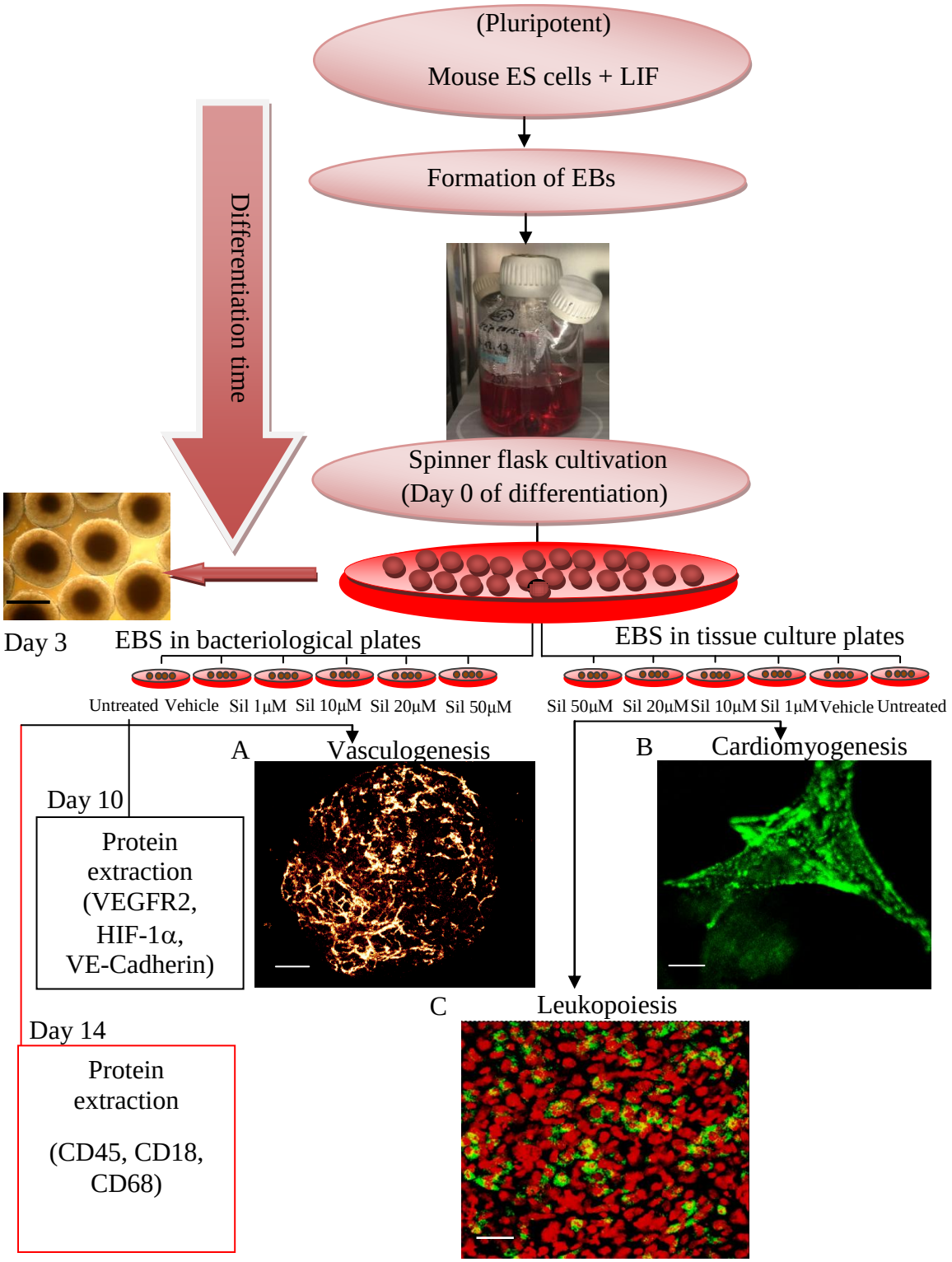

Figure 2.4: Basic Steps of experiments. A-Vasculogenesis in 10-day-old EBs, the bar represents 300µm. B- Cardiomyogenesis in 10-day-old EBs, the bar represents 100µm. C-Leukopoiesis in 14-day-old EBs, the bar represents 75µm.

2.3.3. Measurement of contraction frequency of EBs

The contraction frequency of EBs was assessed from day 7 to day 10 of cell culture by visual inspection using a light microscope (Zeiss Axiovert 40 C) which was connected to a microscope heating stage TRZ 3700 and equipped with a 5/0,12-x objective (CP-Achromat, Zeiss). The frequency of spontaneously contractions in EBs was counted at 37 °C for a time period of 1 min. At least 20 EBs were investigated in each experiment. At least 4 experiments were performed with EB cultures from different passages.

2.3.4. Immunohistochemistry (IHC)

IHC is an important technique used for distinguishing antigens (e.g. proteins) in cells by specific binding of antibodies to antigens in natural tissues (Ramos-Vara and Miller, 2014).

2.3.4.1. PECAM-1 (CD31) staining

PECAM-1 (CD31) staining was performed to visualize three dimensional vascular networks in EBs.

1-Sample collection: 10-day-old EBs were collected in microcentrifuge tubes, and the medium was aspirated before washing EBs 3 times with 1x PBS.

2- Fixation: EBs were covered with ice-cold methanol and kept at -20°C for 20 min.

3- Permeabilization: After fixation, the EBs were washed 4 times with 0.01% PBST (Triton-X-100) buffer, permeabilized with 1% PBST and incubated at RT for 10 min on the shaker.

4- Blocking: After 10 min, the EBs were washed 4 times with 0.01% PBST buffer and were further incubated for 1h at RT on the shaker in 0.01% PBST buffer containing 10% milk powder.

5- Primary Antibody: After blocking, EBs were washed 4 times with 0.01% PBST buffer. The primary antibody against PECAM-1 was freshly prepared by diluting 1:100 in 10% milk and incubated either at RT on the shaker for 2h or overnight at +4°C.

6- Secondary Antibody: The EBs were washed 4 times with 0.01% PBST buffer and left 10 min on the shaker at RT with 0.01% PBST buffer to ensure the removal of surplus primary antibody. The secondary antibody anti-rat Alexa 488 was added at a dilution of 1:100 in 10% milk, and EBs were incubated for 1h in the dark at RT. Then they were

washed 4 times with 0.01% PBST and taken for imaging or stored at +4ºC with 4% PFA until analysis.

7- Imaging: The stained EBs were transferred to the chamber slide, and the branching points were analyzed by confocal microscopy (Leica SP2 AOBS). The pinhole settings of the confocal setup were adjusted to give a full-width half maximum of 5µm. For the quantification of capillary areas within EBs an optical sectioning routine based on confocal laser scanning microscopy was used. Images (512 x 512 pixels) were acquired from PECAM-1 stained EBs using the extended depth of focus algorithm of the confocal setup. In brief, 10 full frame images, separated by a distance of 10µm in *z*-direction, were recorded that included the information of the capillary area and spatial organization in a tissue slice 100µm thick.

8- Analysis: The acquired images were processed to generate a single in-focus image projection of vascular structures in the scanned tissue slice. By use of the image analysis software Metamorph (Molecular Devices), the branching points of vascular structures within the three-dimensional projection were identified and counted in relation to the size (μm^2) of the respective EB.

2.3.4.2. α-actinin staining

α-actinin staining was performed to visualize differentiated cardiac areas in EBs outgrown on cover slips and collected between day 7 and day 10 of cell culture.

1- Sample collections: Cell culture medium was removed from EB tissue cultures. The medium was removed, and they were washed 3 times with 1x PBS.

2- Fixation: The cells were fixed in ice-cold methanol and kept at -20°C for 20 min.

3- Blocking: After fixation the cells were washed 4 times with 0.01% (Triton-X-100) PBST buffer containing 10% FCS and further incubated for 1h at RT.

4- Primary Antibody: After blocking, cells were washed 4 times with 0.01% PBST buffer. The primary antibody against α-actinin was diluted 1:100 in 10% FCS and incubated overnight at +4°C.

5- Secondary Antibody: The EBs were washed 4 times with 0.01% PBST buffer and left 10 min on the shaker with 0.01% PBST buffer to ensure the removal of surplus primary antibody. The secondary antibody Cy5 sheep anti mouse diluted 1:100 in 10% FCS was

added, and cells were incubated for 1h in dark at RT. EBs were washed 4 times with 0.01% PBST and stored at +4ºC until analysis time by embedding EBs on cover slips with Fluoromount-G.

6- Imaging: The stained EBs were transferred to the stage of the Leica confocal microscope and α-actinin-positive cell areas were analysed using 10x objective and z-series**.**

7- Analysis: Sizes of α-actinin positive areas (µm²) in EBs were calculated by use of the image analysis software Metamorph.

2.3.4.3. Leukocyte marker staining

For Leukocyte marker staining, the EBs were treated with Silibinin from day 3 until day 6 of cell culture in bacteriological cell culture plates on the shaker. Subsequently EBs were outgrown on cover slips in tissue culture plates and further treated with Silibinin until day 14 of cell culture. Medium change was performed every day till day 14.

1- Sample collection: On day 14, the EBs were removed from the incubator, the medium was aspirated and washed 3 times with 1x PBS to remove the medium.

2- Fixation: The EBs were fixed in 4% PFA and incubated at +4ºC for 45 min.

3- Blocking: After fixation, the EBs were washed 4 times with 0.01% PBST (Tween-20) buffer, 10% milk powder dissolved in 0.01% PBST (Tween-20) buffer was added, and EBs were further incubated for 1h at RT on the shaker.

4- Primary Antibody: After blocking, EBs cells were washed 4 times with 0.01% PBST (Tween-20). The primary antibody (CD45, CD18 or CD68) diluted 1:100 in 10% milk was added and incubated overnight at +4°C.

5- Secondary Antibody: The EBs were washed 4 times with 0.01% PBST (Tween-20) buffer and left for 10 min on the shaker with 0.01% PBST (Tween-20) buffer to ensure the removal of surplus primary antibody. The secondary antibody anti-rat Alexa 488 (dilution 1:100) in 10% milk was added for 1h in the dark on the shaker at RT. Subsequently EBs were washed 4 times with 0.01% PBST (Tween-20).

6- DRAQ5 staining: The EBs were washed with 1x PBS 3 times and stained with DRAQ5 (1:1000) at RT for 20 min in dark for nuclear staining. Subsequently, the EBs were washed

with 1x PBS buffer 3 times, the cover slips were mounted on object slides with Fluoromount-G and stored at +4°C till analysis.

7- Imaging: EBs on objective slides were transferred to the stage of the Leica confocal microscope and leukocyte markers were assessed using a 20x immersion corrected objective.

8- Analysis: Confocal images were collected from 15-20 EBs. The MetaMorph image analysis software was used to assess the number of leukocyte marker positive cells per total number of cells which were visualized by DRAQ5-labelled cell nuclei.

2.4. Ca^{2+} measurement

2.4.1. Isolation of cardiomyocytes, dissociation of cells and plating

Intracellular Ca^{2+} was recorded in single cardiac contracting cells. Single cell preparations were obtained by enzymatic digestion of 7-day-old EBs for 30 min at 37°C in PBS containing 2mg/ml Collagenase B. Dissociated single cells were plated onto gelatin-coated cover slips in 24-well cell culture plates, and cultivated in Iscove's medium supplemented with 16% FCS.

2.4.2. Ca^{2+} detection (Fluo-4 fluorescence measurement)

Following 24h of culture, cells were loaded in serum-free medium with 1µM Fluo-4-AM for 30 min. Subsequently, the cover slips were transferred in fresh serum-free cell culture medium to the incubation chamber of the confocal laser scanning microscope. Fluorescence excitation was performed at 488nm, emission was recorded at 500-550nm. For analysis of intracellular calcium a HCPL Apo 20x immersion corrected objective was used. Sampling rate was 2 frames/s. The fluorescence emission of single cells was assessed by using the image analysis software of the confocal setup.

2.5. NO measurement

For the measurement of NO the fluorescent NO indicator DAF-FM diacetate was dissolved in DMSO to achieve a stock solution of 5mM. On day 5 of differentiation EBs were treated with Silibinin and stained on day 6 with 5µM DAF-FM for 30 min in dark conditions on a shaker placed in an incubator (37°C and 5% CO_2). Then the medium was replaced for serum-free medium and further incubated for 30 min in dark on the shaker. The

fluorescence of the sample was detected by confocal laser scanning microscopy (Leica SP2 AOBS) with the argon laser (excitation 495nm), and emission was recorded at wavelength of 515nm.

2.6. Western blot (immunoblotting)

2.6.1. Protein extraction

The total protein concentration was measured by the colorimetric Lowry method (Lowry et al., 1951) using a Tecan Infinite M200 Microplate reader instrument (Tecan Group Ltd., Männedorf, Switzerland).

2.6.2. Gel electrophoresis

To perform semi-quantitative western blot, 20µg aliquots of each protein sample were mixed with 1x NuPAGE LDS sample buffer and 1x NuPAGE reducing agent (Thermo Fisher Scientific, Darmstadt, Germany). The freshly prepared protein mixture was incubated for 10 min at 70^{o}C for denaturation, and then was immediately loaded on a 4-12% gradient PAGEr EX Precast polyacrylamide mini-Gel (Lonza, Rockland, USA). The gel electrophoresis was run at 200V for 45-55 min at RT.

After gel electrophoresis, proteins were transferred from the SDS-PAGE gel onto PVDF membranes for 60 min at 375mA using Invitrogen semi-dry apparatus as explained in figure 2.5. Afterwards, the membranes were stained with a Ponceau-S solution (0.1% Ponceau-S in 1% acetic acid) to control transfer of proteins onto membrane.

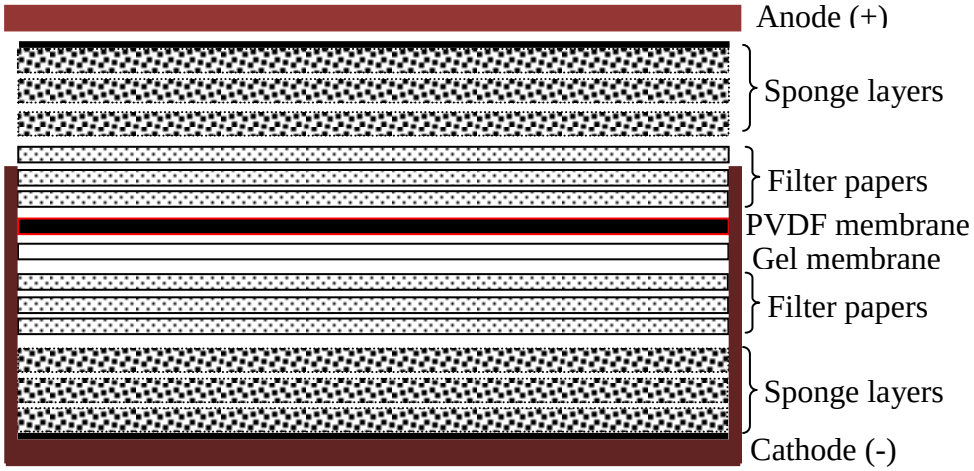

Figure 2.5: Schematic representation of protein transfer from gel membrane to the PVDF membrane in the XCell SureLock^{TM} Mini-Cell Blot Module from Invitrogen, as sandwich layers.

2.6.3. Staining with antibody and detection

Next, the PVDF membrane was washed 2-3 times with ddH_2O until the Ponceau-S staining was completely disappeared from the membranes and then incubated with blocking buffer (5% non-fat milk powder in 0.1% TBS-Tween) for 1h at RT with gentle agitation to reduce unspecific antibody binding. The membranes were washed 2-3 times with TBS-Tween (0.1%) and incubated with primary antibodies, 1:1000 diluted in 5% BSA in 0.1% TBS-Tween, for overnight at 4^oC with gentle agitation. Then, the membranes were washed and incubated with appropriate HRP-conjugated secondary antibodies (1:1000 diluted in 5% BSA in 0.1% TBS-Tween) for 1h at RT with gentle agitation. Finally, the membranes were properly washed with TBS-Tween (0.1%), and the protein bands were detected using chemiluminescent substrates (1.25mM Luminol + 225µM Coumaric acid + 3mM H_2O_2 in 100mM Tris buffer, pH 8.5). The emitted chemiluminescence was visualized and converted into a digital image using a PEQLAB Gel documentation system (VWR Part of Avantor, Erlangen, Germany) assisted with the Chemi-Capt 5000 software (Version 15.01a, Vilber Smart Imaging, Eberhardzell, Germany). Subsequently, a densitometric analysis was performed on these captured digital images using the free available Java software ImageJ (Version 1.46, Wayne Rasband, National Institute of Health, USA) (Schindelin et al., 2012). This densitometric analysis was based on the intensity of each visualized protein band on the captured digital images. The final value of each target protein band was obtained after normalizing with their respective house-keeping protein band. For final protein expression/phosphorylation quantification, this final value of each treated samples was compared with the final value of untreated control sample.

Stripping: For reprobing the same membrane with another set of target proteins, the membranes were 2-3 times washed with TBS-Tween (0.1%) and afterwards stripped using the Restore PLUS western blot Stripping Buffer from Thermo Fisher Scientific (Darmstadt, Germany). For stripping procedure, the membranes were incubated in the above mentioned stripping buffer for 20 min in dark at RT on the shaker with gentle agitation. Next, the membranes were rinsed in TBS-Tween (0.1%) buffer. To control the success of the stripping procedure, the membranes were incubated with the chemiluminescent substrates to confirm that the previous antibody staining was completely removed from the membranes. After this confirmation step, the membranes were 2-3 times washed with TBS-

Tween (0.1%) and the reprobing procedure was started from the blocking step as described before.

2.7. Statistical analysis

For statistical analysis GraphPad InStat statistics software (GraphPad Software Inc. La Jolla, CA) was used. Data are given as mean values $\pm$ standard deviation (SD), with *n* denoting the number of experiments performed with independent ES cell cultures. In each experiment at least 20 culture objects were analyzed unless otherwise indicated. Student's *t* test for unpaired data and one-way ANOVA was applied as appropriate for statistical analysis. A value of * $P \leq 0.05$ was considered to be significant; ** $P \leq 0.01$ (very significant) and *** $P \leq 0.001$ as a highly significant.

2.8. Software

1- Chemicapt 500 - Western blot imaging software, PEQLAB Biotechnologie, Version 15.01a, Vilber Smart Imaging, Eberhardzell, Germany.

2- GraphPad Instat - Statistical analysis software. GraphPad Software Inc. La Jolla, CA USA.

3- Image J - Western blot analysis software, Version 1.46, Wayne Rasband, National Institute of Health, USA.

4- Leica Application Suite Advanced Fluorescence Leica Microsystems, Wetzlar, Germany

5- MetaMorph offline- Microscopy Automation & Image Analysis Software- Molecular Devices, Sunnyvale, CA, USA.

6- Microsoft Office - Data documentation Microsoft, California, USA.

7- Tecan Magellan™ -ELISA Software Tecan, Tecan Group Ltd., Männedorf, Switzerland.

3. Results

3.1. Effect of Silibinin on cardiomyogenesis of ES cells

3.1.1. Effect of Silibinin on contraction frequency and number of contracting foci

To examine the effects of Silibinin on the differentiation of cardiomyocytes, EBs were treated from day 3 until day 10 with different concentrations of Silibinin (1µM, 10µM, 20µM and 50µM). From day 7 until day 10, contraction frequency, the number of contracting foci and the number of contracting EBs were assessed. It was observed that Silibinin treatment dose-dependently decreased contraction frequency (figure 3.1), the number of contracting foci (figure 3.2) as well as the number of contracting EBs (figure 3.3).

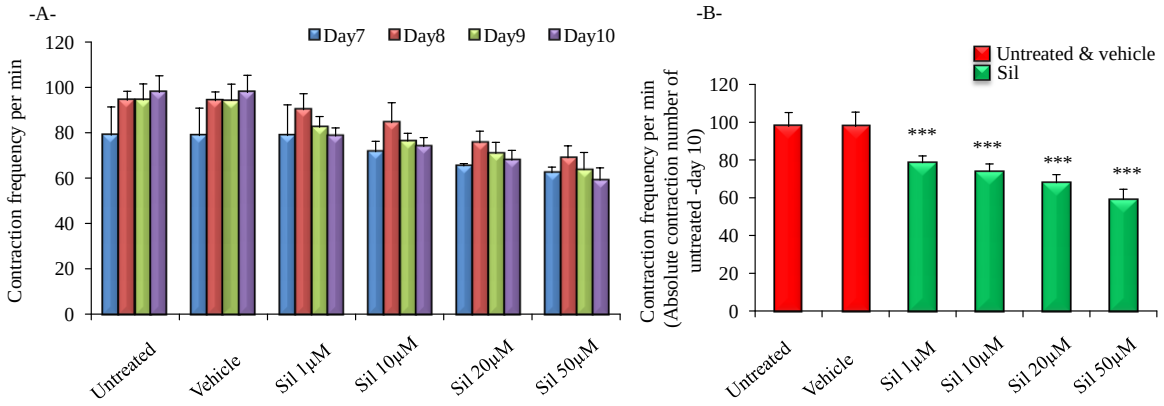

Figure 3.1: Effect of Silibinin on contraction frequency of EBs. (A) Decrease of contraction frequency per min upon treatment of EBs with increasing concentrations of Silibinin. **(B)** Dose-dependent decrease in contraction frequency following treatment with different concentrations of Silibinin compared to the untreated control on day 10, the bar chart shows the means $\pm$ SD of n = 4 experiments; *** P $\leq$ 0.001.

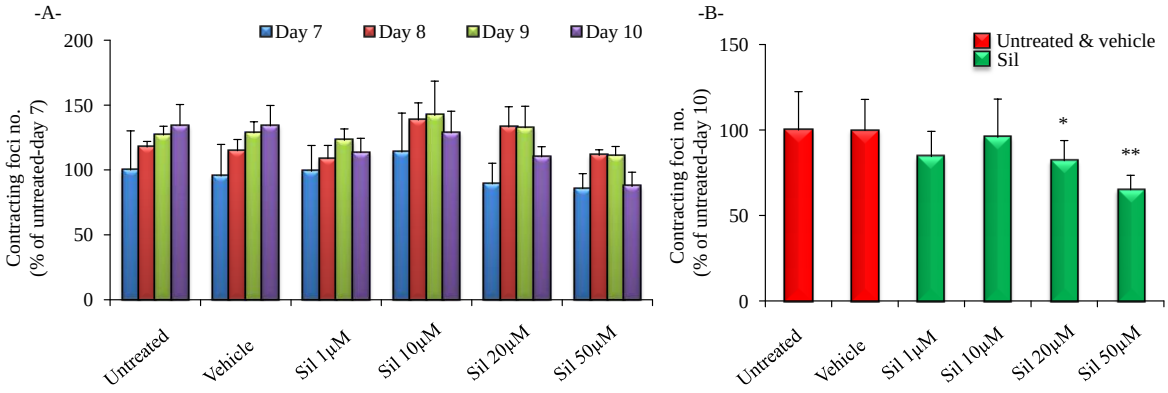

Figure 3.2: Effect of Silibinin on the differentiation of contracting of cardiac foci. **(A)** Dose-dependent decrease of contracting foci number (% of untreated, day 7). **(B)** Dose-dependent decrease of contracting foci number compared to the untreated control on day 10, the bar chart shows the means ± SD of n = 4 experiments; * P ≤ 0.05, ** P ≤ 0.01.

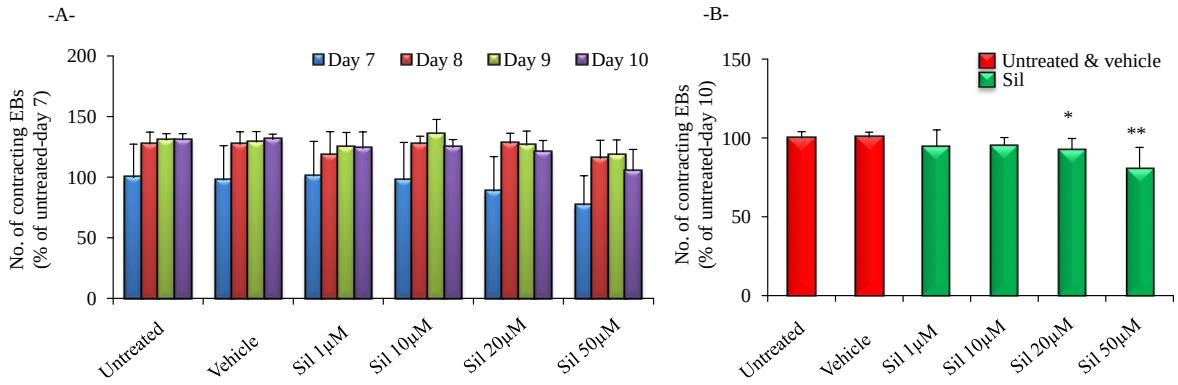

Figure 3.3: Effect of Silibinin on the number of spontaneously contracting EBs. (A) Dose-dependent decrease of contracting EB number (% of untreated, day 7). **(B)** Dose-dependent decrease of contracting EB number compared to the untreated control on day 10, the bar chart shows the means ± SD of n = 4 experiments; * P ≤ 0.05, ** P ≤ 0.01.

3.1.2. Effect of Silibinin on the size of cardiac cell areas

To investigate whether Silibinin affected the size of cardiomyocyte cell areas differentiated from mouse ES cells, 3-day-old EBs were treated for 7 days with different concentrations of Silibinin (1µM, 10µM, 20µM and 50µM). On day 10, EBs were immunostained with an antibody against α-actinin and the size of cardiac areas was determined by confocal laser scanning microscopy. It was observed that Silibinin treatment dose-dependently decreased the size of α-actinin positive cell areas in EBs (figure 3.4).

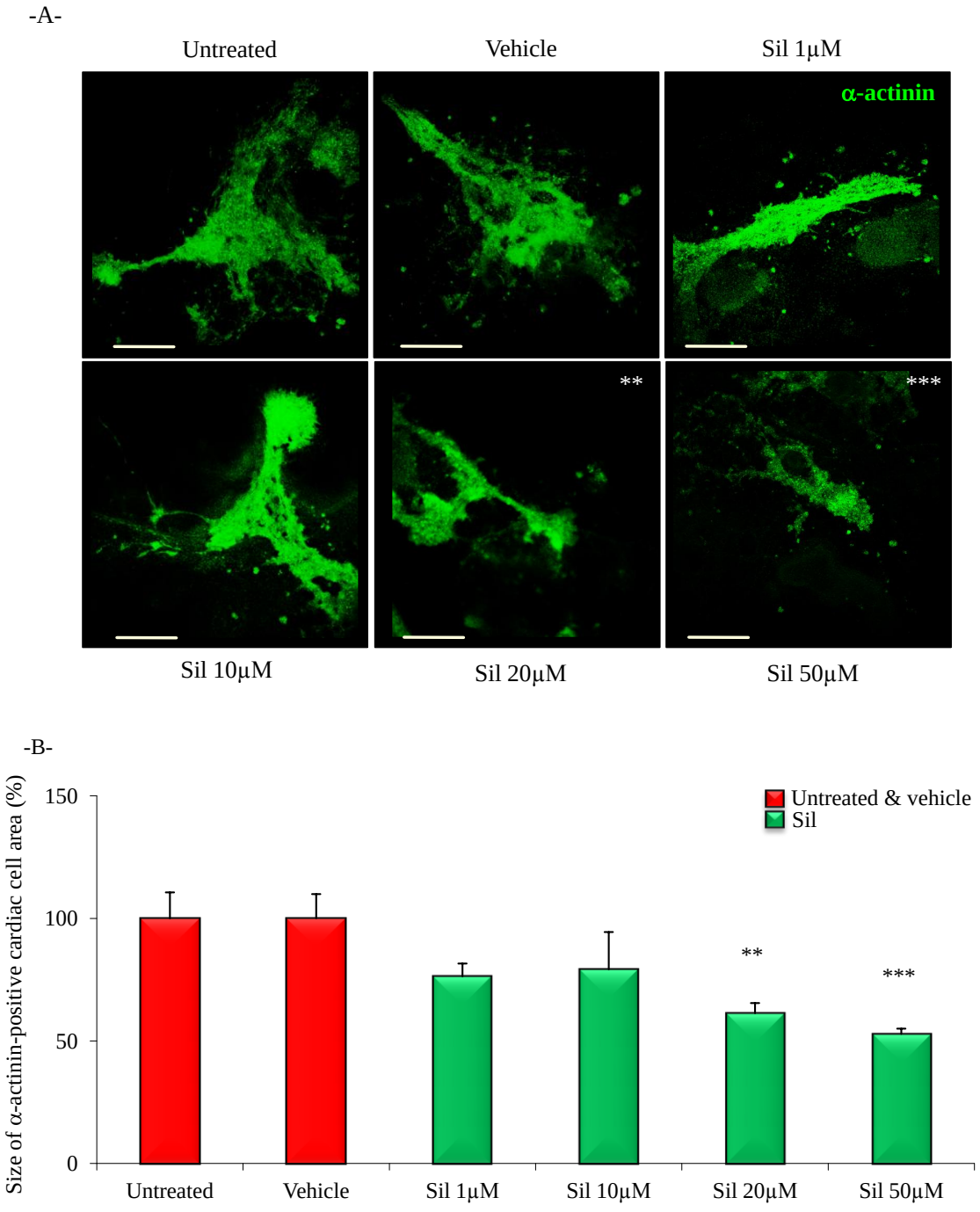

Figure 3.4: Effect of Silibinin on the size of α-actinin positive cell areas of cardiomyocytes derived from mouse ES cells. **(A)** Confocal images of representative EBs stained against α-actinin (green) to determine the size of the positive areas. The bar represents 300µm. **(B)** Quantification of the size of α-actinin positive areas on day 10, the bar chart shows the means ± SD of n = 3 experiments; ** $P \leq 0.01$, *** $P \leq 0.001$.

3.2. Effect of Silibinin on angiotensin II- (Ang II) induced cardiomyogenesis of mouse ES cells

Previous studies have shown that the vasoactive hormone Ang II is stimulating cardiomyogenesis of ES cells (Wu et al., 2013). Moreover, a recent study demonstrated that Silibinin may act as an AT1 receptor antagonist (Bahem et al., 2015). Since the data of the present study demonstrated that Silibinin decreased cardiomyogenesis of ES cells and the frequency of contractions, we investigated whether Silibinin would interfere with Ang II-induced cardiomyogenesis, contraction frequency and Ca^{2+} oscillations.

3.2.1. Effect of Silibinin and Ang II on contraction frequency and number of contracting foci

To investigate whether the contraction frequency was affected by Silibinin and Ang II treatment, we calculated the frequency of contractions per min. Three-day-old EBs were treated for 11 days, (from day 3 to day 14 of differentiation) either with Silibinin (20µM) alone, with Ang II (1µM) alone or with a combination of Silibinin and Ang II. We found that the contraction frequency was significantly increased upon Ang II treatment compared to untreated (control), whereas Silibinin (20µM) alone significantly decreased contraction frequency. Pre-incubation with Silibinin abolished the increase in contraction frequency achieved with Ang II (figure 3.5).

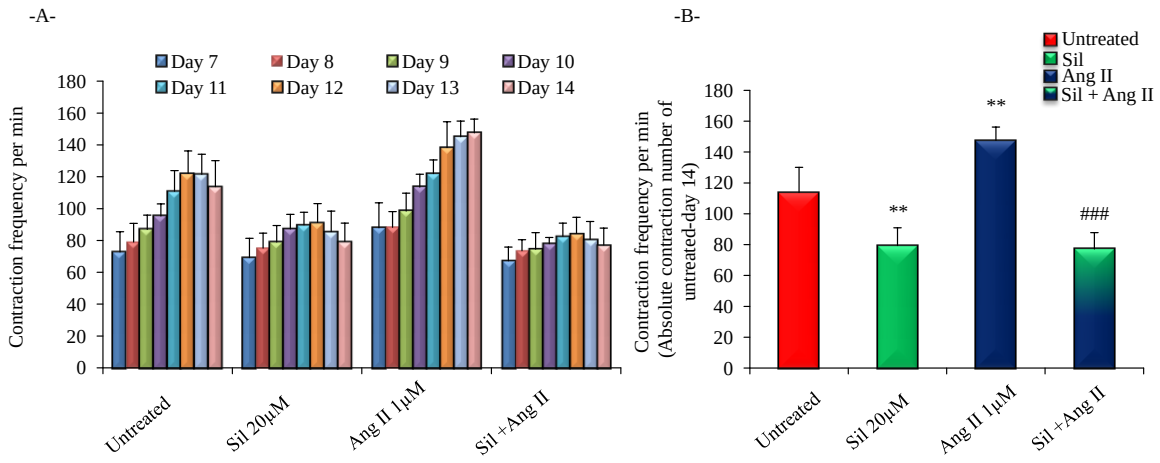

Figure 3.5: Effect of Silibinin and Ang II on contraction frequency of EBs. (A) Contraction frequency per min of EBs after different times of cell culture (day 7 to day 14). EBs remained either untreated or were treated with Silibinin (20µM), Ang II (1µM) or with a combination of Silibinin and Ang II (from day 3 to day 14) **(B)** Effect of Silibinin treatment on Ang II-mediated stimulation of contraction frequency as evaluated on day 14 of cell culture. Silibinin (20µM) reduced the contraction frequency on day 14, the bar chart shows the means $\pm$ SD of n = 5 experiments; ** $P \leq 0.01$, significantly different to the untreated control, ### $P \leq 0.001$ significantly different to Ang II alone.

To further characterize the effect of Silibinin on Ang II-mediated cardiomyogenesis of ES cells the number of contracting cardiac foci (figure 3.6) as well as the number of contracting EBs (figure 3.7) were counted from day 7 until day 14 of cell culture. We found that Ang II increased the number of contracting foci and EBs as compared to the untreated control, while Silibinin (20µM) alone exerted an inhibitory effect. Pre-treatment with Silibinin abolished the stimulation of cardiomyogenesis achieved with Ang II.

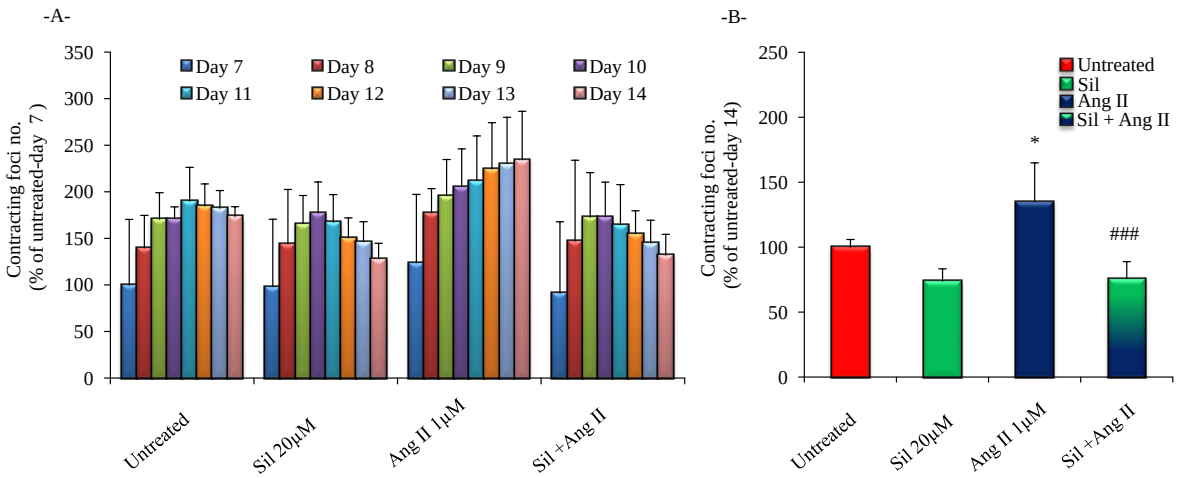

Figure 3.6: Effect of Silibinin and Ang II on contracting cardiac foci number. (A) EBs were treated with Silibinin (20µM), Ang II (1µM) or with a combination of Silibinin and Ang II (from day 3 to day 14). **(B)** Number of contracting foci (% of untreated control, day 14). Pre-treatment with Silibinin (20µM) abolished the stimulation of cardiomyogenesis achieved with Ang II, the bar chart shows the means $\pm$ SD of n = 5 experiments; * $P \leq 0.05$ significantly different to the untreated control, ### $P \leq 0.001$ significantly different to Ang II alone.

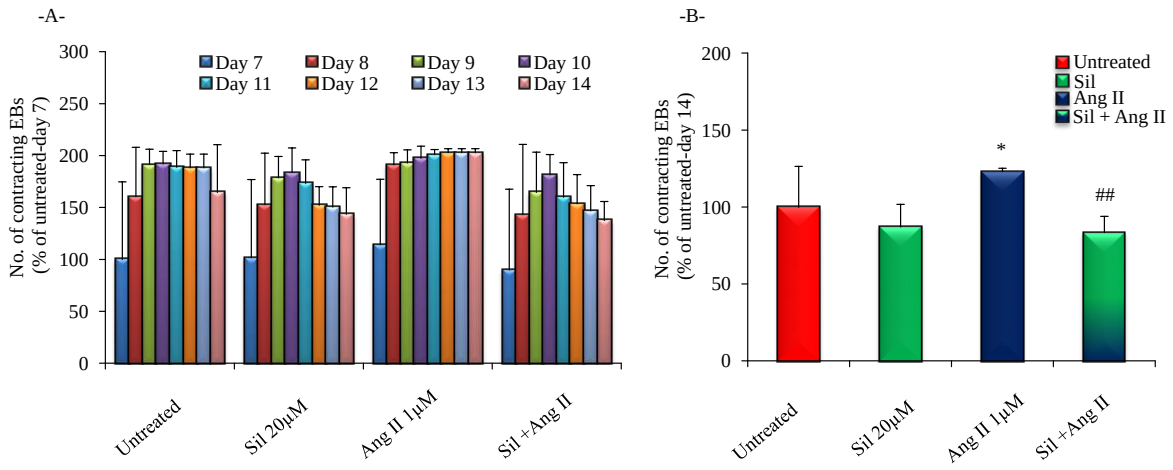

Figure 3.7: Effect of Silibinin and Ang II on spontaneously contracting EBs. (A) Number of contracting EBs (% of untreated day 7). EBs were treated with Sil (20µM), Ang II (1µM) and Sil + Ang II from (day 3 - 14), while the number of contracting EBs was calculated from (day 7 - 14). **(B)** Effect of Silibinin and Ang II on the number of contracting EBs (day 14). Silibinin treatment alone decreased the number of contracting EBs compared to untreated controls, whereas Ang II significantly increased the number of contracting EBs. The stimulation of contraction activity achieved with Ang II was abolished upon co-treatment with Silibinin, the bar chart shows the means $\pm$ SD of n = 5 experiments; * $P \leq 0.05$ significantly different to the untreated control, ## $P \leq 0.01$ significantly different to Ang II alone.

3.2.2. Effect of Silibinin and Ang II on the size of contracting cardiac areas

To examine the effect of Silibinin and Ang II on the size of cardiac areas, EBs remained untreated, were treated with Ang II (1µM) (from day 3 to day 14 of cell culture) alone or pre-incubated for 30 min with Silibinin (20µM) either in absence of presence of Ang II. Cardiac differentiation was investigated by assessing the size of α-actinin-positive cell areas at day 14 (figure 3.8).

Silibinin alone significantly reduced the size of the α-actinin-positive areas compared to the untreated control, whereas a significant increase was observed upon Ang II treatment. Co-treatment with Silibinin and Ang II abolished the stimulation of cardiomyogenesis achieved with Ang II.

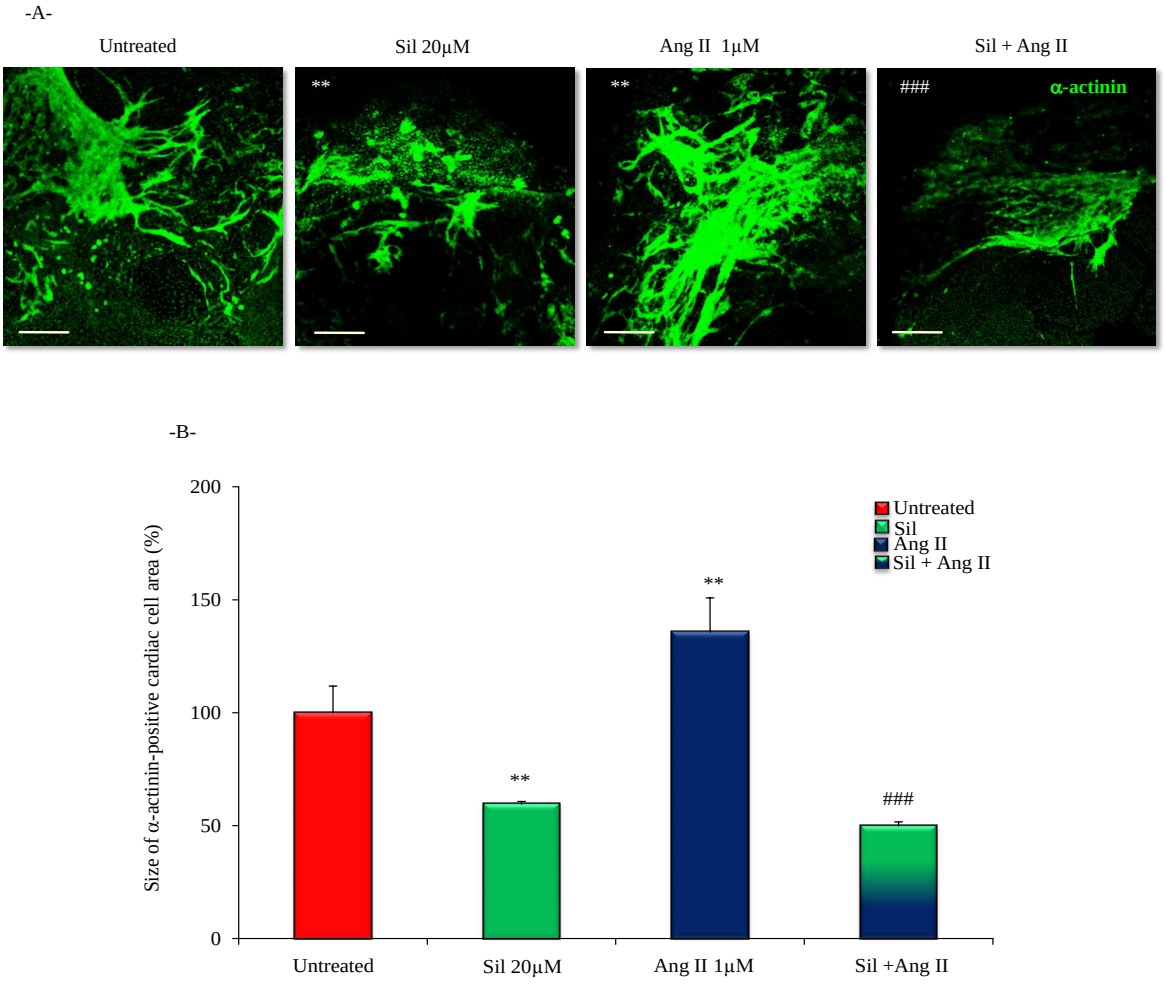

Figure 3.8: Effect of Silibinin and Ang II on the size of α-actinin positive cardiac areas differentiated from mouse ES cells. (A) Representative α-actinin-positive cardiac areas (green) under the following experimental conditions (from the left to the right): untreated, Silibinin (20µM), Ang II (1µM), Sil + Ang II. The bar represents 300µm. **(B)** Quantification of the relative size of cardiac areas at day 14. The untreated control was set to 100%, the bar chart shows the means $\pm$ SD of n = 4 experiments; ** $P \leq 0.01$ significantly different to the untreated control, ### $P \leq 0.001$ significantly different to Ang II alone.

3.3. Effect of Silibinin and Ang II on Ca^{2+} oscillations in cardiomyocytes

Spontaneous contractions and action potentials in cardiac cells are associated to rhythmic Ca^{2+} oscillations. Since our data demonstrated that Ang II treatment stimulated cardiomyogenesis of ES cells, we investigated whether Ang II treatment would have an impact on cardiac cell function. To achieve this aim, contracting EBs (day 7 of cell culture)

were enzymatically dissociated, labeled with the Ca^{2+}-sensitive fluorescence dye Fluo-4-AM on day 8, and intracellular Ca^{2+} oscillations were recorded in single cardiac cells after different times of incubation (200 s, 600 s, 1500 s) with either Ang II (1µM), Silibinin (20µM) or a combination of both. It was evident that Silibinin treatment decreased the frequency of Ca^{2+} spikes which was significant after 1500 s of incubation. In contrast an increase in spiking frequency was observed upon Ang II treatment. However, when Ang II was applied after pre-incubation with Silibinin the stimulation of Ca^{2+} spiking frequency was abolished, which indicates that Silibinin interferes with Ang II-mediated signaling pathways (figure 3.9 A, B).

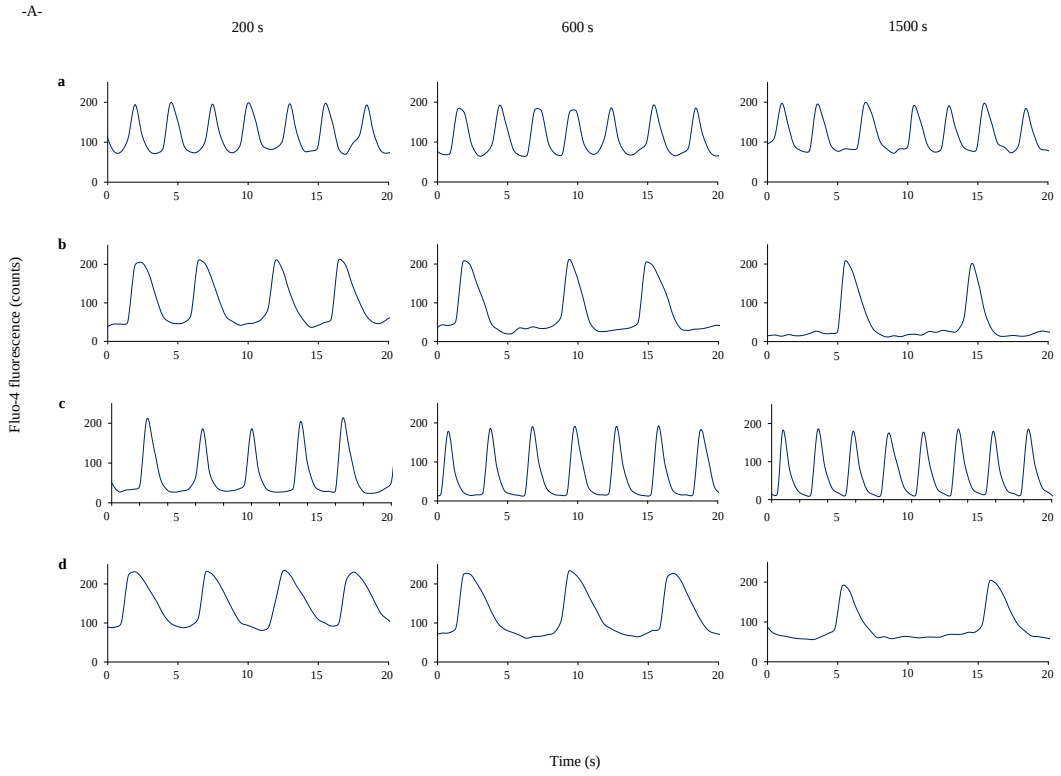

Figure 3.9 A: Effects of Silibinin and Ang II on the frequency of Ca^{2+} transients in cardiac cells differentiated from ES cells. Cardiac cells were enzymatically dissociated from 7-day-old EBs and labeled on day 8 with the Ca^{2+}-sensitive fluorescence dye Fluo-4. Ca^{2+} spiking was evaluated in 3 different time windows, i.e. 200 s, 600 s and 1500 s. Shown are representative traces of individual cells. (a) Untreated controls, (b) Silibinin (20µM) treated cells; (c) Ang II (1µM) treated cells, (d) cells treated with a combination of Silibinin (20µM) and Ang II (1µM).

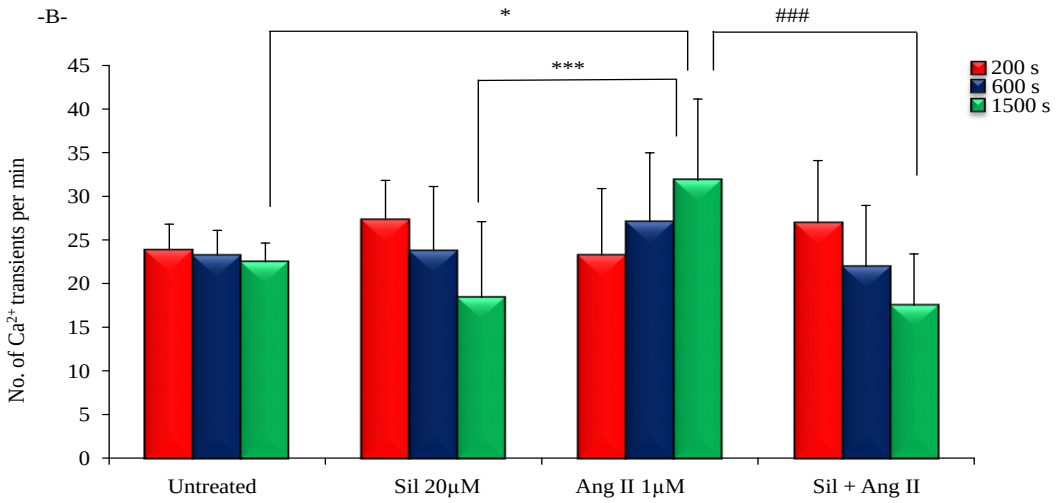

Figure 3.9 B: Bar chart of Silibinin and Ang II effects on the frequency of Ca^{2+} transients. The bar chart shows the means ± SD of 10 experiments and indicates, that Ang II increased the Ca^{2+} spiking frequency which was completely reversed upon co-treatment with Silibinin. * $P \leq 0.05$, significantly different to the untreated control. *** $P \leq 0.001$, significantly different to Silibinin, ### $P \leq 0.001$, significantly different to the Ang II treated sample.

3.4. Effects of Silibinin and Ang II on the function of adult rat cardiomyocytes

Since cardiomyocytes differentiated from ES cells may be immature and represent a fetal phenotype, we investigated whether Silibinin would interfere with Ang II-mediated changes in cardiac cells isolated from the ventricles of adult rat hearts. To achieve this aim, the protocol developed by Mufti et al., 2008 was applied. Our data demonstrated that after 24h incubation with Ang II (10µM) a significant decrease in contraction as well as relaxation velocity occurred. Moreover, Ang II significantly reduced the contraction velocity indicated by diastolic cell lengths of individual cells (dL/L) and decreased the time to reach 50% of peak contraction (TTP50). Treatment with Silibinin alone (20µM) was without effect. Upon co-incubation of Ang II with Silibinin for 24h, the effects observed with Ang II alone were totally abolished (figure 3.10 A, B, C and D).

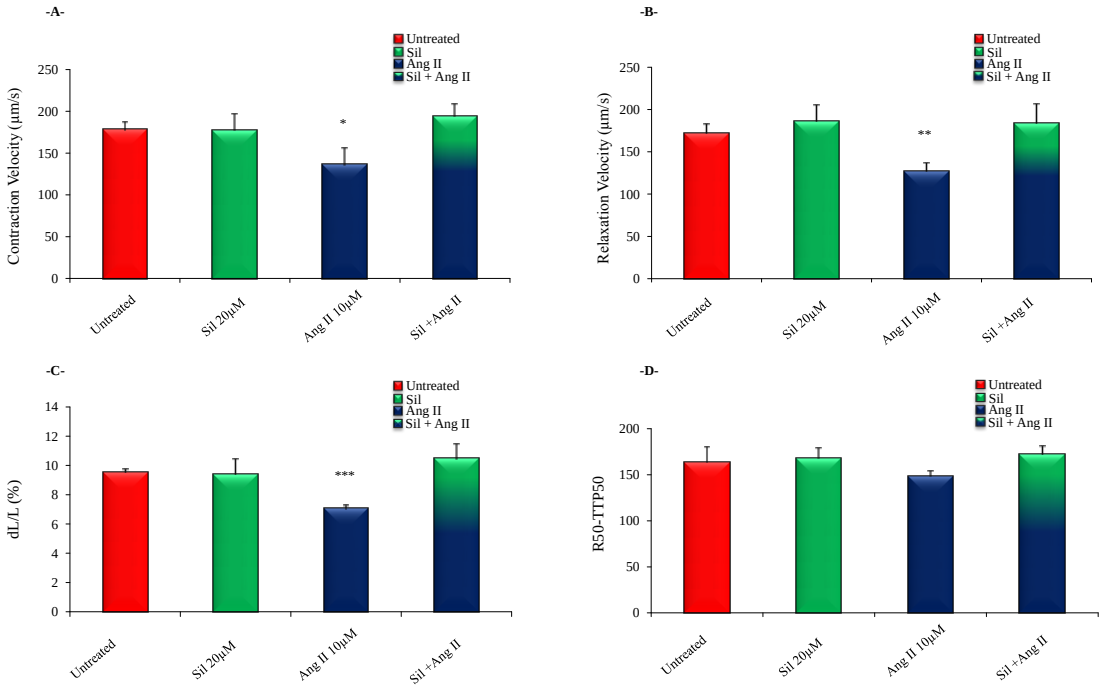

Figure 3.10 A-D: The effect of Silibinin and Ang II on cardiac cell function. (A) Isolated rat cardiomyocytes were incubated for 24h with either Silibinin (Sil) (20µM) alone, Ang II (10µM) alone or a combationation of both, and contraction velocity was investigated. Ang II caused significant decrease in contraction velocity compared to the untreated control which was reversed upon co-treatment with Silibinin. **(B)** Effect of Silibinin and Ang II on relaxation velocity. Ang II (10µM) caused significant decrease in relaxation velocity which was reversed upon co-treatment with Silibinin. **(C)** Effect of Silibinin and Ang II on changes in diastolic cell lengths (dL/L (%)). The observed decrease in diastolic cell lengths was reversed upon co-treatment with Silibinin. **(D)** Effect of Silibinin and Ang II on R50-TTP 50. The decrease in R50-TTP 50 observed with Ang II was reversed upon co-treatment with Silibinin. n = 4 experiments; * $P \leq 0.05$, ** $P \leq 0.01$, *** $P \leq 0.001$.

3.5. Inhibition of Ang II-mediated extracellular signal-regulated kinase 1/2 (ERK1/2), p38 and c-Jun N-terminal kinase (JNK) phosphorylation by Silibinin

Previous data of our group (unpublished data) on adult rat smooth muscle cells demonstrated that Silibinin could not blunt the Ang II-induced Ca^{2+} response, thus ruling out that Silibinin acted on the AT1 receptor. We therefore assumed that Silibinin may interfere with downstream signaling cascades. Since it has been previously shown that Ang II activates ERK1/2, p38 and JNK in differentiating ES cells (Wu et al., 2013), we investigated whether Silibinin (20µM) would abolish MAPK activation upon treatment of EBs with Ang II (1µM). Indeed, Silibinin treatment of 6-day-old EBs efficiently abolished the Ang II-mediated activation of ERK1/2, p38 and JNK (figure 3.11) as evaluated using phospho-specific antibodies. These data corroborated our assumption that Silibinin interfered with Ang II signaling downstream of the AT1 receptor.

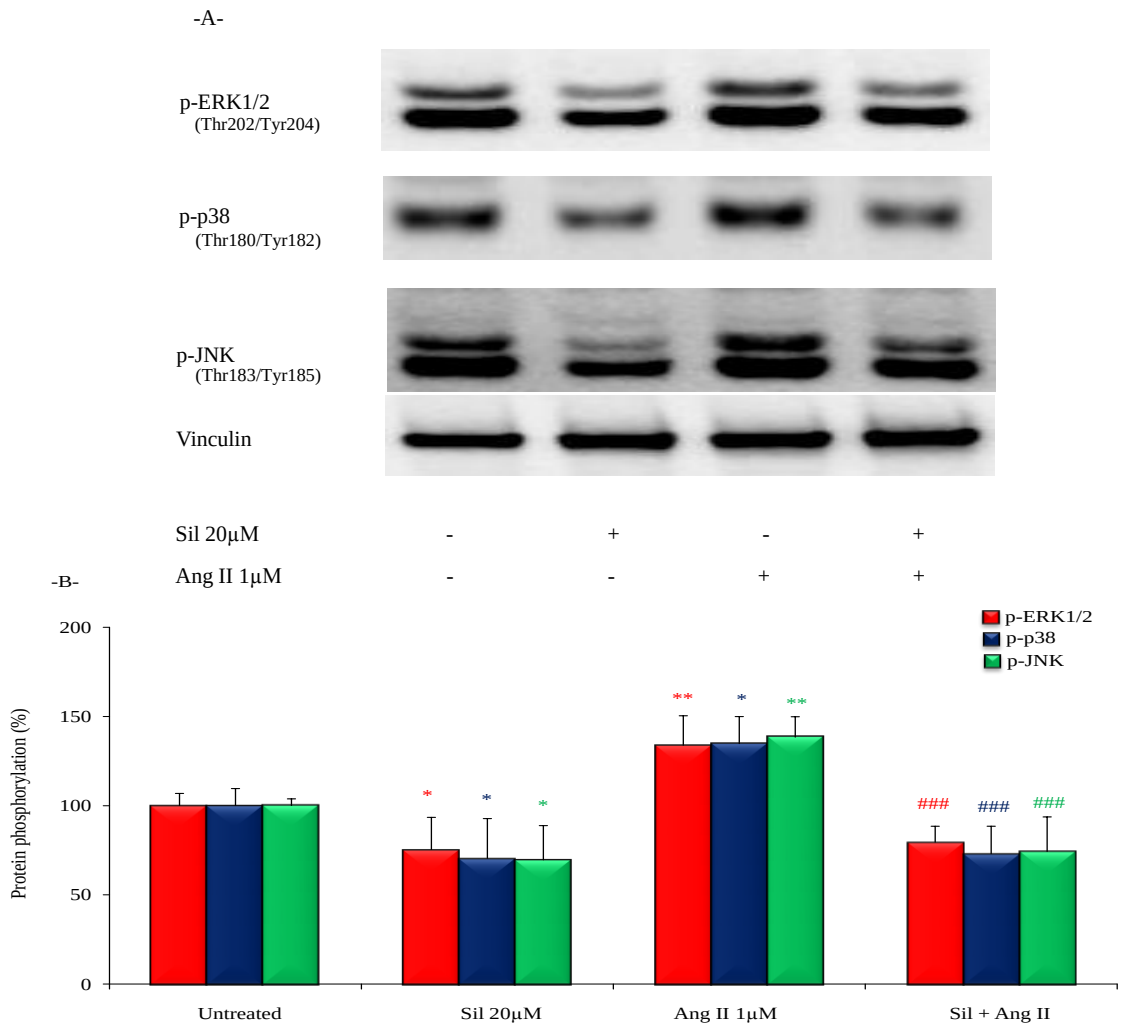

Figure 3.11: Effects of Silibinin and Ang II on MAP kinase (ERK1/2, p38 and JNK) phosphorylation. 6-day-old EBs remained either untreated or were treated with Ang II (1µM), Silibinin (20µM) or a combination of both. MAPK activation was monitored after 15 min of incubation with Ang II by western blot analysis using phospho-specific antibodies. Vinculin was used as house-keeping protein. In **(A)** representative western blots are shown. Upper panel ERK1/2 (42-44 kDa), middle panel p-p38 (43 kDa), bottom panel p-JNK (46 kDa, phospho-JNK1; 54 kDa, phospho-JNK2/3). The bar in **(B)** charts show the means $\pm$ SD of (n = 6) experiments for ERK1/2 and (n = 5) experiments for p38 and JNK, respectively. Note that Silibinin pre-treatment completely abolished MAPK activation achieved with Ang II. * $P \leq 0.05$, ** $P \leq 0.01$, significantly different to the untreated control. ### $P \leq 0.001$, significantly different to the Ang II treated sample.

3.6. Stimulation of vasculogenesis in differentiating mouse ES cells upon Silibinin treatment

Cardiac and vascular cells are known to originate from a common cardiovascular progenitor cell (Ishida et al., 2012). We therefore investigated whether Silibinin would affect vasculogenesis from ES cells. To address this point, EBs were incubated from day 3 to day 10 of differentiation with increasing concentrations of Silibinin, ranging from 1 - 50µM. At day 10 the EBs were collected, fixed and stained against the endothelial marker CD31/ PECAM-1 which is expressed at the intercellular junctions of endothelial cells. Vascular branching points were assessed by confocal laser microscopy and computer-assisted image analysis (figure 3.12). Silibinin treatment resulted in a dose-dependent increase of branching points with maximum effects achieved with 10µM, whereas higher concentrations (20 - 50µM) exerted adverse effects.

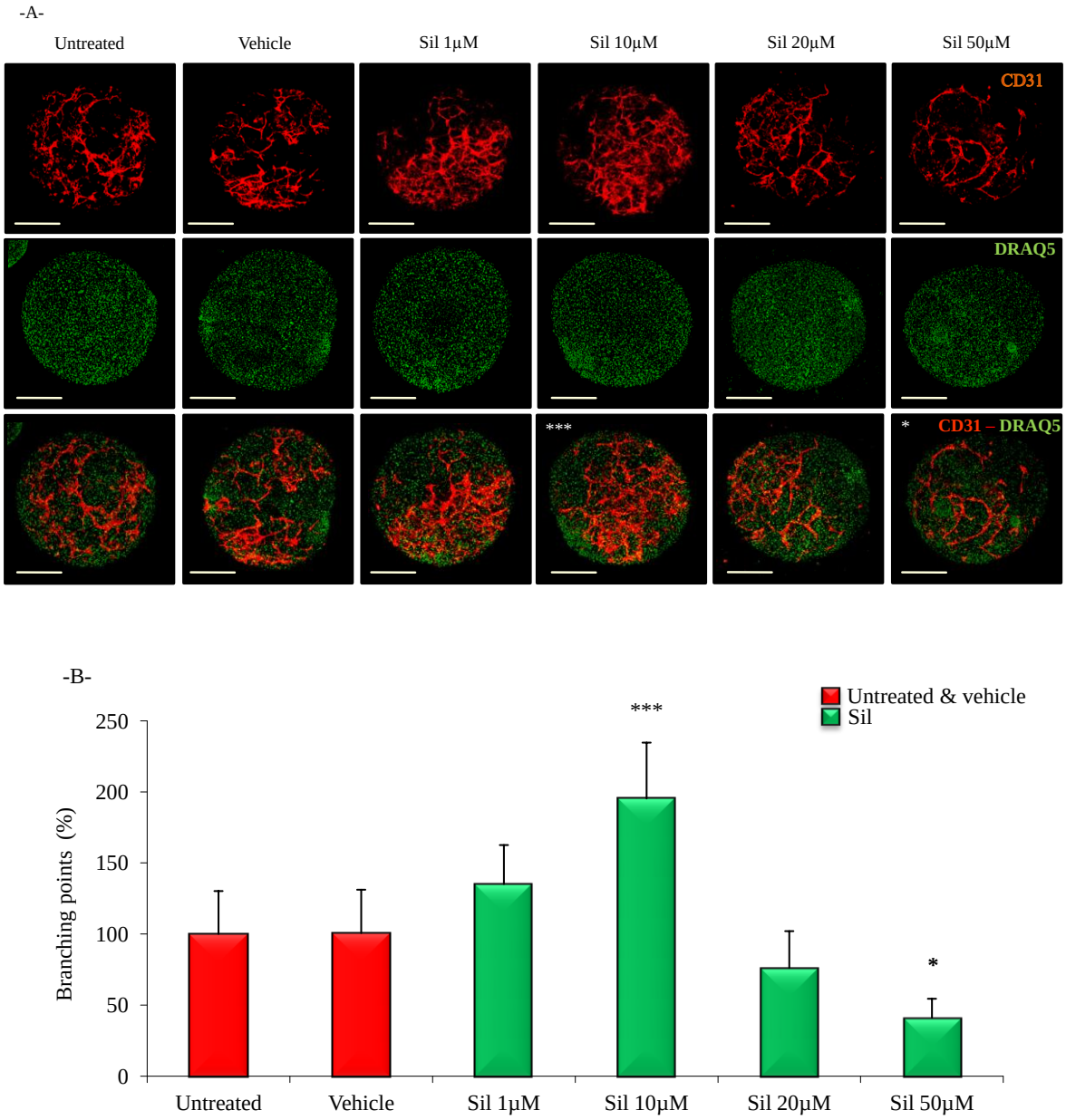

Figure 3.12: Effect of increasing concentrations of Silibinin on vascular branch formation. (A) Representative images of EBs treated with different concentrations of Silibinin or vehicle and stained against CD31 at day 10. CD31 staining (red), DRAQ5-positive cell nuclei (green). The bar represents 300µm. **(B)** The bar chart shows the means $\pm$ SD of n = 5 experiments as percentage values. (25 - 30 EBs were analyzed in each experiment), * $P \leq 0.05$, *** $P \leq 0.001$.

3.7. Expression of angiogenesis-related proteins upon Silibinin treatment

To assess whether the increased branching of vascular structures achieved with Silibinin was associated to pro-angiogenic proteins, the expression of VEGFR2 (FLK-1), VE-Cadherin and HIF-1α was investigated. 3-day-old EBs were treated with different concentrations of Silibinin for 7 days. On day 10, EBs were collected for determination of protein expression (figure 3.13). Silibinin treatment induced protein expression for VEGFR2, HIF-1α and VE-Cadherin which was significant at 10µM.

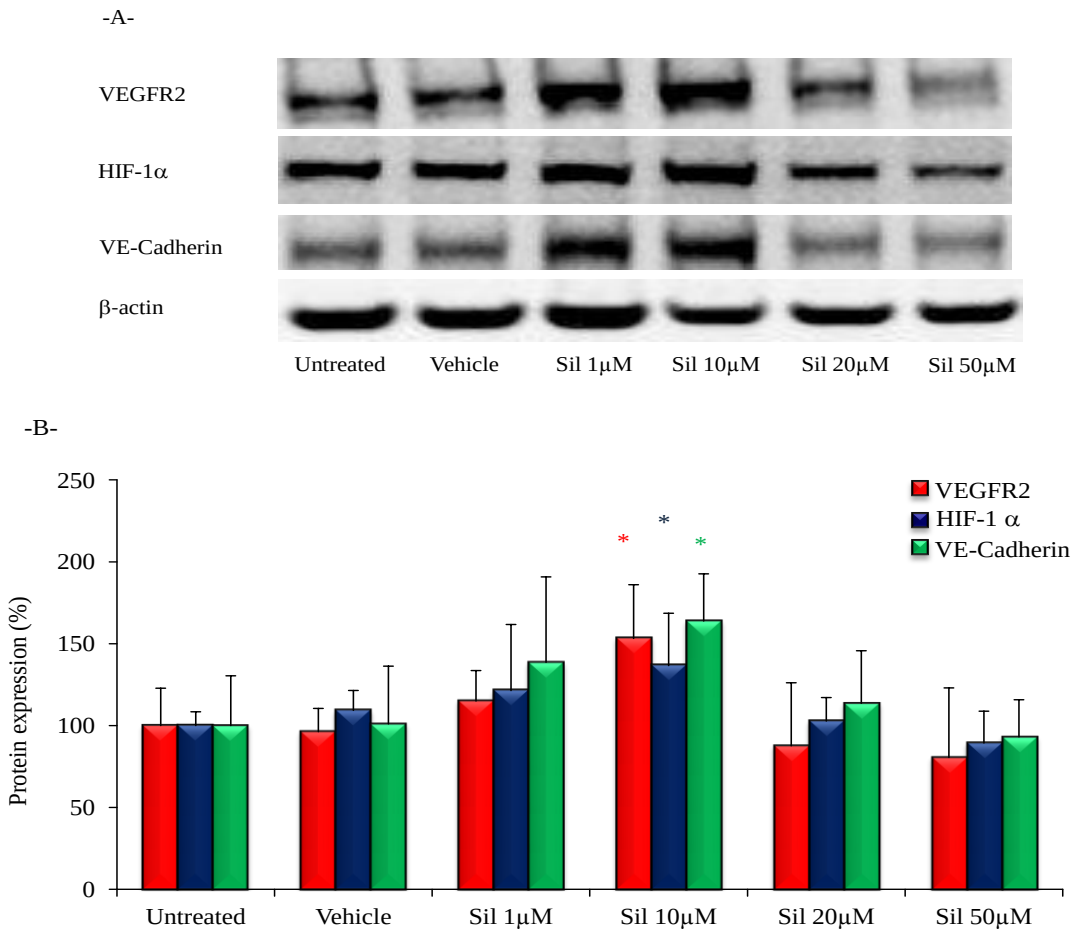

Figure 3.13: Induction of VEGFR2, HIF-1 α and VE-Cadherin expression upon Silibinin treatment. (A) Representative western blots of protein expression in EBs treated with different concentrations of Silibinin. **(B)** Graphical representation of protein expression upon treatment with different concentrations of Silibinin, the bar chart shows the means ± SD of (n = 5 experiments) for VEGFR2, HIF-1α (n = 6) and VE-Cadherin (n = 5). β-actin was used as house-keeping protein, * $P \leq 0.05$, significantly different to the untreated control.

3.8. Generation of NO upon Silibinin treatment of EBs

NO plays important roles in vascular biology and pathology (Walford and Loscalzo, 2003). Notably NO has been previously shown to regulate processes of vasculogenesis of EB cells (Sauer et al., 2013; Sharifpanah et al., 2016). Therefore, it was investigated whether Silibinin treatment would stimulate NO generation in EBs. To achieve this aim, 5-day-old EBs were treated with different doses of Silibinin (1µM, 10µM, 20µM and 50µM). After 24h (day 6), the EBs were incubated with the fluorescent NO indicator DAF-FM and DAF fluorescence was recorded. It was observed that Silibinin in concentrations of 1µM and 10µM significantly increased NO generation, whereas higher concentrations (20µM and 50µM) exerted adverse effects (figure 3.14).

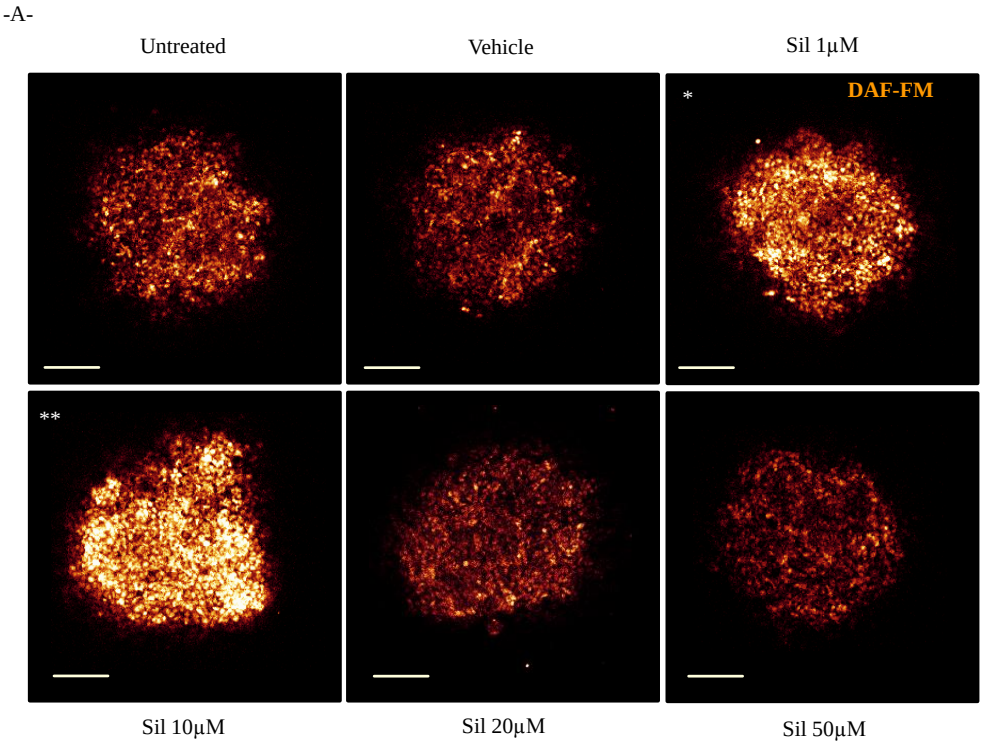

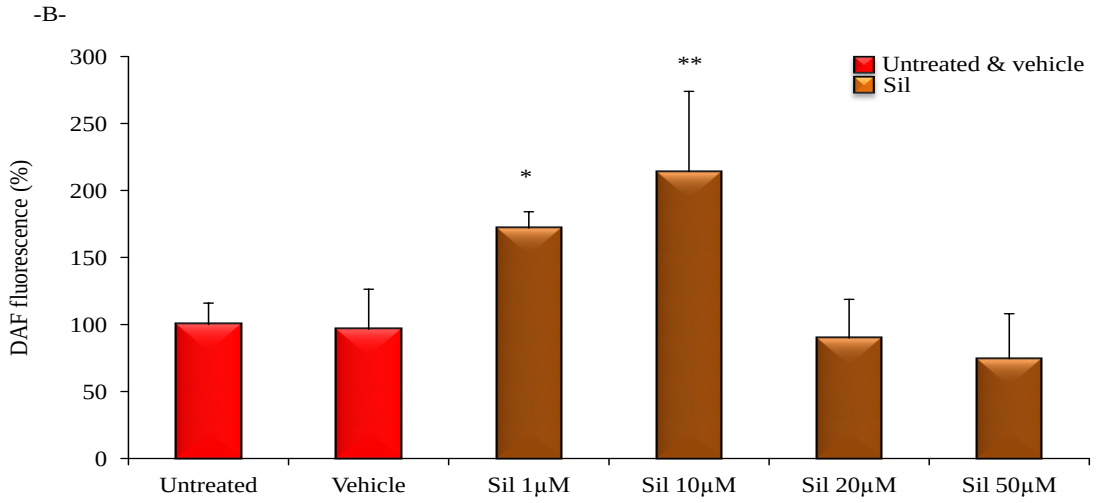

Figure 3.14: Effect of Silibinin on NO generation of EBs. (A) NO generation upon treatment of EBs (6-day-old) with different concentrations (1-50µM) of Silibinin. Silibinin significantly induced NO generation at concentrations of 1µM and10µM compared to the untreated control. NO production was assessed by use of the fluorescence dye DAF-FM. The bar represents 300µm. **(B)** Graphical representation of NO generation at different doses of Silibinin. Shown are the means $\pm$ SD of n = 4 experiments with 20 EBs in each experiment, * $P \leq 0.05$, ** $P \leq 0.01$.

3.9. Enhancement of eNOS phosphorylation upon Silibinin treatment of EBs

In the vascular system, the main NOS isoform is eNOS / NOS III (Shaul, 2002; Liu and Huang, 2008). Therefore, eNOS phosphorylation was assessed following 5, 10, 15, 30, 60 and 120 min pre-incubation with Silibinin (10µM) by western blot assays in 6-day-old EBs. Our data showed that eNOS phosphorylation was significantly up-regulated within 30 min after Silibinin treatment compared to the untreated control (figure 3.15).

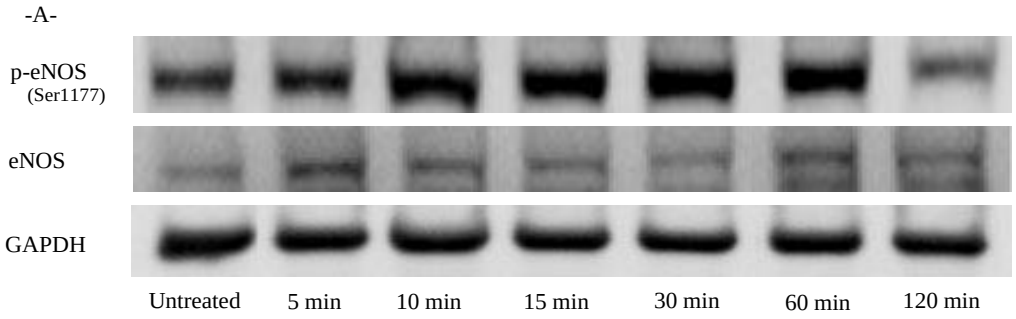

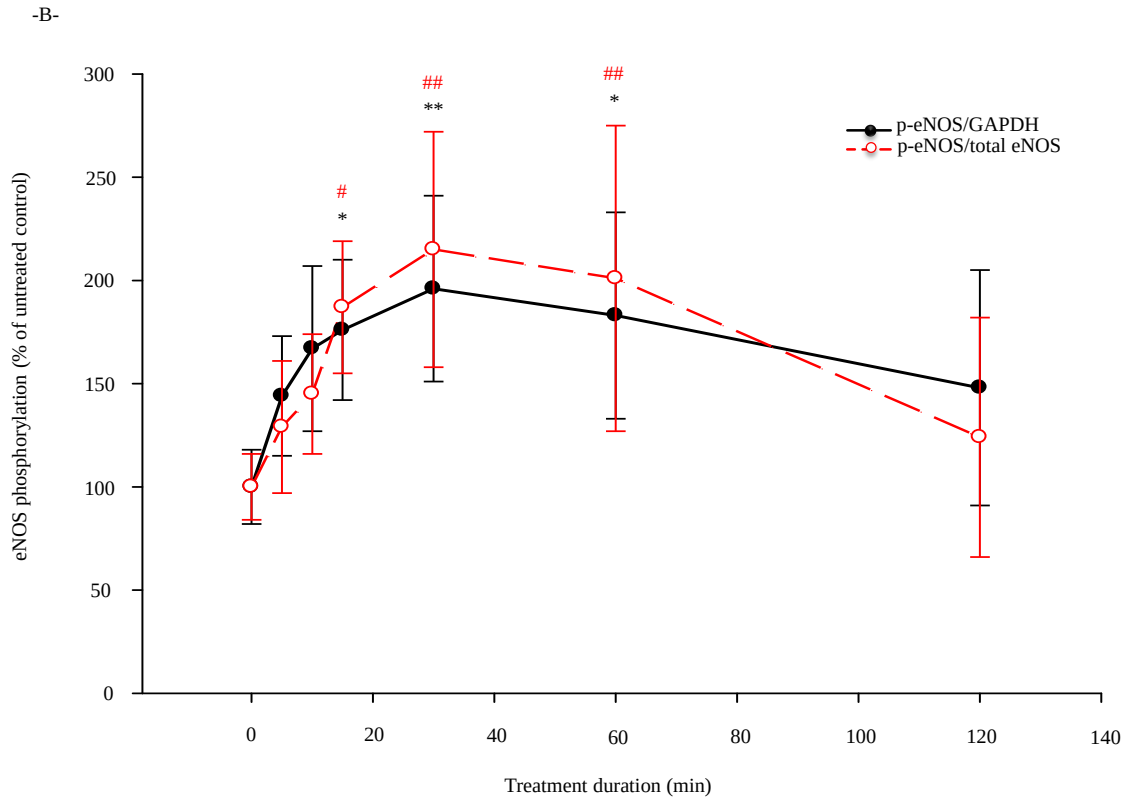

Figure 3.15: Phosphorylation of eNOS upon treatment of EBs with Silibinin (10µM). **(A)** Representative western blot using a phospho eNOS-specific antibody. GAPDH was used as house-keeping protein. The bar chart in **(B)** shows the means ± SD of n = 5 experiments for eNOS phosphorylation to GAPDH and eNOS phosphorylation to total eNOS. * $P \leq 0.05$, ** $P \leq 0.01$, # $P \leq 0.05$, ## $P \leq 0.01$.

3.10. Inhibition of eNOS by L-NAME

3.10.1. Effect of the eNOS inhibitor L-NAME on Silibinin-induced NO generation

To confirm that NO was generated through eNOS, 5-day-old EBs were treated either with the NOS inhibitor L-NAME (100µM) alone, with Silibinin (10µM) alone or with a combination of both, and compared with untreated controls. NO was assessed using the NO indicator DAF-FM. Upon L-NAME treatment NO generation upon Silibinin treatment was completely abolished, indicating that NO production was due to stimulation of eNOS by Silibinin (figure 3.16).

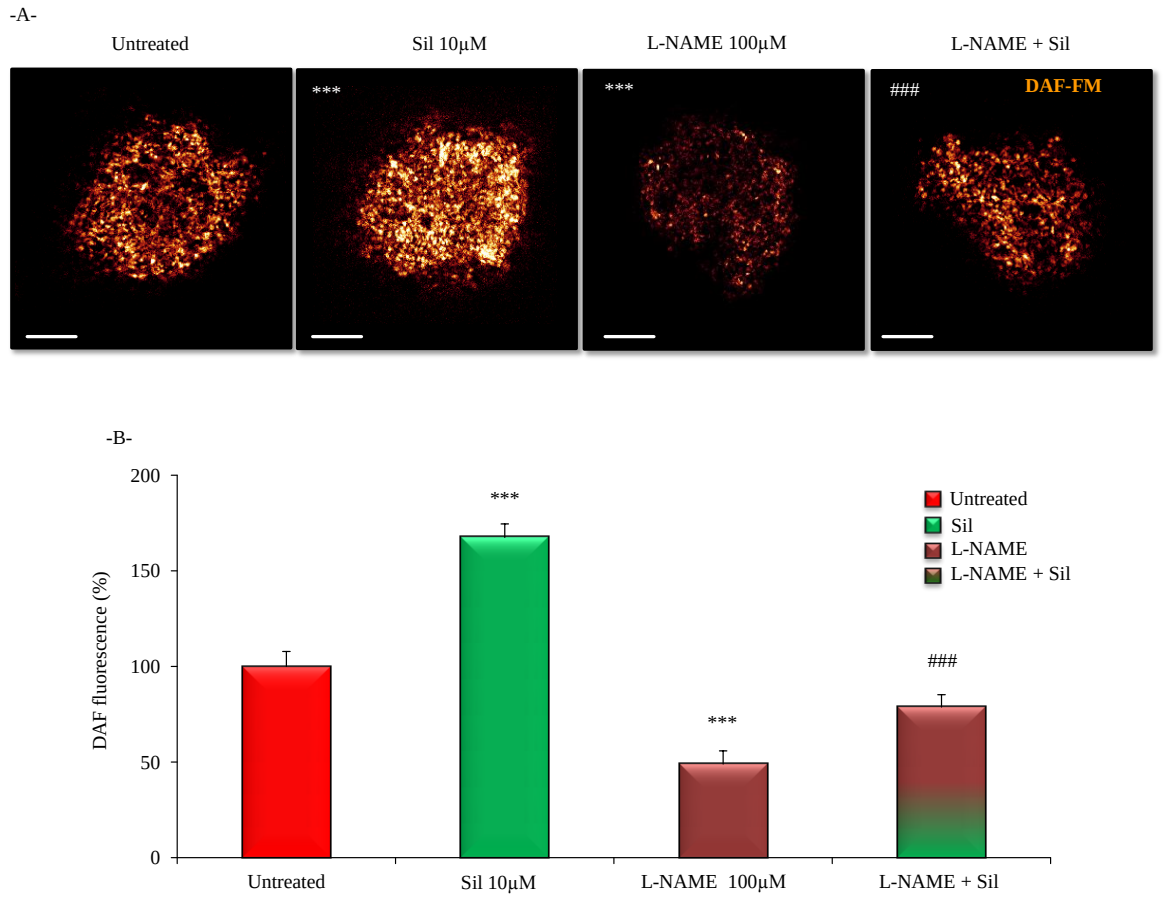

Figure 3.16: Inhibition of Silibinin-induced NO generation by the NOS inhibitor L-NAME (100µM). (A) Confocal images show representative EBs displaying DAF fluorescence. The bar represents 300µm. The bar chart in **(B)** shows the means ± SD of n = 5 experiments. *** $P \leq 0.001$ significantly different to the untreated control, ### $P \leq 0.001$ significantly different to Silibinin alone.

3.10.2. Effect of the eNOS inhibitor L-NAME on Silibinin-induced eNOS phosphorylation

The effect of L-NAME on NO generation may be due to inhibition of eNOS phosphorylation. To address this point 6-day-old EBs were pre-treated for 2h with L-NAME (100µM) and subsequently with Silibinin (10µM). It was apparent that the Silibinin-induced eNOS phosphorylation was completely abolished in the presence of L-NAME. Notably, L-NAME treatment alone decreased eNOS activity below the control

value, indicating that NO generation occurs in EBs during cardiovascular differentiation processes (figure 3.17).

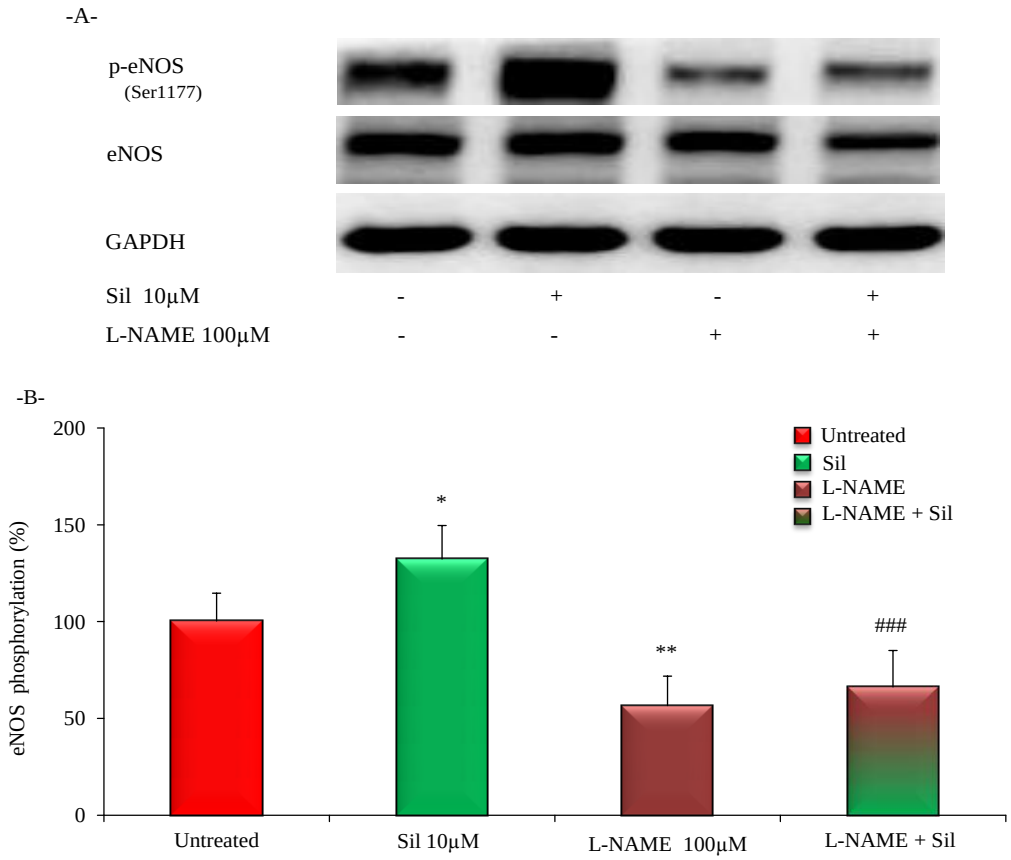

Figure 3.17: Blocking of Silibinin-induced eNOS phosphorylation by the NOS inhibitor L-NAME. (A) Western blot analysis of eNOS phosphorylation which was detected by using an anti p-eNOS (ser1177) antibody. GAPDH was used as house-keeping protein. L-NAME (100µM) completely blocked eNOS phosphorylation compared to the untreated control as well as in the Silibinin-treated sample **(B)** The bar chart shows the means $\pm$ SD of n = 4 experiments * $P \leq 0.05$, ** $P \leq 0.01$ significantly different to the untreated control, ### $P \leq 0.001$ significantly different to Silibinin alone.

3.10.3. Effect of the eNOS inhibitor L-NAME on Silibinin-induced vasculogenesis of mouse ES cells

The data of the present study demonstrate that Silibinin efficiently raises NO in EBs through activation of eNOS. Since vasculogenesis is well known to require NO generation (Milosevic et al., 2010), 3-day-old EBs were treated until day 10 of cell culture every 24h

with Silibinin (10µM), L-NAME (100µM) or a combination of Silibinin with L-NAME. At day 10, EBs were fixed, staining against CD31 antibody and analyzed by confocal laser microscopy. L-NAME significantly decreased branching points in the absence of Silibinin compared to the untreated control and abolished the stimulation of vasculogenesis achieved upon Silibinin treatment, thus supporting the notion that Silibinin-stimulated vasculogenesis by elevating intracellular NO levels (figure 3.18).

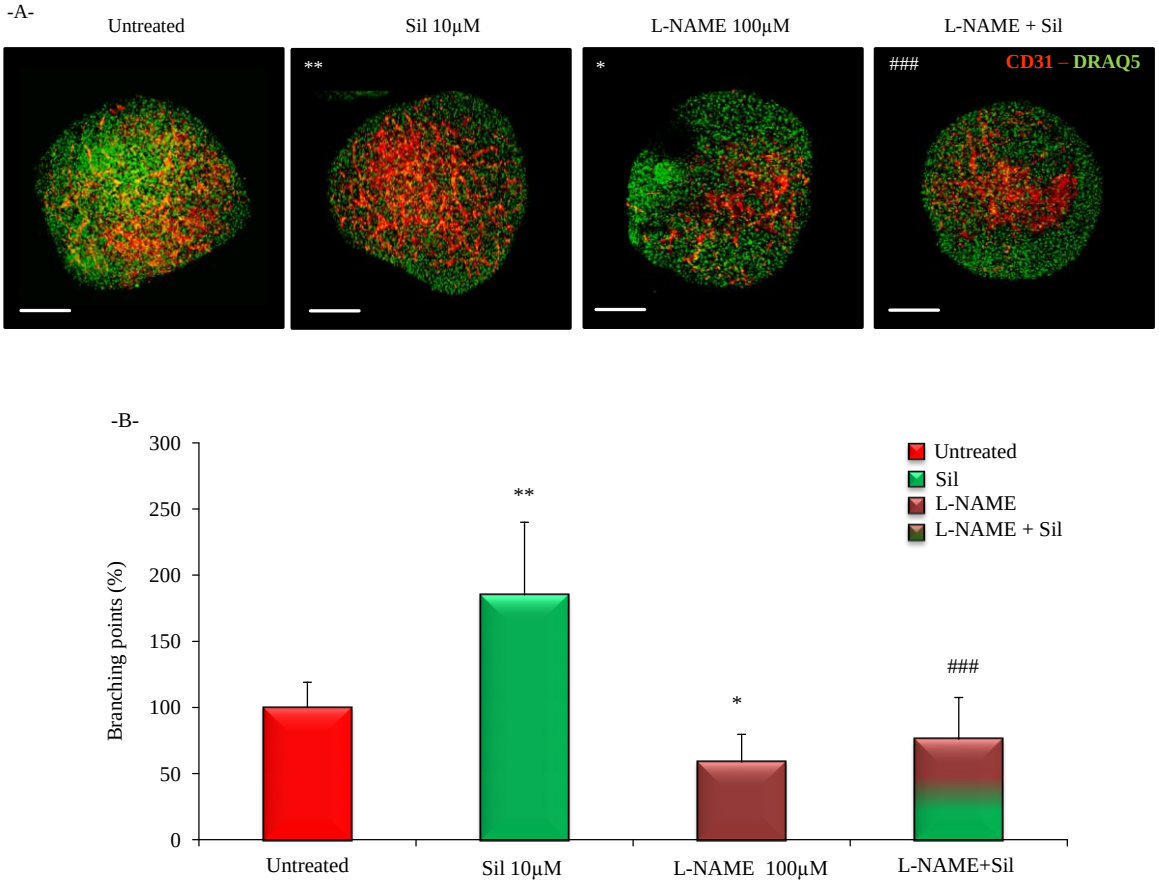

Figure 3.18: Inhibition of Silibinin-induced vasculogenesis upon NOS inhibition by L-NAME. (A) The increase in branching points observed upon Silibinin (10µM) treatment was completely abolished in the presence of L-NAME (100µM). Shown are representative EBs treated from day 3 to day 10 of differentiation. CD31 staining (red), DRAQ5-positive cell nuclei (green). The bar represents 300µm. **(B)** Bar chart showing the means ± SD of n = 5 experiments * $P \leq 0.05$, ** $P \leq 0.01$ significantly different to the untreated control, ### $P \leq 0.001$ significantly different to Silibinin alone.

3.10.4. Effect of the NOS inhibitor L-NAME on Silibinin-stimulated VEGFR2 and VE-Cadherin expression

The data of the present study demonstrate that L-NAME inhibited branching point formation (see 3.10.3). To investigate whether L-NAME would affect the expression of VEGFR2 and VE-Cadherin, EBs were treated from day 3 to day 10 of differentiation with Silibinin (10µM) either in presence or absence L-NAME (100µM). At day 10, EBs were collected and protein extraction was performed. As expected Silibinin-stimulated expression of the endothelial cell progenitor marker VEGFR2 and the endothelial marker VE-Cadherin, while the observed effect was completely abolished by L-NAME (figure 3.19).

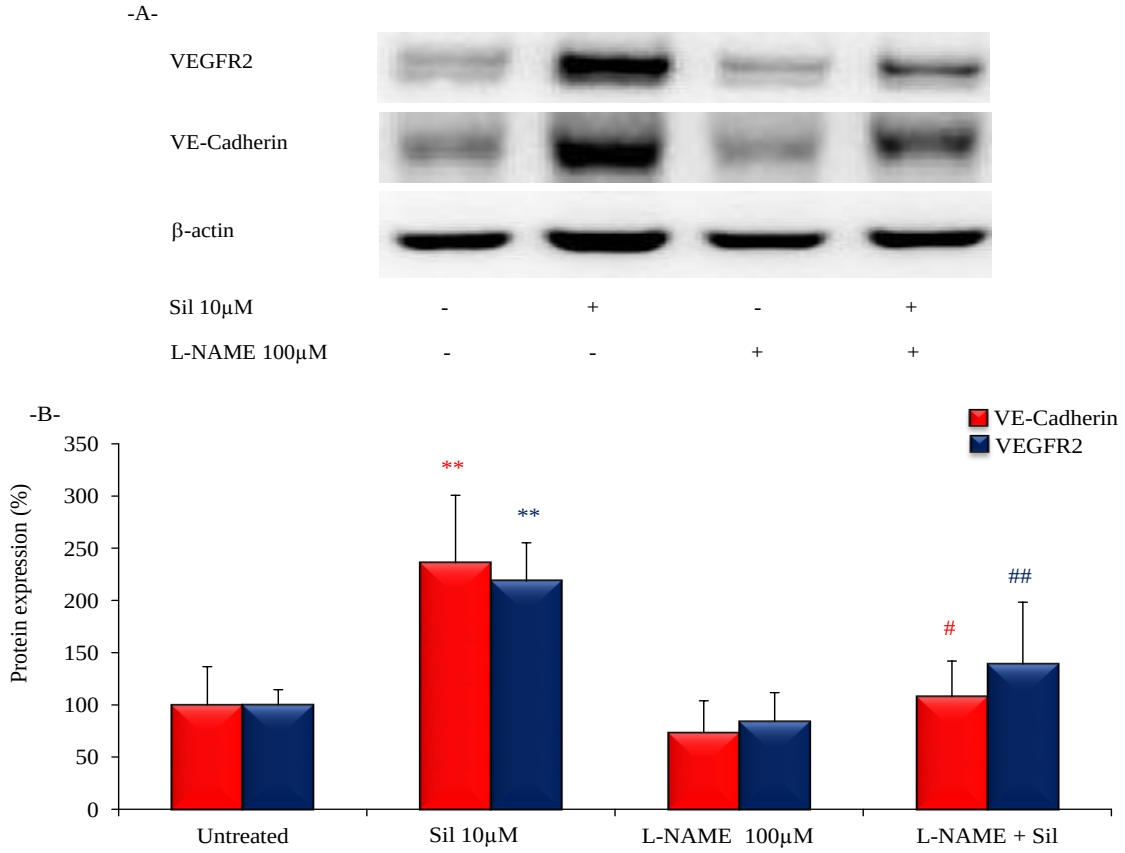

Figure 3.19: Inhibition of VEGFR2 and VE-Cadherin by L-NAME upon Silibinin treatment. (A) Representative western blot for VEGFR2 and VE-Cadherin. β-actin was used as house-keeping protein. At day 10, protein extraction and western blot analysis were performed. Silibinin significantly increased the expression of VEGFR2 and VE-Cadherin. Moreover, pre-treatment with L-NAME (100µM) decreased VEGFR2 and VE-Cadherin expression. **(B)** The bar chart shows the means $\pm$ SD of n = 4 experiments; ** $P \leq 0.01$ significantly different to the untreated control, # $P \leq 0.05$, ## $P \leq 0.01$ significantly different to Silibinin alone.

3.11. Induction of STAT3, AKT, PI3K and VEGFR2 phosphorylation upon treatment of EBs with Silibinin

To examine, whether Silibinin could regulate STAT3, PI3K/AKT and VEGFR2 activation, 6-day-old differentiating EBs were treated with 10µM Silibinin and STAT3, AKT, PI3K and VEGFR2 phosphorylation was analyzed using phospho-specific antibodies. 6-day-old differentiating EBs were treated with Silibinin (10µM), collected at 5, 10, 15, 30, 60 and 120 min and analyzed by western blot technique (figure 3.20). Indeed Silibinin (10µM) transiently increased the phosphorylation of STAT3, AKT and PI3K following 5 - 10 min of treatment. The activation remained on an elevated plateau for more than 30 min and reached control values approximately 60 min after Silibinin application. Significant activation of VEGFR2 was observed following 30 min of Silibinin treatment.

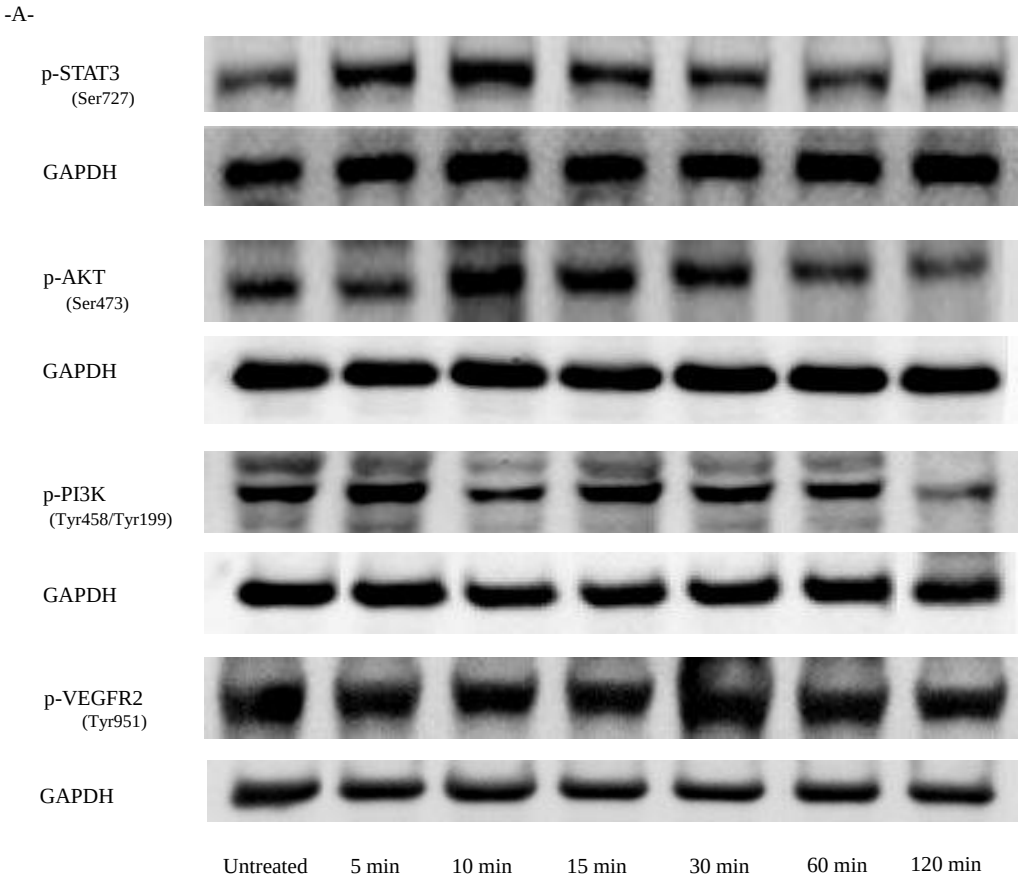

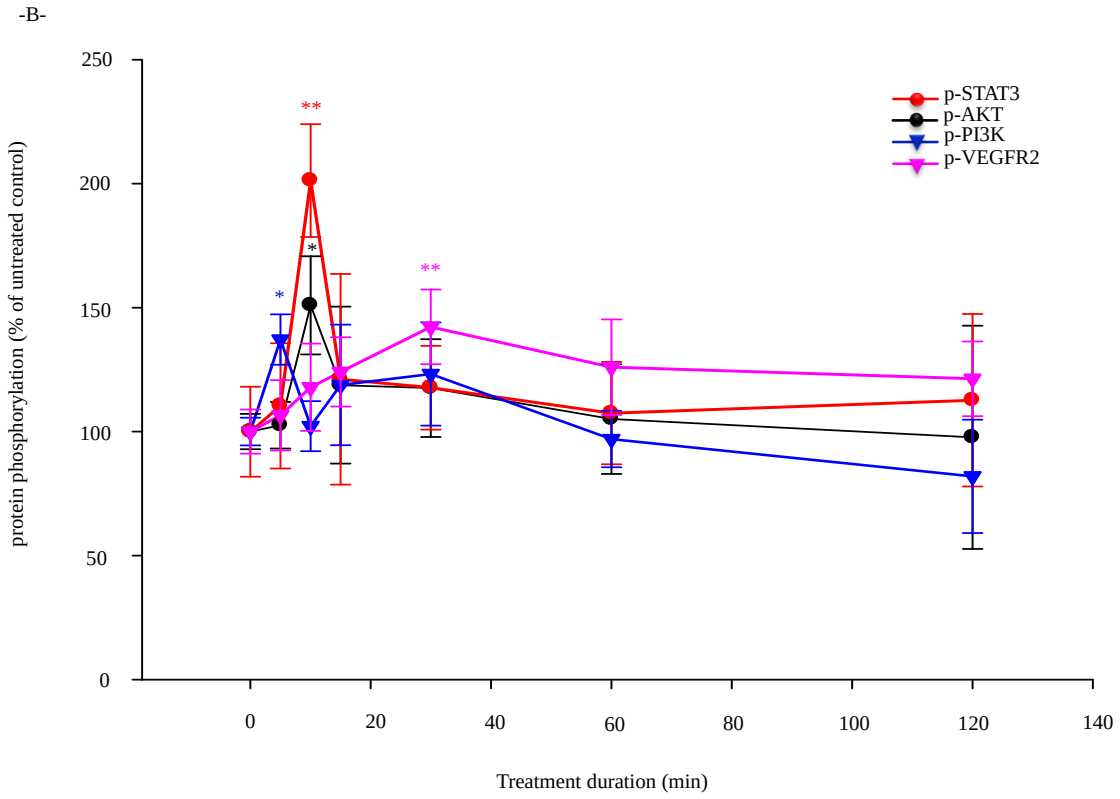

Figure 3.20: Phosphorylation of STAT3, AKT, PI3K and VEGFR2 upon Silibinin treatment. **(A)** Representative western blots for activation of phospho-STAT3 (ser727), phospho-AKT (ser473), phospho-PI3K and phospho-VEGFR2. GAPDH was used as house-keeping protein. Silibinin treatment of EBs was performed on day 6 of cell differentiation. **(B)** The bar chart shows the means $\pm$ SD of n = 4 experiments for phospho-STAT3, n = 5 experiments and n = 4 experiments for phospho-AKT and phospho-PI3K respectively, and n = 5 experiments for phospho-VEGFR2. * $P \leq 0.05$, ** $P \leq 0.01$ significantly different to the untreated control.

3.12. Effect of pharmacological inhibitors on STAT3, AKT and PI3K activation upon Silibinin treatment of EBs

The data of the present study show that Silibinin treatment activates angiogenesis-related signalling pathways, e.g. STAT3, AKT or PI3K. These protein kinases may be activated independently or may interfere in a common signal transduction cascade. We therefore applied specific pharmacological inhibitors, i.e. the PI3K inhibitor LY294002 (5µM), the STAT3 inhibitor Stattic (7µM), or the AKT inhibitor AKT inhibitor VIII (5µM) and assessed activation of PI3K (figure 3.21), STAT3 (figure 3.22), or AKT (figure 3.23). Our

data demonstrated that the PI3K inhibitor LY294002 abolished the activation of PI3K, STAT3 and AKT. Upon co-treatment of Silibinin with Stattic, activation of STAT3 and AKT was inhibited. Treatment with Silibinin in presence of AKT inhibitor VIII inhibited AKT as well as STAT3 phosphorylation. Taken together these data demonstrate that Silibinin activates PI3K, STAT3 and AKT in the same signal transduction cascade.

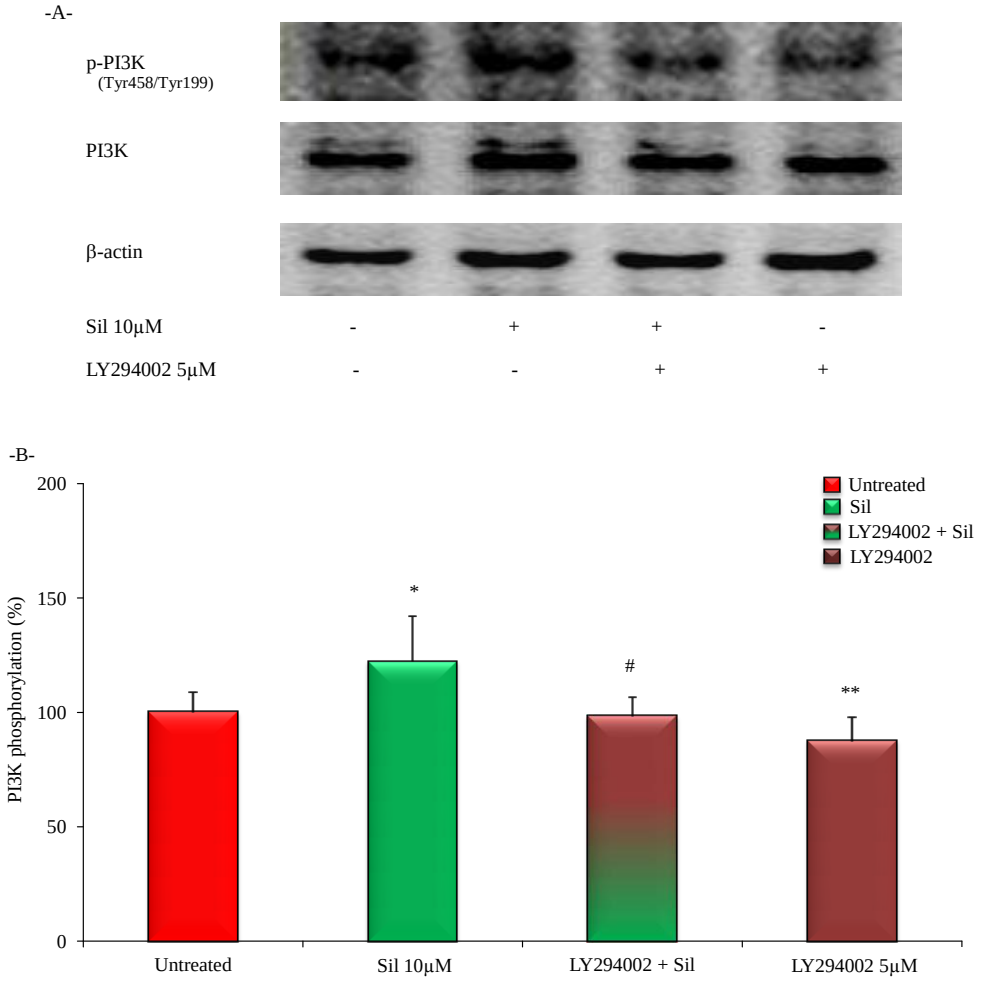

Figure 3.21: Effect of PI3K inhibitor LY294002 on Silibinin-mediated PI3K phosphorylation. (A) Representative western blots showing PI3K activation by use of a phospho-specific anti-PI3K antibody in the presence or absence of PI3K inhibitor LY294002 (5µM). β-actin was used as house-keeping protein. **(B)** The bar chart shows the means $\pm$ SD of n = 6 experiments for LY294002. * $P \leq 0.05$, ** $P \leq 0.01$ significantly different to the untreated control, # $P \leq 0.05$ significantly different to Silibinin alone.

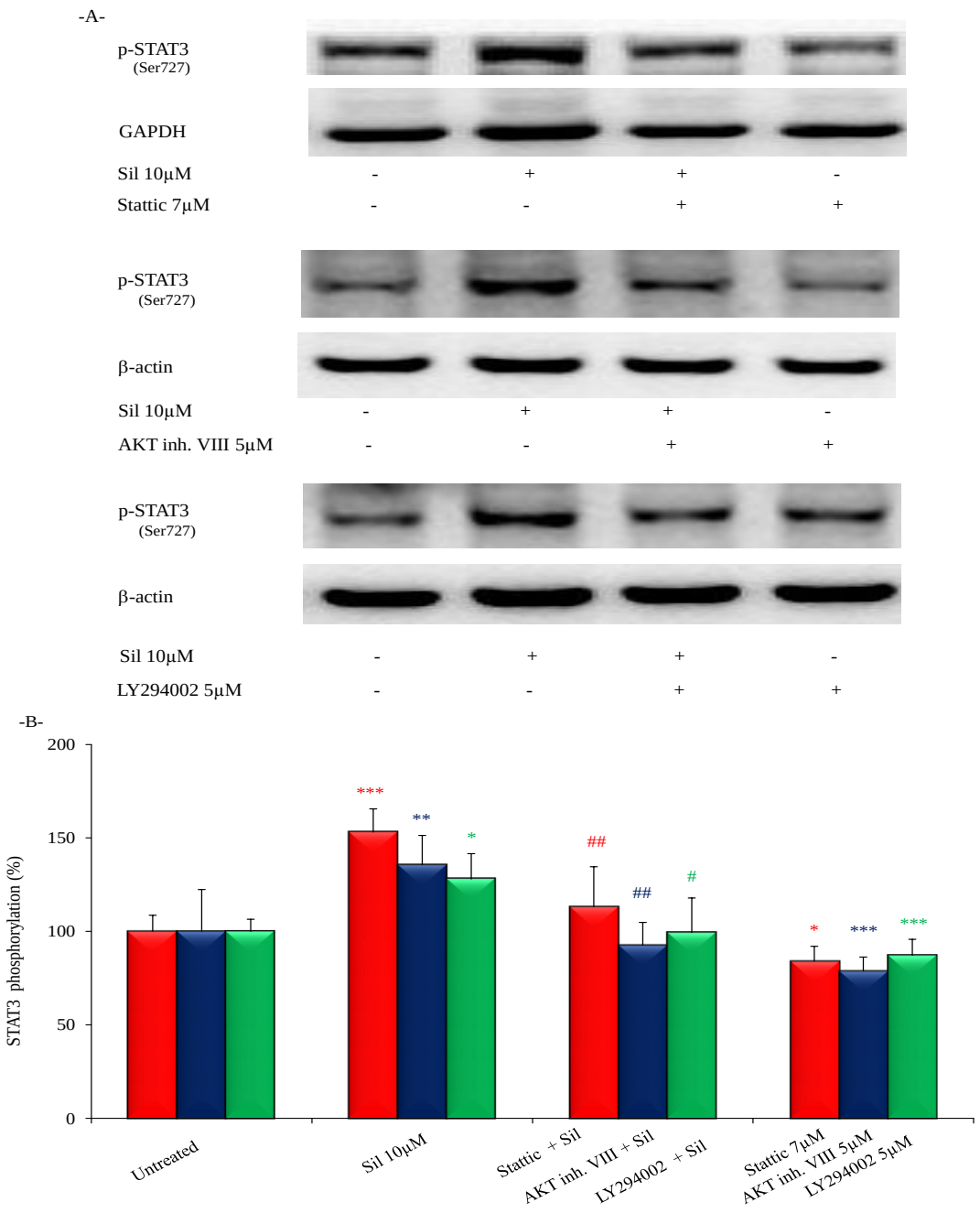

Figure 3.22: Effect of STAT3 inhibitor Stattic, AKT inhibitor AKT VIII and PI3K inhibitor LY294002 on Silibinin-mediated STAT3 phosphorylation. (A) Representative western blots showing STAT3 activation by use of a phospho-specific anti-STAT3 antibody in the presence or absence of either STAT3 inhibitor Stattic (7µM) (upper panel), AKT inhibitor VIII (5µM) (middle panel) or PI3K inhibitor LY294002 (5µM) (lower panel). GAPDH and β-actin were used as house-keeping proteins. **(B)** Bar chart showing the means $\pm$ SD of n = 4 experiments for Stattic (red bars), n = 5 experiments for AKT inhibitor VIII (blue bars), and n = 5 experiments for LY294002 (green bars). * $P \leq 0.05$, ** $P \leq 0.01$, *** $P \leq 0.001$ significantly different to the untreated control, # $P \leq 0.05$, ## $P \leq 0.01$ significantly different to Silibinin alone.

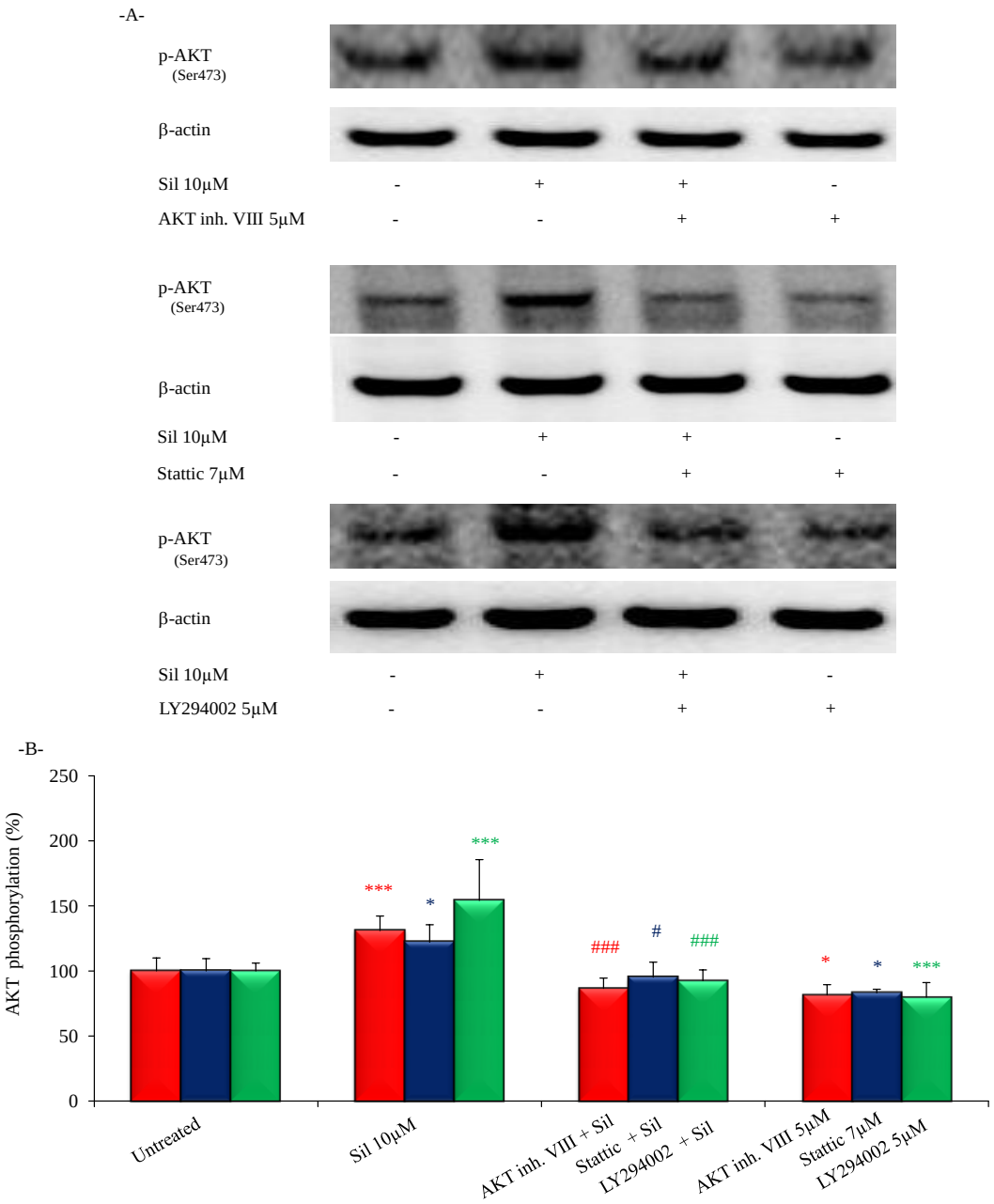

Figure 3.23: Effect of AKT inhibitor AKT VIII, STAT3 inhibitor Stattic and PI3K inhibitor LY294002 on Silibinin-mediated AKT phosphorylation. (A) Representative western blots showing AKT activation by use of a phospho-specific anti-AKT antibody in the presence or absence of either AKT inhibitor VIII (5µM) (upper panel), STAT3 inhibitor Stattic (7µM) (middle panel) or PI3K inhibitor LY294002 (5µM) (lower panel). β-actin was used as house-keeping protein. **(B)** The bar chart shows the means ± SD of n = 5 experiments for AKT inhibitor VIII (red bars), n = 4 experiments for Stattic (blue bars) and n = 6 experiments for LY294002 (green bars). * $P \leq 0.05$, *** $P \leq 0.001$ significantly different to the untreated control, # $P \leq 0.05$, ### $P \leq 0.001$ significantly different to Silibinin alone.

3.13. Effect of STAT3 inhibitor Stattic, AKT inhibitor AKT inhibitor VIII and PI3K inhibitor LY294002 on Silibinin-mediated NO generation

To interpret the potential involvement of Stattic, AKT inhibitor VIII and LY294002 in Silibinin-induced NO generation of mouse ES cells, 6-day-old EBs were assessed for NO generation by utilizing the NO-sensitive fluorescence indicator DAF-FM (1µM). Generation of NO in EBs increased upon Silibinin (10µM) treatment, Stattic (7µM), AKT inhibitor (5µM) and LY294002 (5µM) treatment strongly inhibited NO production (figure 3.24). These results indicate that the NO production following Silibinin treatment is occurring downstream of the STAT3 and PI3K/AKT signaling pathways.

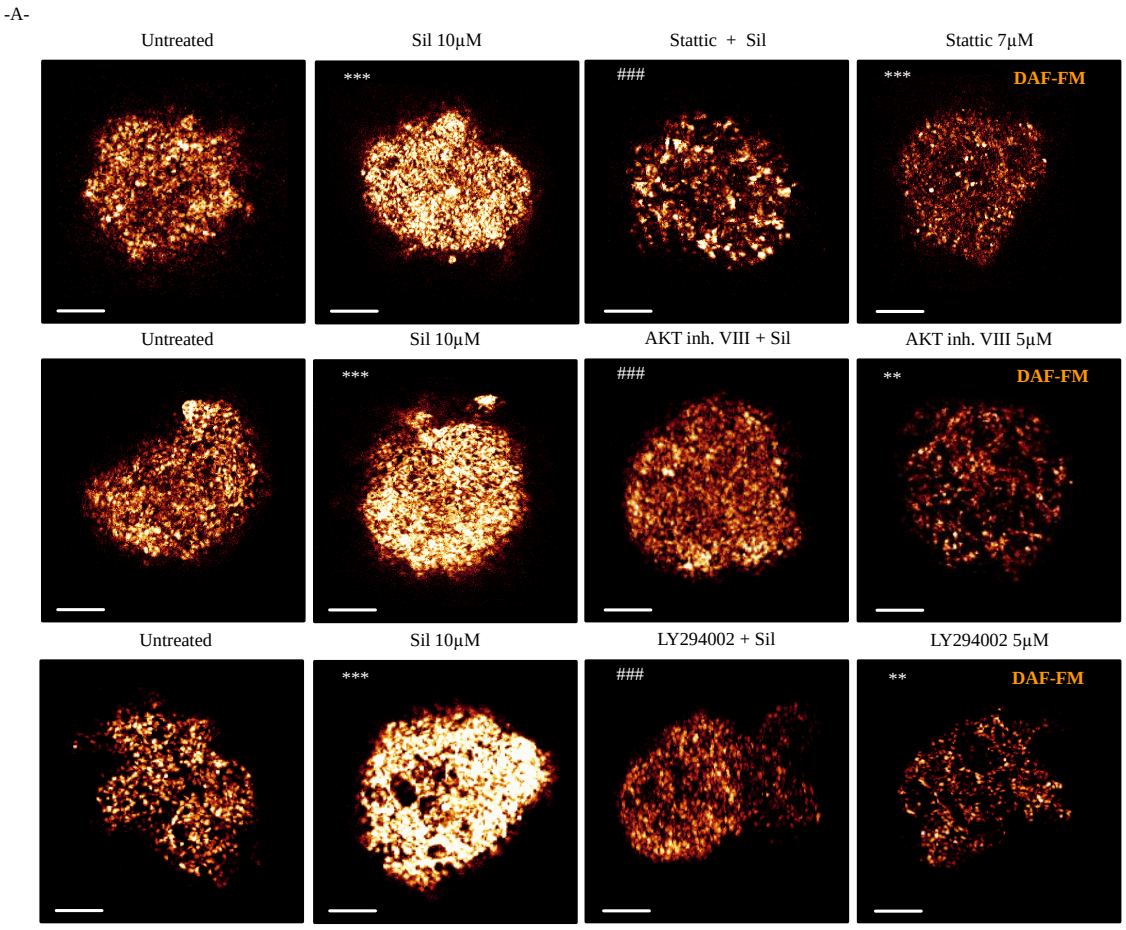

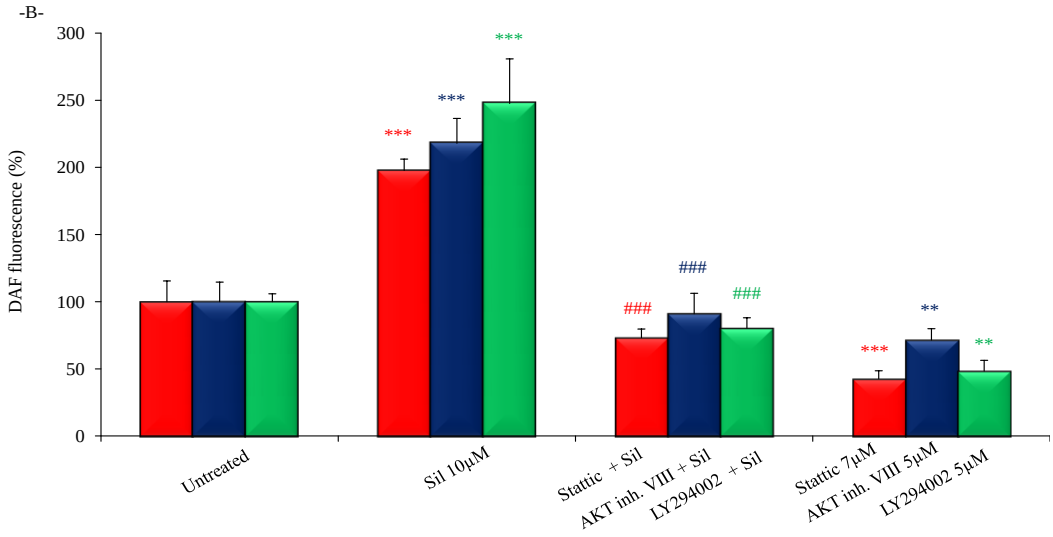

Figure 3.24: Effect of STAT3 inhibitor Stattic, AKT inhibitor AKT inhibitor VIII and PI3K inhibitor LY294002 on Silibinin-mediated NO generation. (A) Representative 6-day-old DAF stained EBs which either remained untreated or were treated with Silibinin (Sil) in the absence or presence of either STAT3 inhibitor Stattic (7µM), AKT inhibitor AKT inhibitor VIII (5µM) or PI3K inhibitor LY294002 (5µM). EBs were stained with fluorescence indicator DAF-FM and the elevation DAF fluorescence was assessed. The bar represents 300µm. **(B)** The bar chart represents the means ± SD of n = 4 experiments for Stattic (red bars), n = 4 experiments for AKT inhibitor (blue bars) and n = 5 experiments for LY294002 (green bars), ** $P \leq 0.01$, *** $P \leq 0.001$ significantly different to the untreated control, ### $P \leq 0.001$ significantly different to Silibinin alone.

3.14. Effect of STAT3 inhibitor Stattic, AKT inhibitor AKT inhibitor VIII and PI3K inhibitor LY294002 on Silibinin-induced eNOS activation

To explain whether the signaling cascade elicited upon Silibinin treatment affected the activity of eNOS, the effects of STAT3 inhibitor Stattic, AKT inhibitor AKT inhibitor VIII and PI3K inhibitor LY294002 on the phosphorylation of eNOS was investigated. 6-day-old EBs were treated with Silibinin (10µM) for 30 min in absence and presence of Stattic (7µM), AKT inhibitor AKT inhibitor VIII (5µM) and PI3K inhibitor LY294002 (5µM) (figure 3.25). It was shown that inhibition of STAT3 and PI3K/AKT significantly inhibited the phosphorylation achieved with Silibinin, thus corroborating the data on NO generation and suggesting that NO was generated by eNOS.

-A-

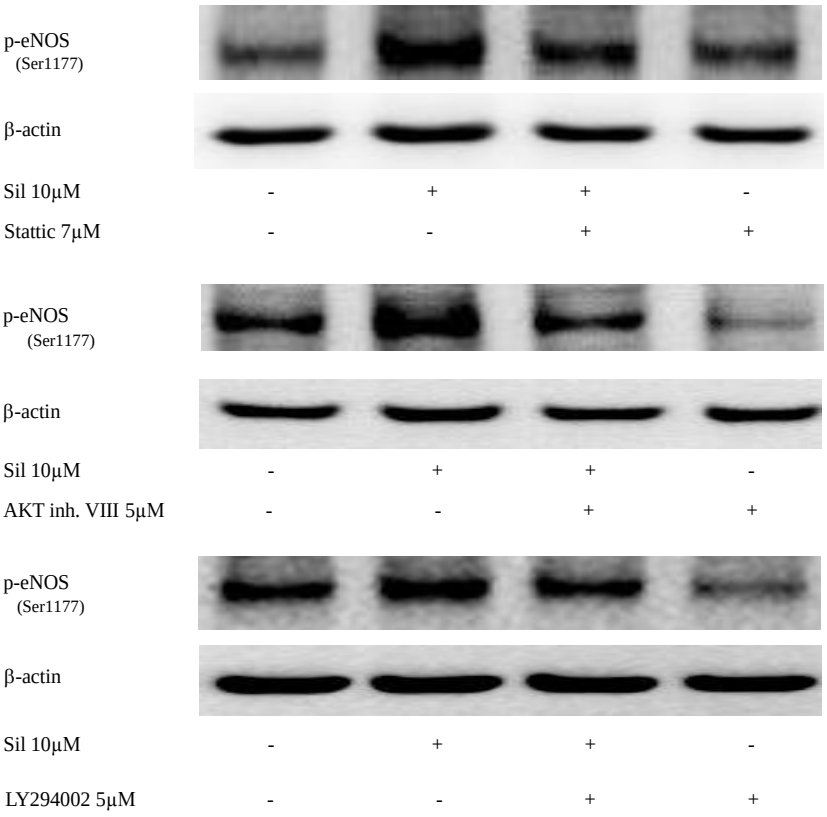
p-eNOS
(Ser1177)
β-actin
Sil 10μM - + + -
Stattic 7μM - - + +
p-eNOS
(Ser1177)
β-actin
Sil 10μM - + + -
AKT inh. VIII 5μM - - + +
p-eNOS
(Ser1177)
β-actin
Sil 10μM - + + -
LY294002 5μM - - + +

-B-

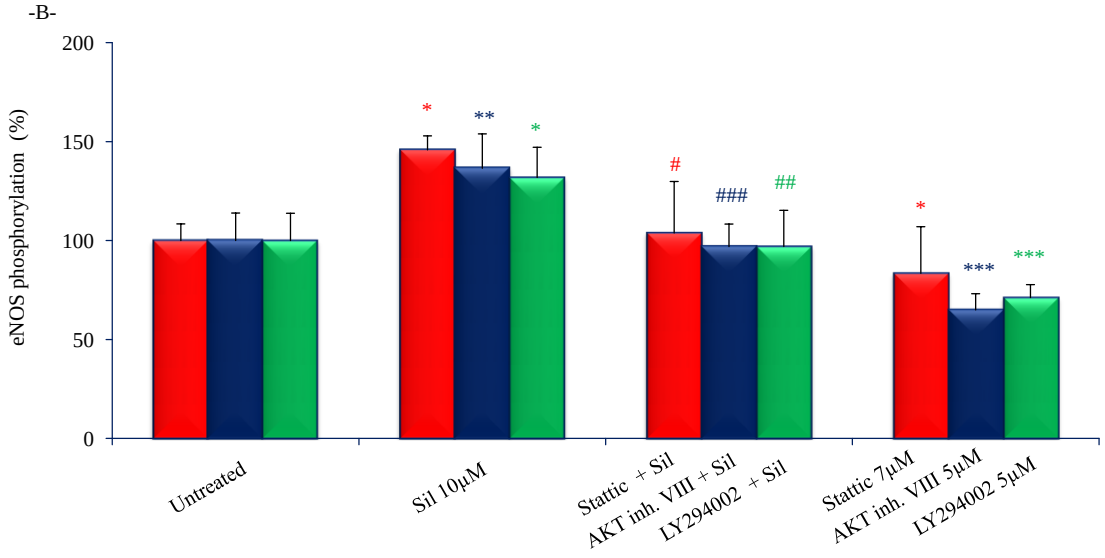
eNOS phosphorylation (%)
200
150
100
50
0
*
**
*
#
###
##
*
***
***
Untreated
Sil 10μM
Stattic + Sil
AKT inh. VIII + Sil
LY294002 + Sil
Stattic 7μM
AKT inh. VIII 5μM
LY294002 5μM

Figure 3.25: Inhibition of Silibinin-induced eNOS activation by STAT3 inhibitor Stattic, AKT inhibitor AKT inhibitor VIII and PI3K inhibitor LY294002 (A) Representative western blots of 6-day-old EBs showing eNOS activation by use of a phospho-specific anti-eNOS antibody in the presence or absence of either STAT3 inhibitor Stattic (7µM) (upper panel), AKT inhibitor VIII (5µM) (middle panel) or PI3K inhibitor LY294002 (5µM) (lower panel). β-actin was used as house-keeping protein. **(B)** Bar chart showing the means $\pm$ SD of n = 4 experiments for Stattic (red bars), n = 5 experiments for AKT inhibitor VIII (blue bars) and n = 5 experiments for LY294002 (green bars). * $P \leq 0.05$, ** $P \leq 0.01$, *** $P \leq 0.001$ significantly different to the untreated control, # $P \leq 0.05$, ## $P \leq 0.01$, ### $P \leq 0.001$ significantly different to Silibinin alone.

3.15. Effect of STAT3 inhibitor Stattic, AKT inhibitor AKT inhibitor VIII and PI3K inhibitor LY294002 on Silibinin-induced vasculogenesis

Differentiation of mouse ES cells to vascular-like structures positive for the vascular marker CD31/PECAM-1 occurs within 10 days (Wartenberg et al., 2006). To unravel participation of STAT3, AKT and PI3K in vasculogenesis initiated by Silibinin, EBs were treated for 7 days, i.e. from day 3 to day 10 of cell culture with Silibinin (10µM) alone in the absence or presence of Stattic (7µM), AKT inhibitor VIII (5µM) or LY294002 (5µM). Silibinin treatment resulted in a significant increase in vascular-like structures as compared to the untreated control, which was totally abrogated upon Stattic, AKT inhibitor VIII and LY294002 treatment (figure 3.26).

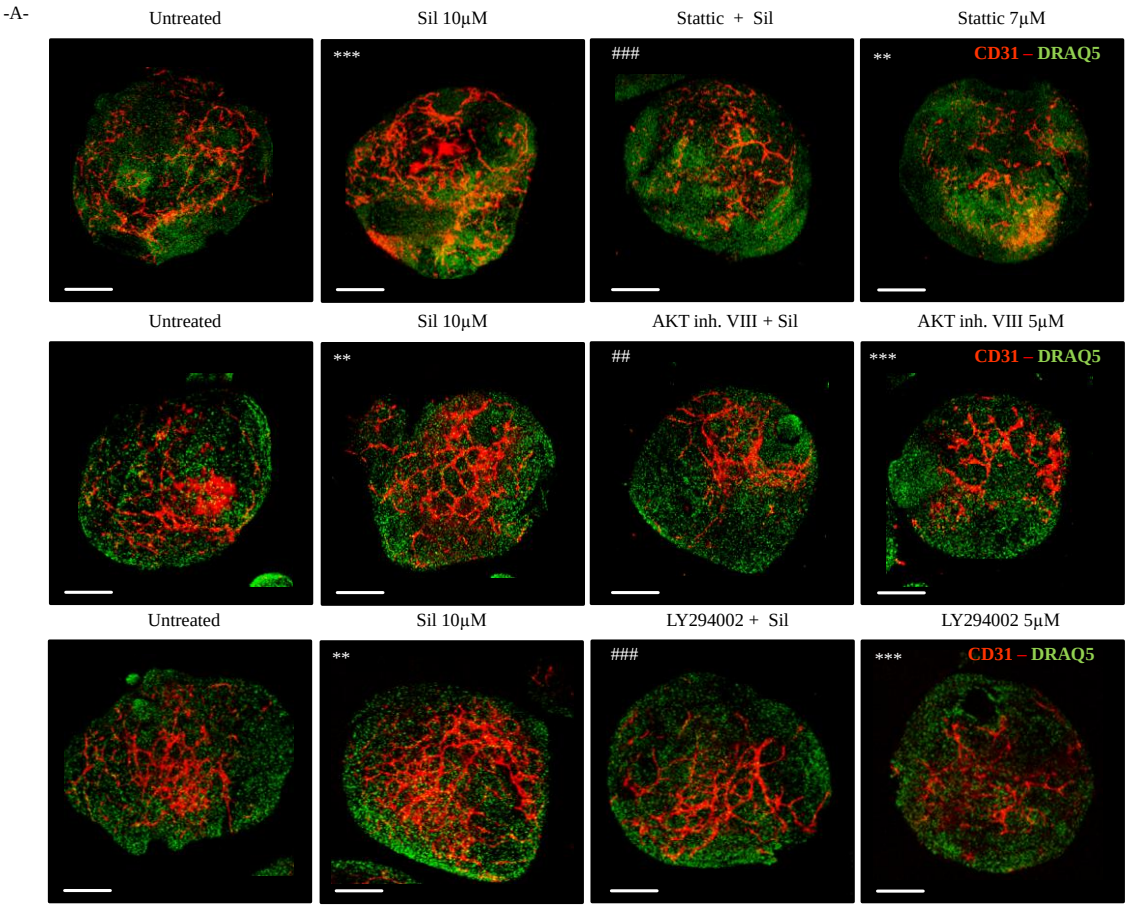
-A-
Untreated
Sil 10µM
Stattic + Sil
Stattic 7µM
CD31 – DRAQ5
***
###
**
Untreated
Sil 10µM
AKT inh. VIII + Sil
AKT inh. VIII 5µM
CD31 – DRAQ5
**
##
***
Untreated
Sil 10µM
LY294002 + Sil
LY294002 5µM
CD31 – DRAQ5
**
###
***

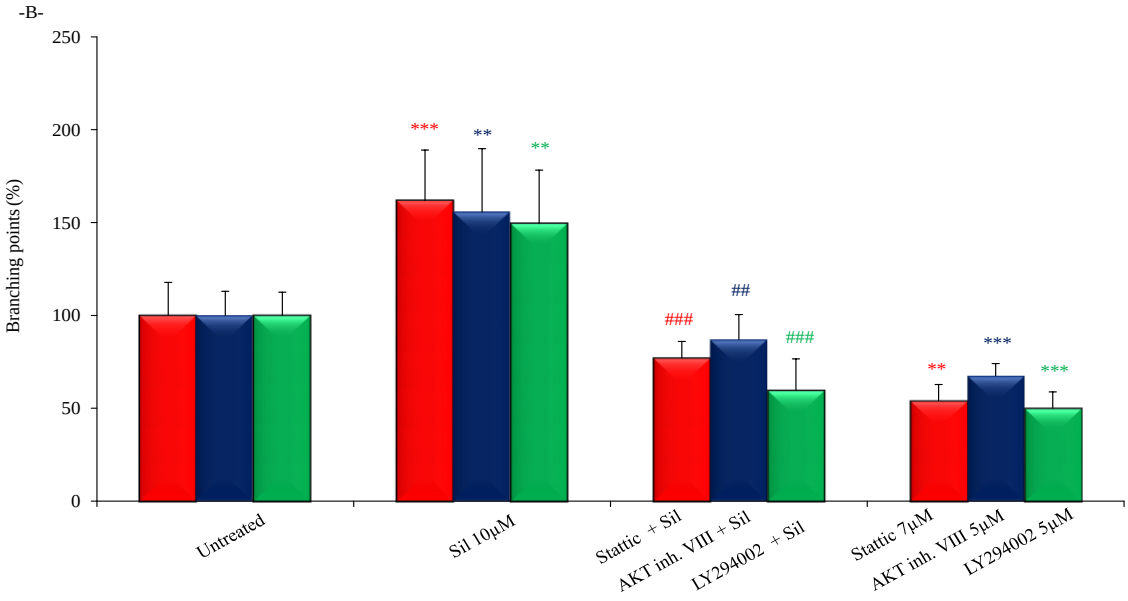
-B-
Branching points (%)
250
200
150
100
50
0
***
**
**
###
##
###
**
***
***
Untreated
Sil 10µM
Stattic + Sil
AKT inh. VIII + Sil
LY294002 + Sil
Stattic 7µM
AKT inh. VIII 5µM
LY294002 5µM

Figure 3.26: Effect of STAT3 inhibitor Stattic, AKT inhibitor AKT inhibitor VIII and PI3K inhibitor LY294002 on Silibinin-induced vascular-like structures. (A) Representative EBs differentiated for 10 days with treatments as indicated. On day 10, EBs were collected fixed, stained against endothelial marker CD31/PECAM-1 and examined by confocal microscopy. CD31 staining (red), DRAQ5-positive cell nuclei (green). Silibinin treatment significantly increased the number of branching points which was completely reversed by Stattic (7µM), AKT inhibitor VIII (5µM) and LY294002 (5µM). The bar represents 300µm. **(B)** Graphic representation of the effects of Stattic, AKT inhibitor VIII and LY294002. The bar chart shows the means $\pm$ SD for n = 5 experiments Stattic (red bars), n = 4 experiments AKT inhibitor VIII (blue bars) and n = 5 experiments LY294002 (green bars). ** $P \leq 0.01$, *** $P \leq 0.001$ significantly different to the untreated control, ## $P \leq 0.01$, ### $P \leq 0.001$ significantly different to Silibinin alone.

3.16. Effect of STAT3 inhibitor Stattic, AKT inhibitor AKT inhibitor VIII and PI3K inhibitor LY294002 on vasculogenic protein expression

Vasculogenesis is regulated in ES cells by activation of VEGFR2 and the transcription factor HIF-1α (Koch and Claesson-Welsh, 2012; Zimna and Kurpisz, 2015). To investigate, whether the signaling pathways identified in the present study to regulate vascular structure formation by Silibinin, affected vasculogenic protein expression, we treated differentiating EBs either with STAT3 inhibitor Stattic (7µM), AKT inhibitor AKT inhibitor VIII (5µM) or PI3K inhibitor LY294002 (5µM) and investigated VEGFR2 (figure 3.27) as well as HIF-1α (figure 3.28) expression. In additional experiments we investigated VE-Cadherin expression (figure 3.29), which is an endothelium-specific protein required for proper vasculogenesis (Gory-Fauré et al., 1999). Indeed the data of the present study clearly demonstrate that inhibition of STAT3 and PI3K/AKT abolished the stimulation of VEGFR2, HIF-1α as well as VE-Cadherin expression by Silibinin. Taken together these data corroborate our previous data on a stimulation of vasculogenesis by Silibinin and demonstrate that basic vasculogenic signaling pathways via VEGFR2 and HIF-1α are involved in this process.

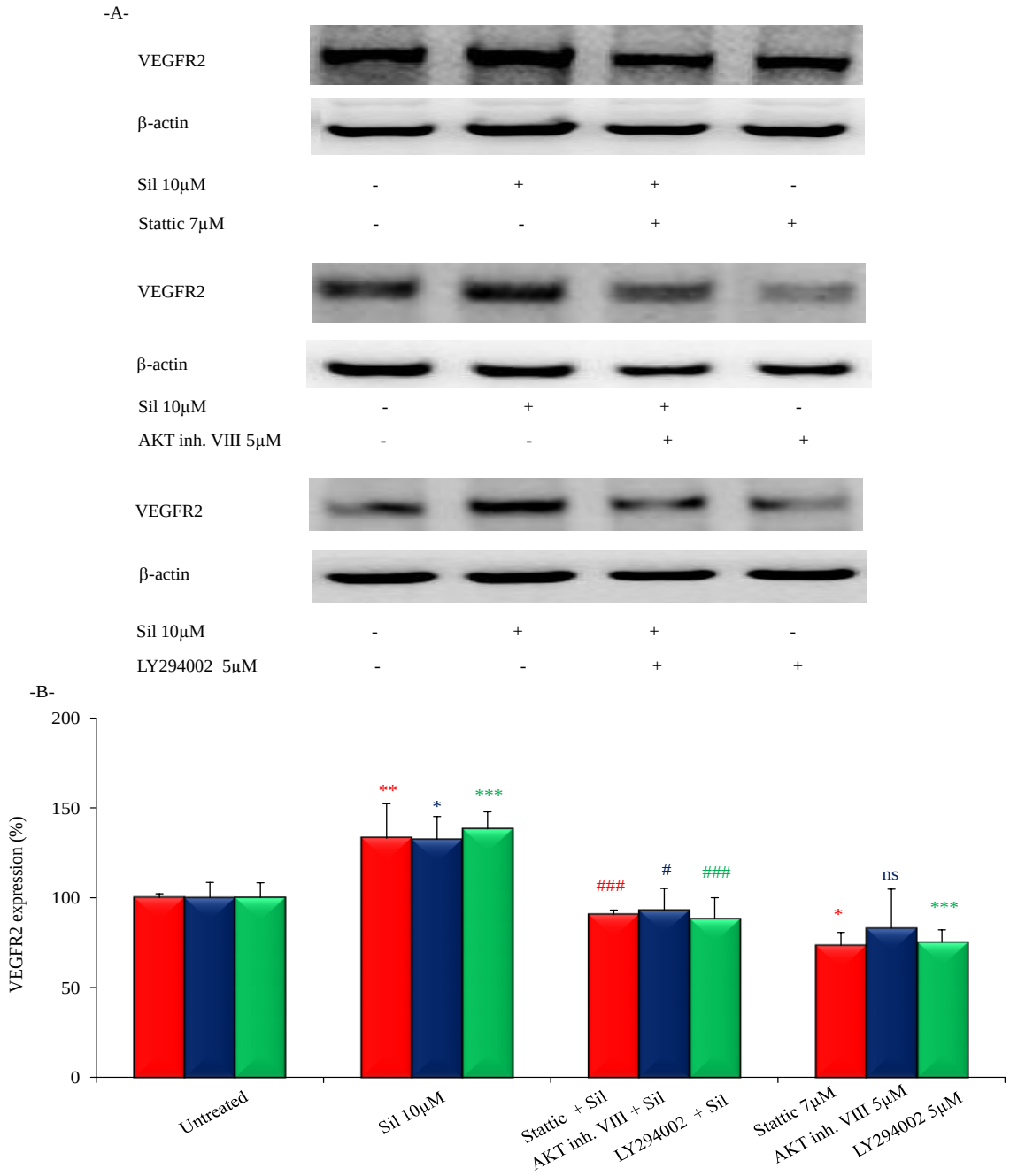

Figure 3.27: Effect of STAT3 inhibitor Stattic, AKT inhibitor AKT inhibitor VIII and PI3K inhibitor LY294002 on Silibinin-induced VEGFR2 expression. (A) Representative western blots for VEGFR2. EBs were treated from day 3-10 with Silibinin (10µM), in the absence or presence of either Stattic (7µM) (upper panel), AKT inhibitor VIII (5µM) (middle panel) and LY294002 (5µM) (lower panel). β-actin was used as house-keeping protein. **(B)** The bar chart shows the means ± SD of n = 4 experiments for Stattic (red bars), n = 4 experiments for AKT inhibitor VIII (blue bars) and n= 6 experiments for LY294002 (green bars). * $P \leq 0.05$, ** $P \leq 0.01$, *** $P \leq 0.001$ significantly different to the untreated control, # $P \leq 0.05$, ### $P \leq 0.001$ significantly different to Silibinin alone and ns (non-significant), $P \geq 0.05$.

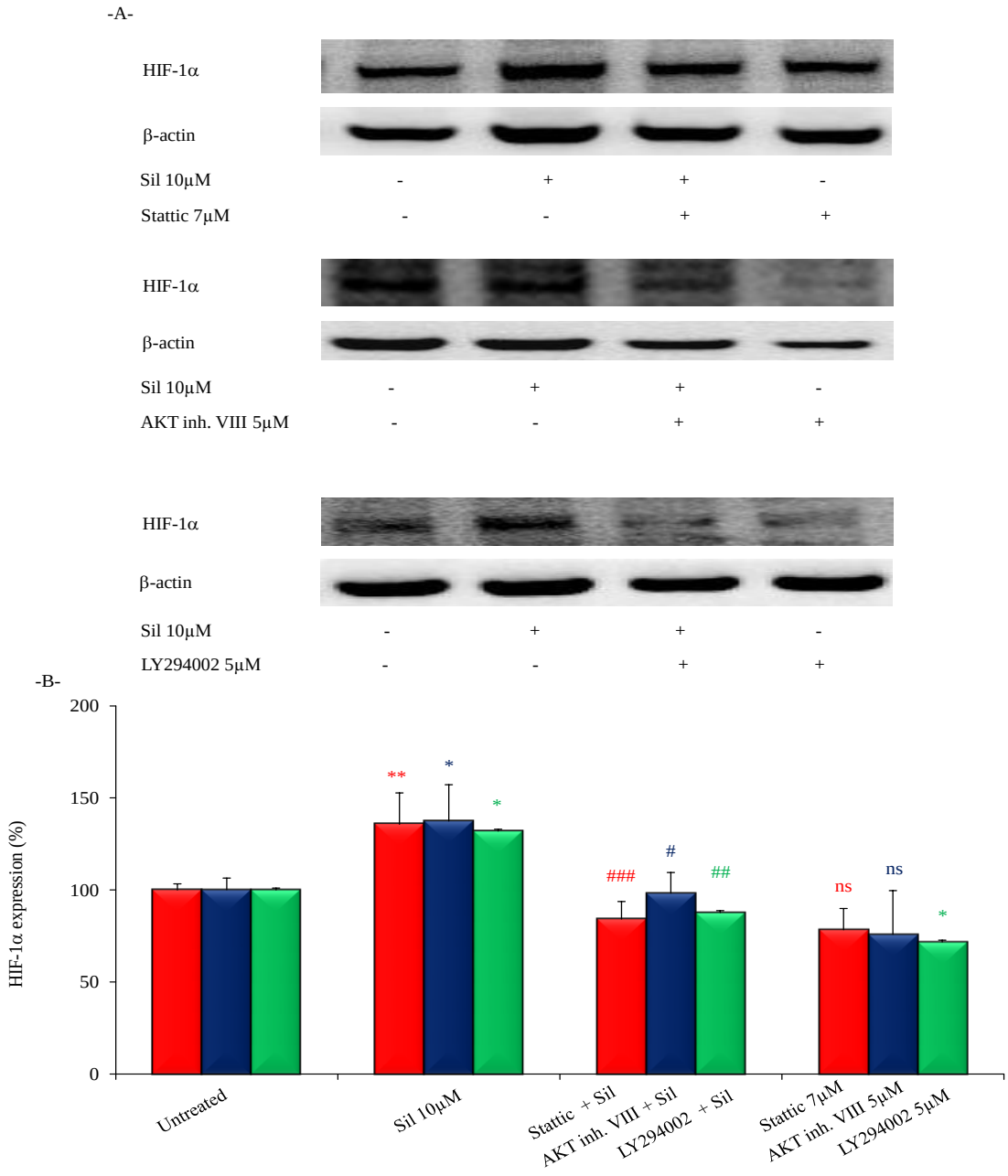

Figure 3.28: Effect of STAT3 inhibitor Stattic, AKT inhibitor AKT inhibitor VIII and PI3K inhibitor LY294002 on Silibinin-induced HIF-1α expression. (A) Representative western blots for HIF-1α. EBs were treated from day 3-10 with Silibinin (10µM), in the absence or presence of either Stattic (7µM) (upper panel), AKT inhibitor VIII (5µM) (middle panel) or LY294002 (5µM) (lower panel). β-actin was used as house-keeping protein. **(B)** The bar chart show the means ± SD of n = 4 experiments for Stattic (red bars), n = 4 experiments for AKT inhibitor VIII (blue bars) and n = 6 experiments for LY294002 (green bars). * $P \leq 0.05$, ** $P \leq 0.01$, significantly different to the untreated control, # $P \leq 0.05$, ## $P \leq 0.01$, ### $P \leq 0.001$, significantly different to Silibinin alone and ns (non-significant), $P \geq 0.05$.

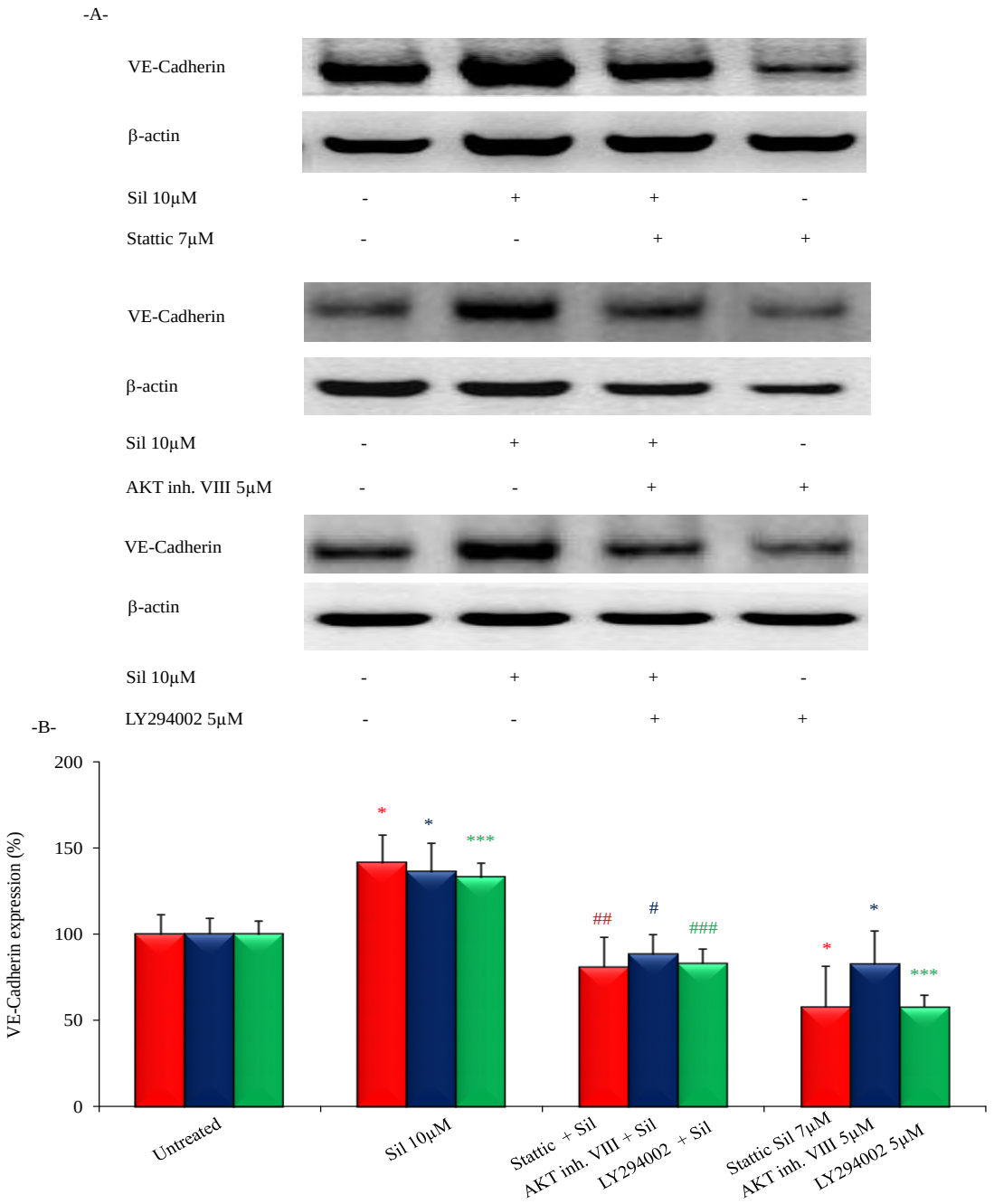

Figure 3.29: Effect of STAT3 inhibitor Stattic, AKT inhibitor AKT inhibitor VIII and PI3K inhibitor LY294002 on Silibinin-induced VE-Cadherin expression. (A) Representative western blots for VE-Cadherin expression. EBs were treated from day 3-10 with Silibinin (10µM), in the absence or presence of either Stattic (7µM) (upper panel), AKT inhibitor VIII (5µM) (middle panel) or LY294002 (5µM) (lower panel). β-actin was used as house-keeping protein. **(B)** The bar chart shows the means $\pm$ SD of n = 4 experiments for Stattic (red bars), n = 4 experiments for AKT inhibitor VIII (blue bars) and n = 6 experiments for LY294002 (green bars). * $P \leq 0.05$, *** $P \leq 0.001$ significantly different to the untreated control, # $P \leq 0.05$, ## $P \leq 0.01$, ### $P \leq 0.001$ significantly different to Silibinin alone.

3.17. Stimulation of leukocyte differentiation upon Silibinin treatment

Previous studies demonstrated that leukopoiesis is closely associated to vasculogensis of mouse ES cells (Sharifpanah et al., 2015). Our data (shown in 3.6) have demonstrated that Silibinin stimulates vasculogenesis in mouse ES cells, therefore we investigated whether Silibinin would likewise induce leukocyte differentiation, EBs were treated from day 3 to day 14 with increasing doses of Silibinin (1µM, 10µM, 20µM and 50µM). On day 14 the expression of the leukocyte marker CD45, the leukocyte integrin marker CD18 and the macrophage marker CD68 (Suga et al., 2014; Hutterer et al., 2015; Kaser-Eichberger et al., 2016) were assessed by immunohistochemistry. Maximum effects were achieved with 10µM Silibinin which increased the number of $CD45^+$, $CD18^+$ and $CD68^+$ cells per total cells from 8 $\pm$ 1 % to 14 $\pm$ 2 %, 9 $\pm$ 1 % to 14 $\pm$ 1 % and 11 $\pm$ 2 to 20 $\pm$ 6 %, respectively (figure 3.30 A, B, C and D). Taken together these results demonstrate that Silibinin not only increased vasculogenesis and NO generation but also up-regulated leukocyte differentiation of ES cells.

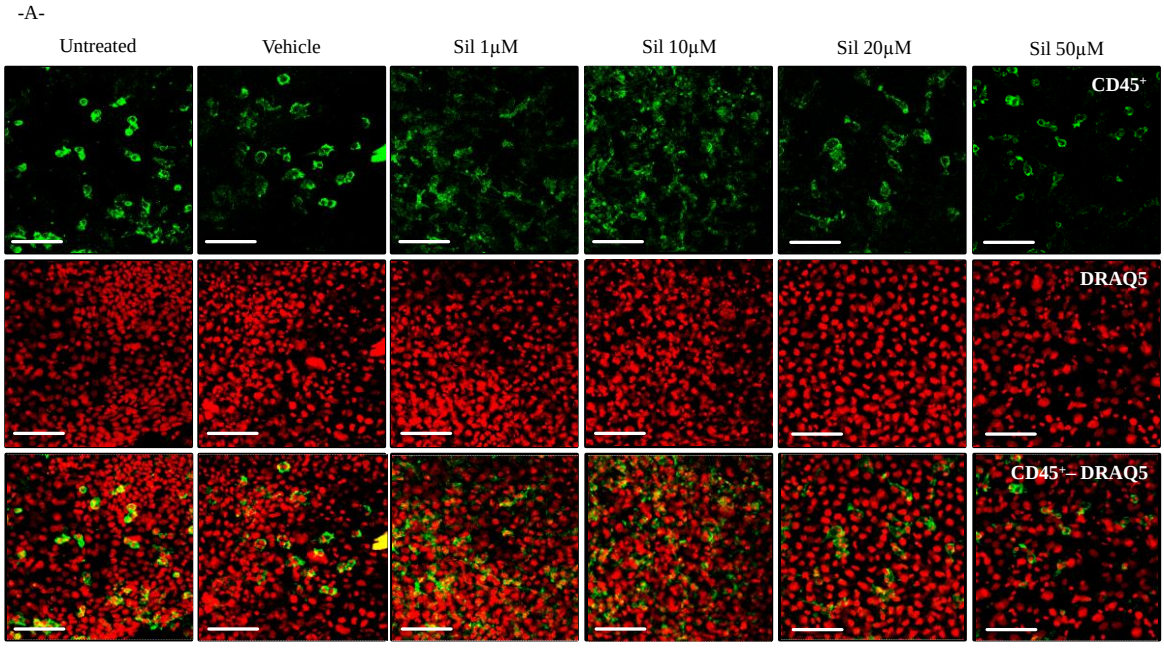

-B-

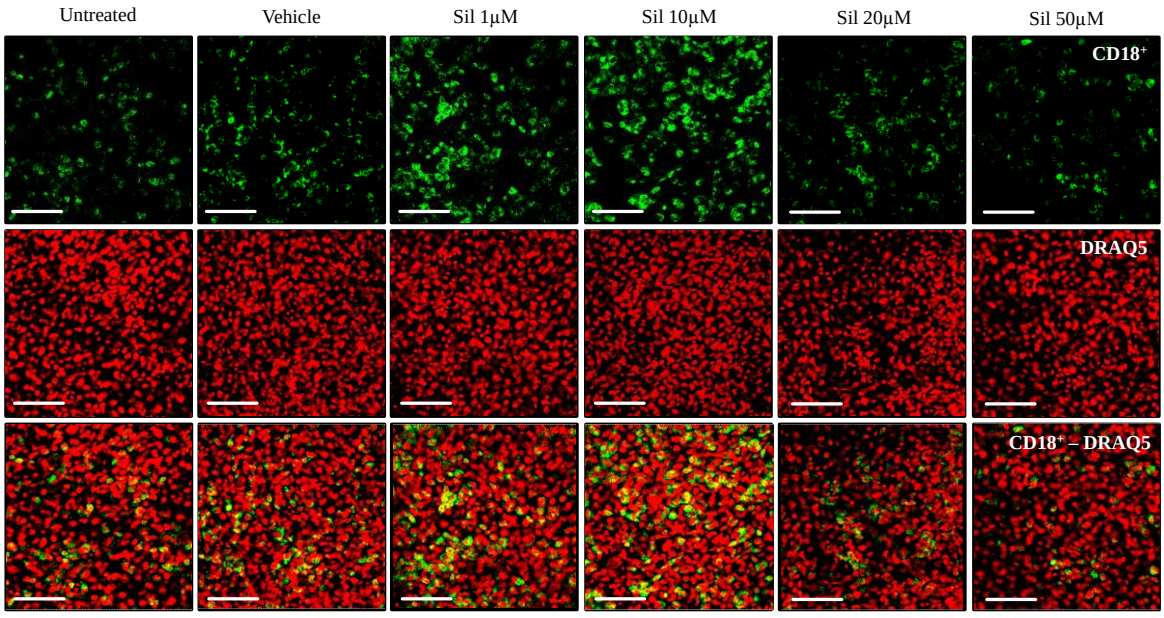
Untreated
Vehicle
Sil 1µM
Sil 10µM
Sil 20µM
Sil 50µM
CD18+
DRAQ5
CD18+ – DRAQ5

-C-

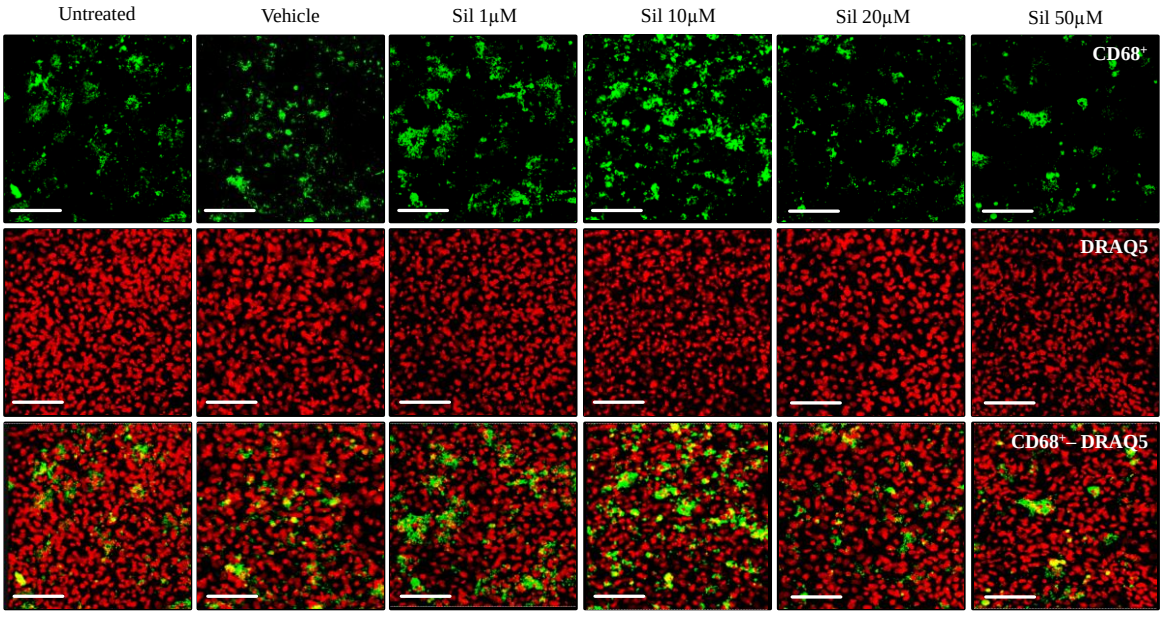
Untreated
Vehicle
Sil 1µM
Sil 10µM
Sil 20µM
Sil 50µM
CD68+
DRAQ5
CD68+– DRAQ5

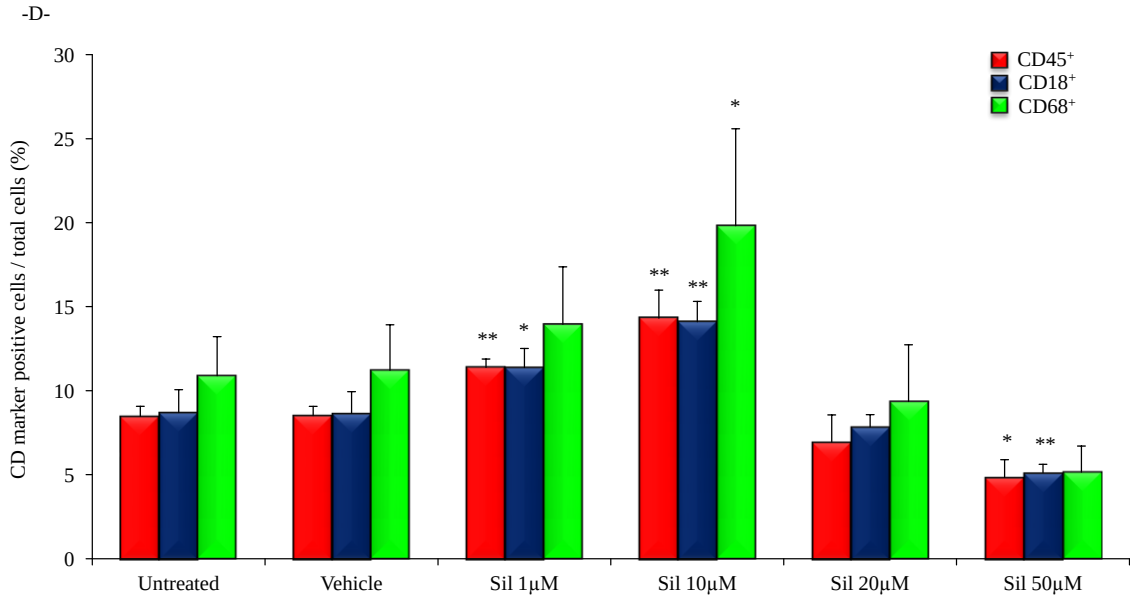

Figure 3.30 A-D: Effect of Silibinin on leukocyte differentiation of mouse ES cells. Immunohistochemical analysis of the number of $CD45^+$, $CD18^+$ and $CD68^+$ cells differentiated in ES cell derived EBs following treatment with Silibinin. **(A-C)** Representative images of outgrown EBs which were treated from day 3 to day 14 with Silibinin (1µM, 10µM, 20µM and 50µM) and subsequently labeled with antibodies against the leukocyte markers **(A)** CD45, **(B)** CD18 and **(C)** CD68 (upper panel, green). Total cells were labeled with DRAQ5 (middle panel, red). The lower panel shows overlay images of CD marker-positive and DRAQ5-labelled cells. The bar represents 75µm. **(D)** Quantitative analysis of the number of cells positive for CD45 (red bars, n = 4), CD18 (blue bars, n = 4) and CD68 (green bars, n = 3) in relation to the total (DRAQ5-positive) cell number (%) upon treatment with different concentrations of Silibinin.* $P \leq 0.05$, ** $P \leq 0.01$ significantly different to the untreated control.

3.18. Expression of leukocyte proteins upon Silibinin treatment

To confirm the observation that Silibinin increased the cell number of $CD45^+$, $CD18^+$ and $CD68^+$ cells, western blot experiments were performed to assess protein expression of CD markers. 3-day-old EBs were treated with different concentrations of Silibinin for 11 days. On day 14, EBs were collected for determination of protein expression (figure 3.31). Our data demonstrated that Silibinin treatment dose-dependently increased protein expression for CD45, CD18 and CD68 which was significant at a concentration of 10µM.

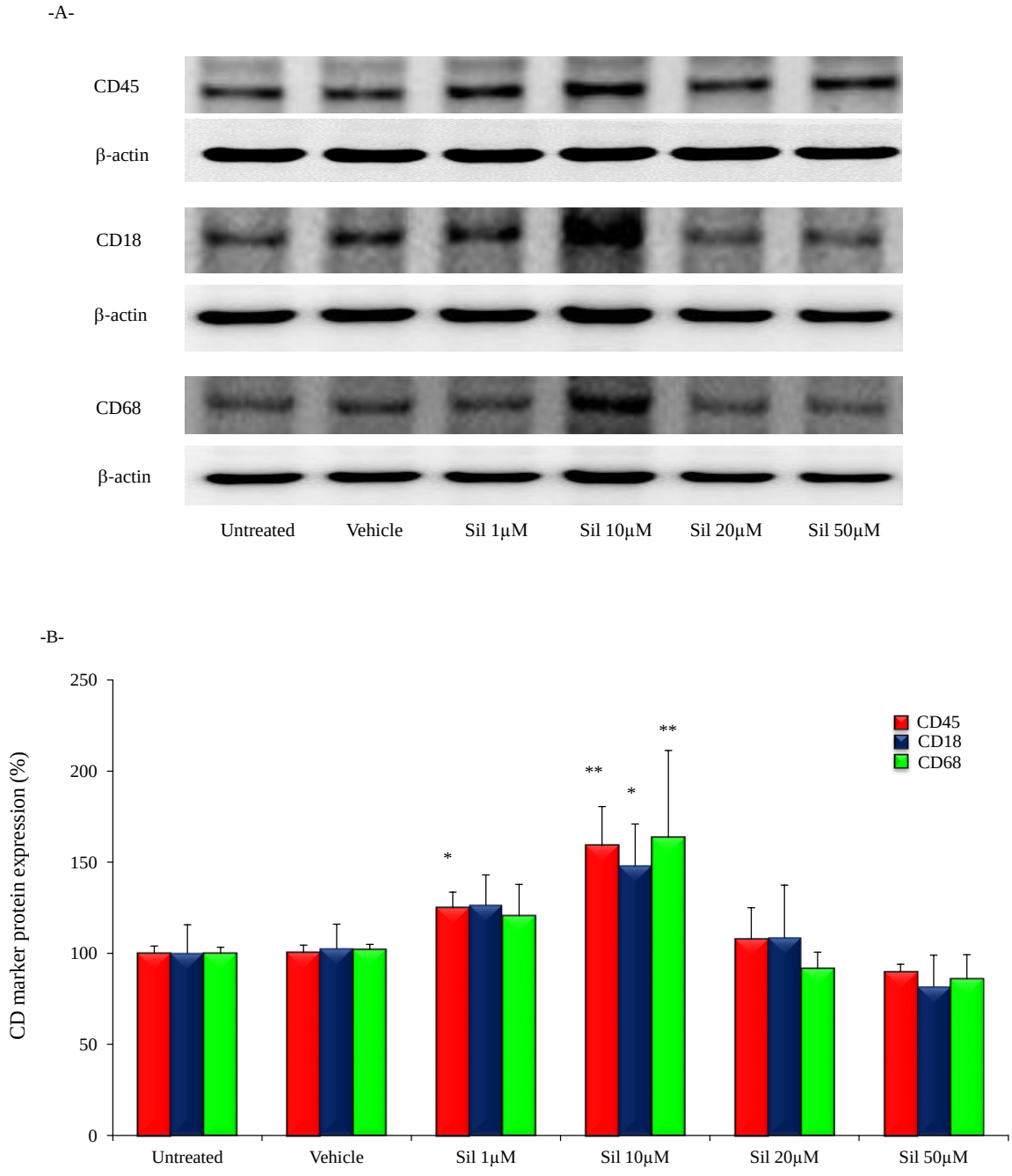

Figure 3.31: Increase of CD45, CD18 and CD68 expression upon Silibinin treatment. (A) Representative western blots of protein expression in EBs treated with different concentrations of Silibinin **(B)** Graphical representation of protein expression for CD45, CD18 and CD68 upon treatment with different concentrations of Silibinin. The bar chart shows the means $\pm$ SD of (n = 4 experiments). β-actin was used as house-keeping protein; * $P \leq 0.05$, ** $P \leq 0.01$, significantly different to the untreated control.

3.19. Effect of the eNOS inhibitor L-NAME, Stattic, AKT inhibitor VIII and LY294002 on leukocyte differentiation upon Silibinin treatment of mouse ES cells

Our previous results demonstrated that Silibinin increased vasculogenesis. The stimulation of vasculogenesis was abolished upon inhibition of NOS, STAT3 and PI3K/AKT. Since vasculogenesis and leukopoiesis are regulated by comparable signaling pathways, it was investigated, whether L-NAME, Stattic, AKT inhibitor VIII and LY294002 would affect leukocyte differentiation upon Silibinin treatment. To achieve this aim, EBs were treated from day 3 to day 14 with Silibinin (10µM) either in the absence or presence of L-NAME (100µM), Stattic (7µM), AKT inhibitor VIII (5µM) and LY294002 (5µM), and western blot analysis for CD45, CD18 and CD68 was performed. Our results showed that L-NAME, Stattic, AKT inhibitor VIII and LY294002, decreased protein expression of the leukocyte markers CD45 (figure 3.32), CD18 (figure 3.33) and the macrophage marker CD68 (figure 3.34) even in the absence of Silibinin. Moreover, the stimulation of leukocyte marker expression achieved upon Silibinin treatment was completely abolished.

-A-

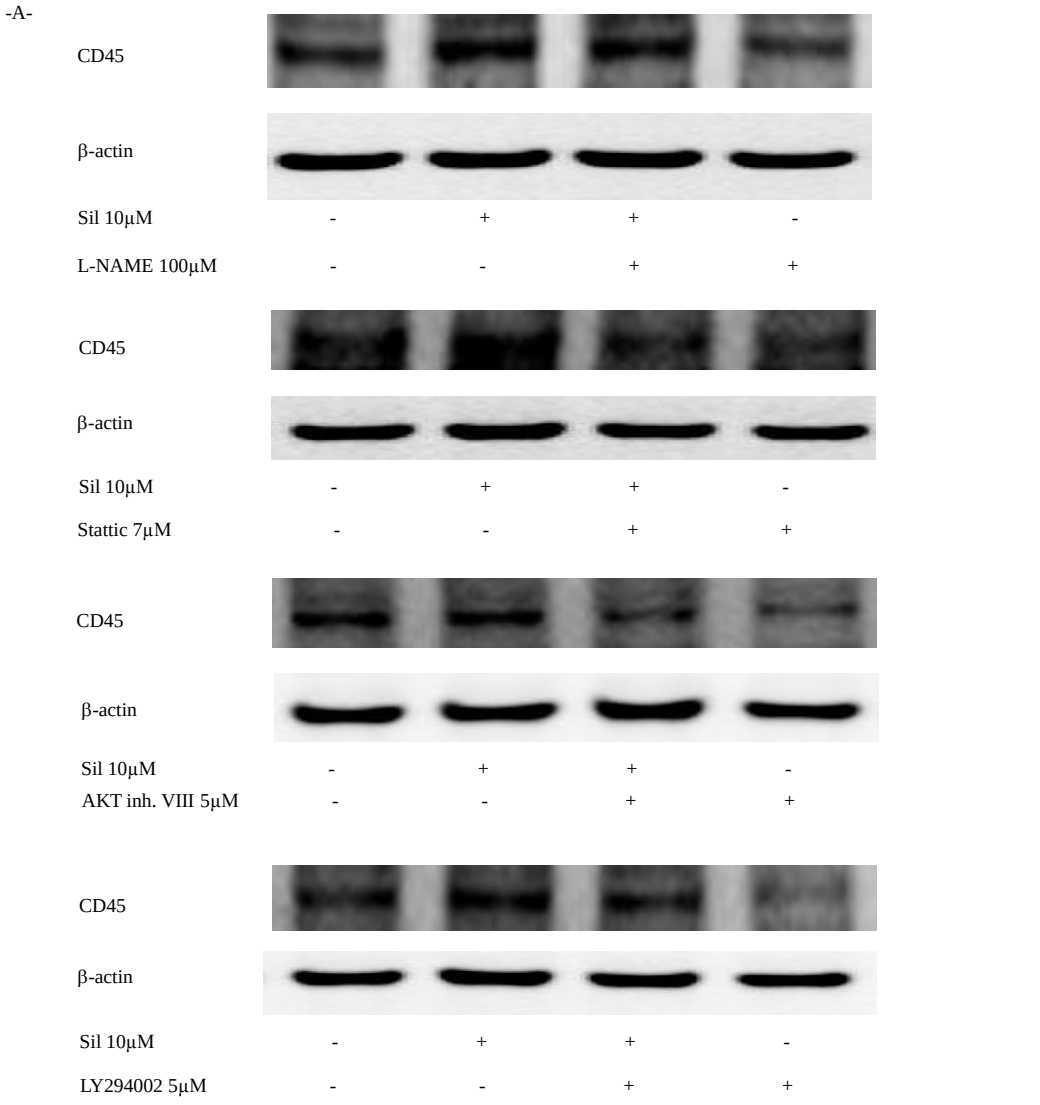
CD45
β-actin
Sil 10μM - + + -
L-NAME 100μM - - + +
CD45
β-actin
Sil 10μM - + + -
Stattic 7μM - - + +
CD45
β-actin
Sil 10μM - + + -
AKT inh. VIII 5μM - - + +
CD45
β-actin
Sil 10μM - + + -
LY294002 5μM - - + +

-B-

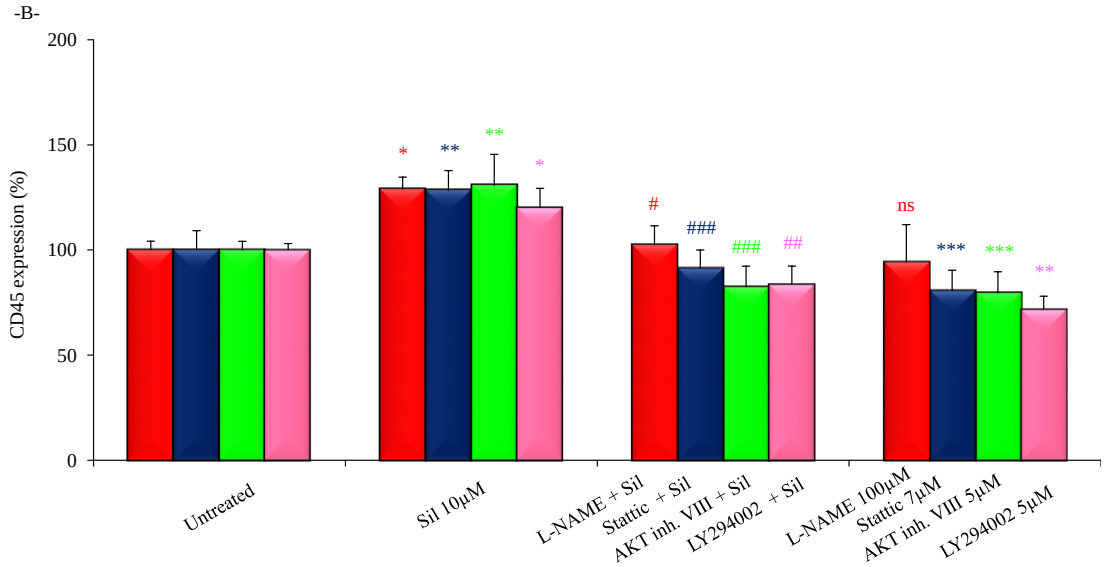
CD45 expression (%)
200
150
100
50
0
*
**
**
*
#
###
###
##
ns
***
***
**
Untreated
Sil 10μM
L-NAME + Sil
Stattic + Sil
AKT inh. VIII + Sil
LY294002 + Sil
L-NAME 100μM
Stattic 7μM
AKT inh. VIII 5μM
LY294002 5μM

Figure 3.32: Effect of L-NAME, Stattic, AKT inhibitor VIII and LY294002 on CD45 expression upon Silibinin treatment of EBs. (A) Representative western blots showing CD45 expression either in the absence (untreated) or presence of Silibinin with or without inhibitors. β-actin was used as house-keeping protein. **(B)** Graphic representation of western blots showing the means ± SD of n = 4 experiments for L-NAME (red bars), Stattic (blue bars), AKT inhibitor VIII (green bars) and n = 3 experiments for LY294002 (pink bars). * $P \leq 0.05$, ** $P \leq 0.01$, *** $P \leq 0.001$ significantly different to the untreated control, # $P \leq 0.05$, ## $P \leq 0.01$, ### $P \leq 0.001$ significantly different to Silibinin alone and ns (non-significant), $P \geq 0.05$.

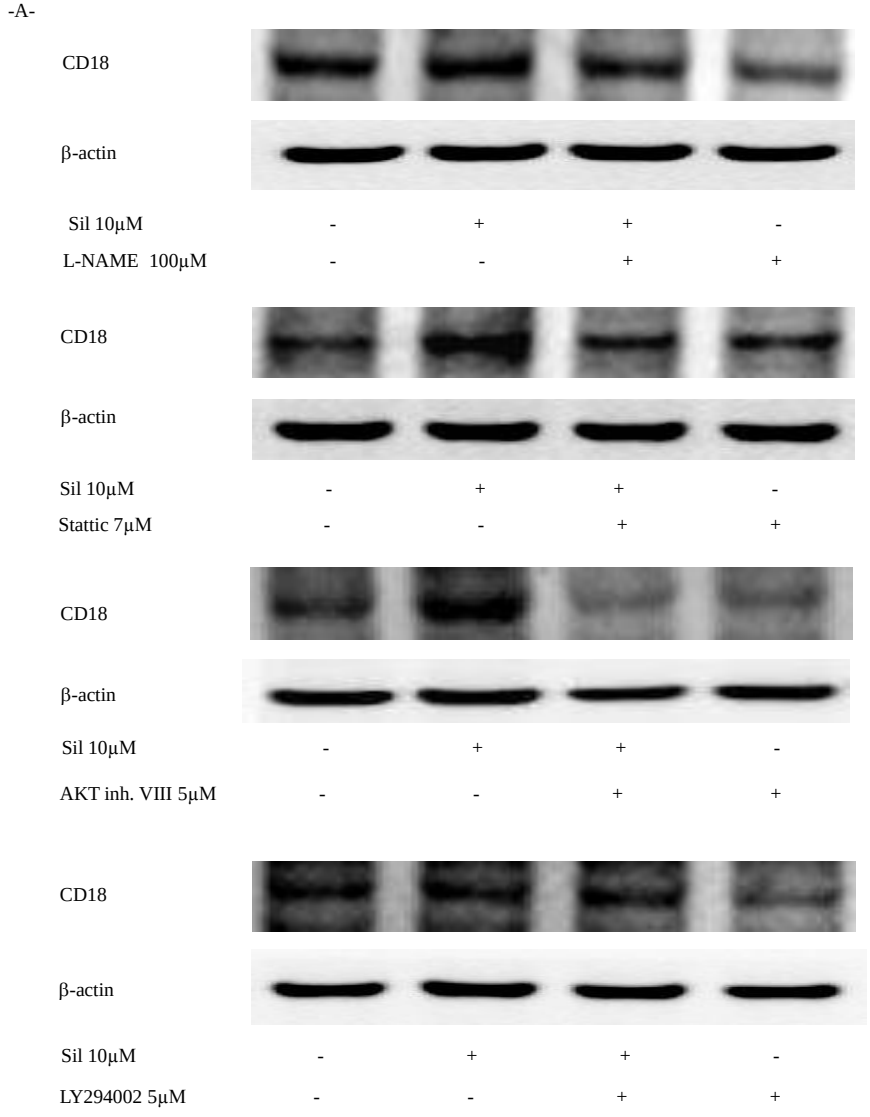

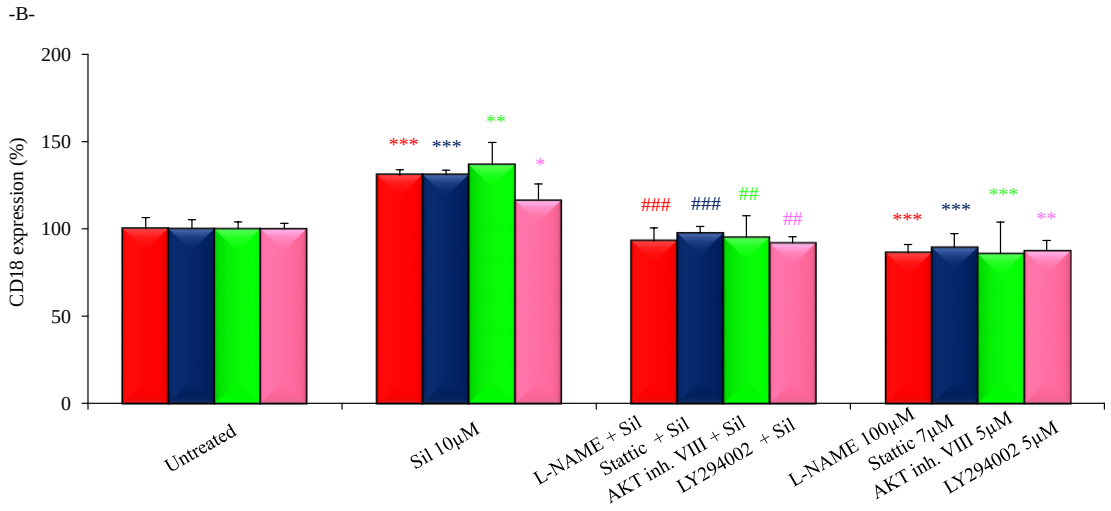

Figure 3.33: Effect of L-NAME, Stattic, AKT inhibitor VIII and LY294002 on CD18 expression upon Silibinin treatment of EBs. (A) Representative western blots showing CD18 expression either in the absence (untreated) or presence of Silibinin with or without inhibitors. β-actin was used as house-keeping protein (**B)** Graphic representation of western blots showing the means $\pm$ SD of n= 4 experiments for L-NAME (red bars), Stattic (blue bars), AKT inhibitor VIII (green bars) and n = 3 experiments for LY294002 (pink bars). * $P \leq 0.05$, ** $P \leq 0.01$, *** $P \leq 0.001$ significantly different to the untreated control, ## $P \leq 0.01$, ### $P \leq 0.001$ significantly different to Silibinin alone.

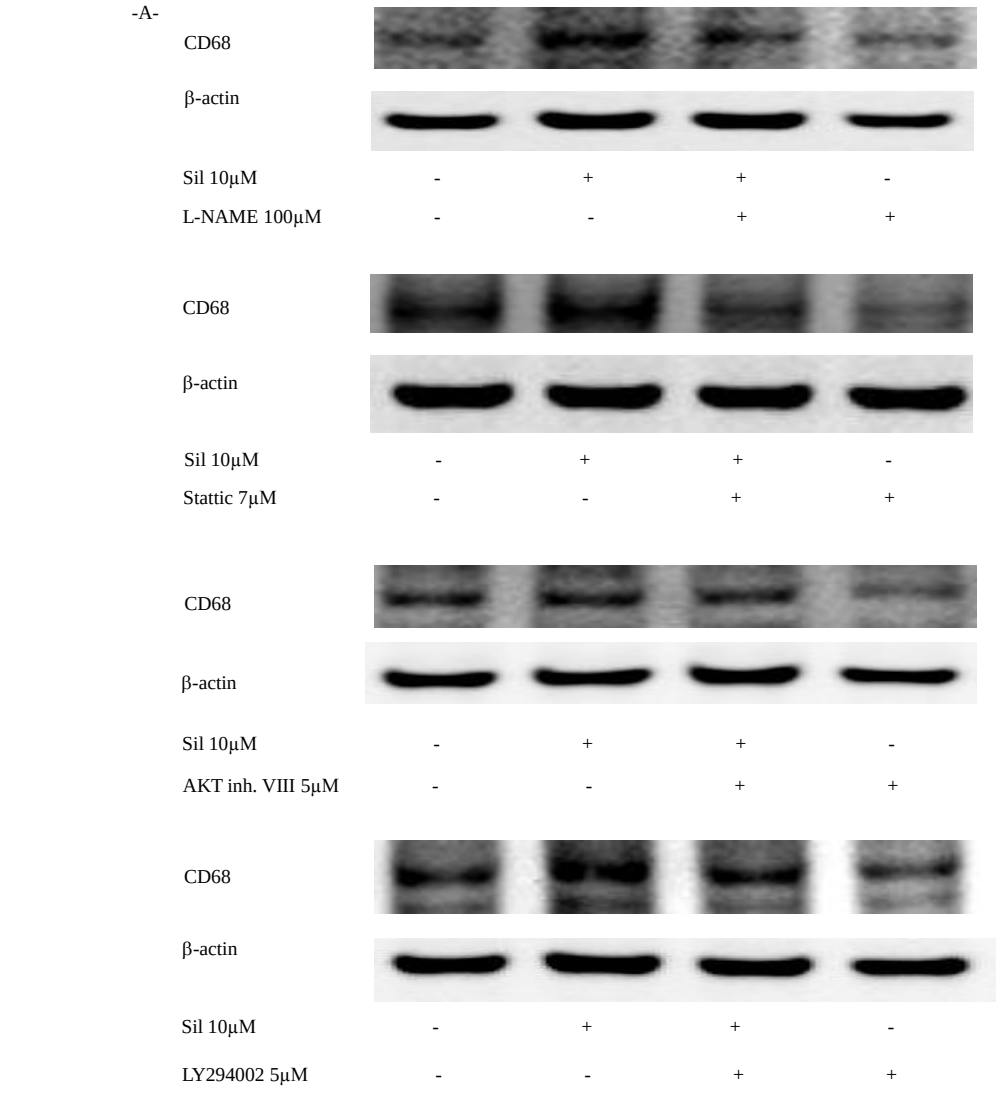
-A-
CD68
β-actin
Sil 10µM - + + -
L-NAME 100µM - - + +
CD68
β-actin
Sil 10µM - + + -
Stattic 7µM - - + +
CD68
β-actin
Sil 10µM - + + -
AKT inh. VIII 5µM - - + +
CD68
β-actin
Sil 10µM - + + -
LY294002 5µM - - + +

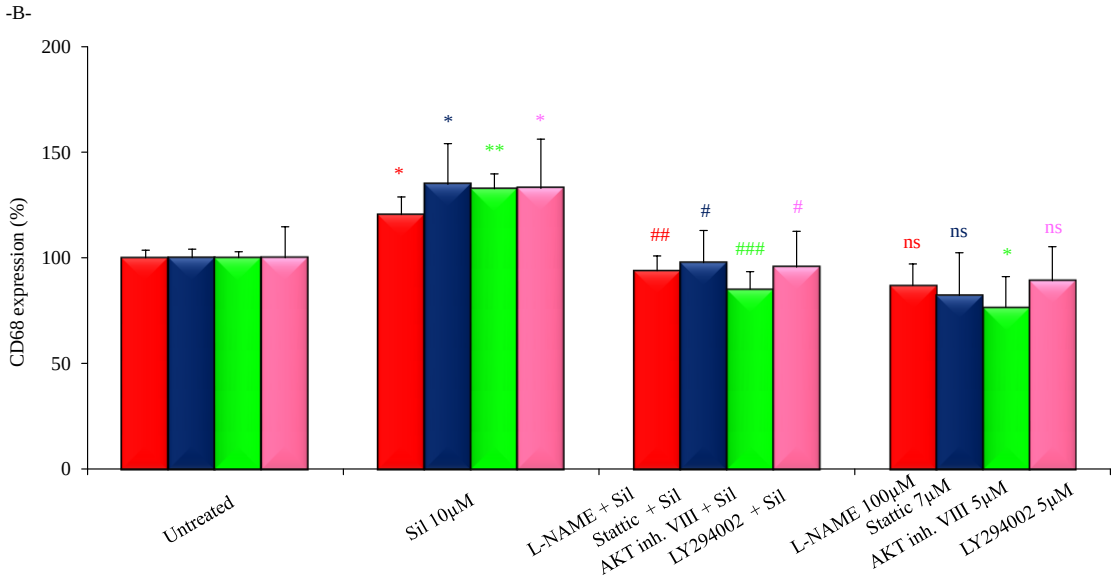
-B-
CD68 expression (%)
200
150
100
50
0
Untreated
Sil 10µM
L-NAME + Sil
Stattic + Sil
AKT inh. VIII + Sil
LY294002 + Sil
L-NAME 100µM
Stattic 7µM
AKT inh. VIII 5µM
LY294002 5µM
ns

Figure 3.34: Effect of L-NAME, Stattic, AKT inhibitor VIII and LY294002 on CD68 expression upon Silibinin treatment of EBs. (A) Representative western blots showing CD68 expression either in the absence (untreated) or presence of Silibinin with or without inhibitors. **(B)** Graphic representation of western blots showing the means $\pm$ SD of n = 4 experiments for L-NAME (red bars), Stattic (blue bars) and AKT inhibitor VIII (green bars) and n = 5 experiments for LY294002 (pink bars). * $P \leq 0.05$, ** $P \leq 0.01$ significantly different to the untreated control, # $P \leq 0.05$, ## $P \leq 0.01$, ### $P \leq 0.001$ significantly different to Silibinin alone and ns (non-significant), $P \geq 0.05$.

4. Discussion

In the present study we investigated the effect of Silibinin on the cardiovascular and leukopoesis differentiation potential of mouse ES cells which share a variety of similarities with resident stem cells of many organs. After tissue injury, stem cells are activated to initiate and promote regenerative processes of tissue and organ repair. Previous studies had shown that DMSO was used as solvent for Silibinin which led to off-target effects and misleading results (Cavas et al., 2005). Silibinin is water insoluble which results in low bioavailability. We therefore used the soluble form of Silibinin, i.e. Silibinin-C-2',3-dihydrogensuccinate, disodium salt (Legalon SIL) for the experiments of the present study.

4.1. Effect of Silibinin on cardiomyogenesis of ES cells and Ang II-mediated cardiac cell function

The pharmacologic actions of Silibinin have been mainly attributed to its hepato-protective and anti-cancer properties (Neha et al., 2016). However, Silibinin has also been shown to be pharmacologically active in the cardiovascular system. In this respect it has been demonstrated to exert cardioprotective properties, e.g. following isoproterenol-induced cardiac myocyte injury (Zhou et al., 2006; Zhou et al., 2006a) or doxorubinin-mediated cardiotoxicity (Raskovic et al., 2011). Moreover, Silibinin reduced blood pressure and the incidence of post-occlusion arrhythmias in spontaneously hypertensive rats, and it was suggested that this compound may be beneficial when used in hypertensive patients who develop acute myocardial infarction (Chen et al., 1993). Silymarin exhibited significant antihypertensive activity in a DOCA salt model of hypertension (Jadhav and Upasani, 2011). In anesthetized open chest cats Silibinin lowered the amplitude and duration of diastolic blood pressure and produced a marked depression of cardiac contractility (Rui et al., 1986), suggesting that Silibinin affects the hemodynamic properties of the heart.

The data of the present study demonstrated that Silibinin dose-dependently inhibited cardiomyogenesis of ES cells. Moreover, Silibinin decelerated the frequency of Ca^{2+} spikes in differentiated cardiac cells. To investigate whether the effects of Silibinin on cardiomyogenesis and cardiac cells were due to inhibition of Ang II-mediated signaling pathways, we investigated whether Silibinin treatment would abolish the stimulation of cardiomyogenesis achieved upon Ang II treatment of differentiating ES cells. In

corroboration with the data of Wu et al. 2013, we observed stimulation of cardiomyogenesis following incubation with Ang II. Moreover, Ang II treatment increased the contraction frequency of cardiac areas differentiated from ES cells and the frequency of Ca^{2+} spikes in differentiated cardiac cells. The stimulation of cardiomyogenesis as well as the increase in Ca^{2+} spiking frequency achieved with Ang II was completely abolished upon co-treatment with Silibinin, supporting the notion that Silibinin is interfering with Ang II signaling. Previous studies of Wu et al., 2013 and Zheng et al., 2013 suggested that the effects of Ang II on cardiac and smooth muscle cell differentiation were mediated via the AT1 receptor, since the specific AT1 receptor antagonist losartan abolished the observed effects. Notably, Silibinin has been discussed to act as an AT1 receptor antagonist in CHO cells which were stably transfected with the human AT1 receptor (Bahem et al., 2015). We therefore investigated, whether Silibinin would abolish the Ang II-mediated Ca^{2+} response in smooth muscle cells which are well known to express the AT1 receptor (Murphy et al., 1992). Interestingly it was observed that Silibinin was not able to inhibit the Ca^{2+} response elicited by Ang II even at high (100µM) concentrations. Comparable data were obtained in DU145 prostate cancer cells which have been described to express the AT1 receptor (Sidorkiewicz et al., 2009) (data not shown). Thus the data of the present study argue against an involvement of AT1 receptor inhibition by Silibinin at least in the physiological Ang II concentrations (1µM) used in our experiments.

If the AT1 receptor activity and Ca^{2+} signaling are not affected, Silibinin could possibly interfere with the further downstream signaling cascade. It has been previously described in rat neonatal cardiomyocytes, that Ang II activates ERK1/2, p38 and JNK, whereby the phosphorylation of p38 and JNK is dependent on reactive oxygen species (ROS) generation (Nishida et al., 2005). In the experiments of the present study Silibinin significantly inhibited ERK1/2, p38 and JNK activity as compared to the untreated control, whereas MAPK stimulation was observed upon Ang II treatment. According to our assumptions Silibinin totally abolished the stimulation of all members of the MAPK family by Ang II, which indicates that the compound interferes with the MAPK signaling cascade downstream of the AT1 receptor. Since NO is well known as a free radical scavenger for ROS (Kumar et al., 2017), it may be assumed that the inhibitory effect of Silibinin on MAPK activity may be due to its capacity to raise NO concentration in the tissue. Previous

data from others who showed that Silibinin protects H9c2 cardiac cells from oxidative stress and inhibits phenylephrine-induced hypertrophy, presumably by repression of the phenylephrine-induced phosphorylation of ERK1/2 kinases (Anestopoulos et al., 2013), are pointing to the same direction. Moreover, the property of Silibinin to act as a free radical scavenger has been validated in several studies (Mira et al., 1994; Dehmlow et al., 1996a; Ali et al., 2018).

The RAAS has been shown to exert deep impact on cardiac development (Price et al., 1997). In humans all components of RAAS are expressed at very early stages of embryogenesis (30-35 days of gestation) in different organs, suggesting that Ang II likely plays a role in the growth and differentiation of various organotypic cells (Schutz et al., 1996). Although triple knockouts of the AT1a, AT1b and AT2 receptors are viable and fertile, the lack of both AT1 receptor subtypes was associated with atrophic changes in the myocardium, a reduced coronary flow and a reduced left ventricular systolic pressure (Gembardt et al., 2008; van et al., 2010). Recently it has been outlined, that anti-hypertensive medication of pregnant women is associated with increased risk for congential heart defects. This was the case for the treatment with ß-blockers as well as with the use of RAAS blockers (Fisher et al., 2017). Milk thistle seeds as well as their pharmacologically active ingredients are frequently used as dietary herbal supplements mainly to detoxify the liver. Since the data of the present study demonstrate that Silibinin inhibits cardiac differentiation of ES cells and affects Ang II-mediated signaling cascades, its use should be avoided in pregnant women.

4.2. Silibinin and Ang II effects on rat adult cardiac cell function

Ang II exerts vasoconstrictor effects and RAAS blockers are used in humans as blood pressure lowering agents. In addition Ang II has been shown to induce cardiac hypertrophy by acting directly on the heart tissue as well as indirectly through hypertension and increased hemodynamic forces within the heart (Steckelings et al., 2007; Danser, 2010; Xu et al., 2010; Zhou et al., 2016). To explain the effect of Silibinin and Ang II on cardiac cell function, adult rat cardiomyocytes were treated overnight with Ang II (10μM) in presence or absence of Silibinin (20μM) and cell shortening, relaxation velocity, diastolic cell length (L diastolic) and R50-TTP 50 (time to reach 50% relaxation- time-to-peak 50% (TTP 50))

were investigated as previously described (Mufti et al., 2008). As previously demonstrated by Mufti et al. (2008) Ang II treatment significantly reduced cell shortening, decreased relaxation velocity, diastolic cell length and the time to reach 50% relaxation compared to untreated controls. The observed inhibition of cardiac cell function achieved with Ang II was completely reversed by Silibinin treatment. The adverse effect of Ang II on cardiac cell function may be due to the increase in cellular oxidative stress which occurs upon AT1 receptor binding by Ang II. Since Silibinin has been demonstrated to exert anti-oxidative properties in several studies (Lu et al., 2009), the preservation of cardiac cell function in the presence of Silibinin may be due to its radical scavenging properties. Increased Ang II levels play a pivotal role in adverse myocardial remodeling and progression to heart failure which are currently treated by ACE inhibitors or AT1 receptor blockers (Patel et al., 2016). Due to its low toxicity and good tolerance Silibinin may be used in future to prevent Ang II-mediated cardiac remodeling and heart failure progression.

4.3. Stimulation of vasculogenesis by Silibinin

Our data demonstrated that very low concentrations (1-10µM) of Silibinin exerted a pro-angiogenic effect associated with increased branching points, VE-cadherin, VEGFR2 and HIF-1α protein expression, whereas higher concentrations of Silibinin (up to 50µM) were anti-angiogenic, however without increasing overall toxicity of this compound (data not shown). The dose-dependent pro- and anti-angiogenic activity may explain the conflicting data of previous studies which demonstrated anti-angiogenic effects at Silibinin concentrations of approximately 100µM (Lin et al., 2013), whereas protective effects on endothelial cells were observed at concentrations below 100µM (Wang et al., 2005).

To unravel the pro-angiogenic effect of Silibinin, we assessed NO generation and eNOS activation since NO is well known to exert pro-angiogenic effects *in vitro* and *in vivo* (Ghimire et al., 2017). Indeed Silibinin treatment dose-dependent increased NO generation with maximum effects at 10µM and adverse effects at higher concentrations. Moreover, activation of eNOS was observed within 30 min of Silibinin treatment. The anti-oxidative activity of Silibinin has been described in numerous studies, and has been attributed to direct radical scavenging, chelation of iron and copper, inhibition of ROS producing enzymes and activation of anti-oxidant enzymes (Surai, 2015). The potential role of NO as

a mediator of Silibinin´s anti-oxidative activity has so far not sufficiently been investigated, although it has been previously shown that very high concentrations of Silibinin (400µM) exerted nitrosative stress in human epidermoid carcinoma A431 cells (Yu et al., 2012) and HeLa cells (Fan et al., 2011). Notably, it has been discussed, that there exists an inter-regulation pattern between reactive nitrogen species (RNS) and ROS generation upon Silibinin treatment of cultured cells (Wang et al., 2010) which may be involved in the cyto-protective versus cyto-toxic effect of this compound. In this respect it has to be kept in mind that the same chemical compound can act as a pro-oxidant as well as anti-oxidant, which is dependent on the overall oxidative milieu in the cell or tissue as well as the concentration of the investigated agent. Therefore, the data of the present study suggest that higher (> 20µM) concentrations of Silibinin may raise ROS towards levels which inhibit eNOS phosphorylation, NO generation and vascular differentiation from ES cells.

To investigate the signaling pathways involved in the generation of NO and stimulation of vasculogenesis of ES cells, we assessed activation of PI3K, STAT3 and AKT and determined whether pharmacological inhibition of these protein kinases would interfere with NO generation as well as vascular structure formation upon treatment with Silibinin. The PI3K/AKT pathway has been previously shown to be essential for several key endothelial cell (EC) functions, including cell growth, migration, survival, and vascular tone (Lee et al., 2014), and has been demonstrated in various studies to activate eNOS in the downstream signaling cascade (Lee et al., 2006; Erdogdu et al., 2010; Yu et al., 2011). STAT3 is required for both basal and growth signal-induced expression of HIF-1α (Hooper et al., 2007) and regulates VEGF expression (Niu et al., 2002). Presumably STAT3 regulates VEGF activation by directly interacting with the binding site on 5' region of VEGF gene (Lv et al., 2017). Recently it has been shown that the RNA-binding protein Quaking isoform 5 (QKI-5) is an important regulator of STAT3 stabilization and VEGFR2 activation during the endothelial cell differentiation process of induced pluripotent stem (iPS) cells (Cochrane et al., 2017).

In the present study it was shown that Silibinin treatment of EBs activated PI3K, STAT3 and AKT. Inhibition of PI3K abolished activation of STAT3, AKT as well as NO generation and vascular structure formation. Comparable results were achieved upon inhibition of STAT3 and AKT, which clearly demonstrates that Silibinin is activating the

PI3K/AKT/STAT3/eNOS pathway to stimulate vasculogenesis of ES cells (figure 4.1). Since NO generation and eNOS phosphorylation upon Silibinin treatment was inhibited upon pharmacological intervention with the PI3K/AKT/STAT3 pathway, it can be concluded, that the action of Silibinin is not just related to its anti-oxidative capacity, but to specific activation of signaling pathways known to be related with NO generation and blood vessel formation.

4.4. Enhancement of leukopoiesis upon Silibinin treatment

Silibinin has been shown to exert organ-protective and regenerative properties which may be related to its reported anti-inflammatory action (Choi et al., 2012; Guo et al., 2016; Kim et al., 2016). Moreover, Silibinin may have impact on immune function in a complex way. Since regenerative processes involve stem cells, we investigated whether Silibinin would affect the differentiation of $CD45^+$, $CD18^+$ and $CD68^+$ cells which are indicative for the monocyte/macrophage cell lineage. Our data demonstrated that indeed Silibinin dose-dependent increased the differentiation of cells which were positive for leukocyte markers, with maximum effects achieved at 10µM Silibinin, whereas higher concentrations exerted adverse effects. The strict concentration dependence of this compound´s biological action may be one of the explanations for the conflicting data existing on the anti-oxidative and anti-inflammatory properties of Silibinin and the activation versus inhibition of specific signaling pathways (Verma and Thuluvath, 2007). In this respect it has been shown that Silymarin inhibits T-lymphocyte function at low doses but stimulates inflammatory processes at high doses (Johnson et al., 2003). It is well known that one and the same substance can act as a pro-oxidant or anti-oxidant, depending on the concentration, the cellular context, the balance between ROS and RNS and the presence of catalyzing metals like Cu and Fe which promote the pro-oxidant activity of natural anti-oxidants (Pisoschi and Pop 2015; Adegbola et al., 2017). To assess the signaling pathways underlying the differentiation of cells expressing leukocyte markers, we investigated the activation of STAT3 which is a central component of the JAK/STAT signaling cascade. STAT3 is an important transcription factor required for growth and differentiation of hematopoietic stem cells (Hillmer et al., 2016). STAT3 deficiency renders hematopoietic progenitor cells and myeloid precursors refractory to the growth-promoting functions of G-CSF (Zhang et al.,

2010). Interestingly, STAT3 has been recently attributed anti-inflammatory activity in haematopoiesis (Martelli et al., 2010), which may contribute to the inflammation lowering capacity, which has been reported for Silibinin in different experimental settings. Moreover, activation of PI3K and AKT, which are involved in central pathways directing cardiovascular differentiation of ES cells (Bekhite et al., 2011), was investigated. Notably, the PI3K/AKT/mTOR signaling network regulates proliferation, survival, and differentiation events during haematopoiesis (Martelli et al., 2010), whereby a signaling pathway consisting of PI3K/AKT-NF-κB-Bcl-xL regulates survival of macrophages during and after differentiation from monocytes (Busca et al., 2014). Our data demonstrate that treatment with Silibinin (10µM) activated STAT3 as well as PI3K and AKT within few minutes of incubation, which may indicate that this compound is directly activating growth factor/cytokine receptors, thereby initiating specific signaling pathways. This assumption would implicate, that the anti-inflammatory action of Silibinin is not just due to the radical scavenging chemical structure of this flavonolignan, but to the initiation of receptor regulated anti-inflammatory signaling cascades, which indirectly results in anti-oxidative action. Our previous observations, that Silibinin activates NO generation by eNOS stimulation, which was inhibited upon interference with STAT3 and PI3K/AKT (Ali et al., 2018) (figure 4.1), and the observation, that Silibinin raised NO in $CD68^+$ cells (data not shown), point in this direction. To underscore the notion that Silibinin is stimulating the differentiation of cells expressing leukocyte markers through STAT3 and PI3K/AKT signaling pathways, we applied pharmacological inhibitors. Notably, inhibition of STAT3 by Stattic, PI3K by LY294002 and AKT by AKT inhibitor VIII totally abolished expression of CD45, CD18 and CD68 achieved upon treatment of differentiating ES cells with Silibinin. Moreover, the applied inhibitors blunted the stimulation of VEGFR2 and HIF-1α expression, which was observed upon Silibinin treatment of differentiating ES cells. In our recent study we demonstrated that Silibinin-stimulated vasculogenesis from ES cells, which is well known to be regulated by VEGFR2 and HIF-1α-mediated signaling pathways (Ali et al., 2018). Vasculogenesis and haematopoiesis are two closely related events, which are regulated by the gene *cloche*, a master regulator of the endothelial and haematopoietic cell fate (Reischauer et al., 2016). Previous studies of us demonstrated that inhibition of VEGFR2 receptors abolished not only vasculogenesis, but also leukopoiesis

(Hannig et al., 2010). Whereas vasculogenesis in mouse ES cells occurs within the first 9 days following removal of LIF from the cell culture medium, the differentiation of leukocytes occurs between day 12 and day 14 of cell culture, which implies that inhibition of vasculogenesis should abolish differentiation of leukocytic cells (Hannig et al., 2010). During embryogenesis haematopoietic stem cells differentiate from a population of endothelial cells called haemogenic endothelium (HE) in a process called the endothelial-to-haematopoietic transition (EHT) and is regulated by the transcription factor Runx1 (Yzaguirre et al., 2018). Recently transcriptional overlap between haemogenic endothelial cells and haematopoietic progenitor cells was reported (Angelos et al., 2018). Moreover, it was reported that HIF-1α and HIF-2α regulate haemogenic endothelium and hematopoietic stem cell formation in zebrafish (Gerri et al., 2018).

The most important biological activity of Silibinin is its liver-protective effect (Wellington and Jarvis, 2001), which may be associated to the initiation of regenerative processes. Recent studies have shown that in a murine model of hepatic injury and fibrosis, treatment with bone marrow derived macrophages (Thomas et al., 2011) or macrophages differentiated from ES cells (Haideri et al., 2017) can improve liver regeneration and reduce fibrosis. Since the data of the present study demonstrate that leukocytic differentiation occurs from ES cells upon Silibinin treatment, it may be speculated that differentiation of resident stem cells in the liver towards cells of the monocyte/macrophage lineage may be an important corner mark in the regenerative properties of this milk thistle ingredient.

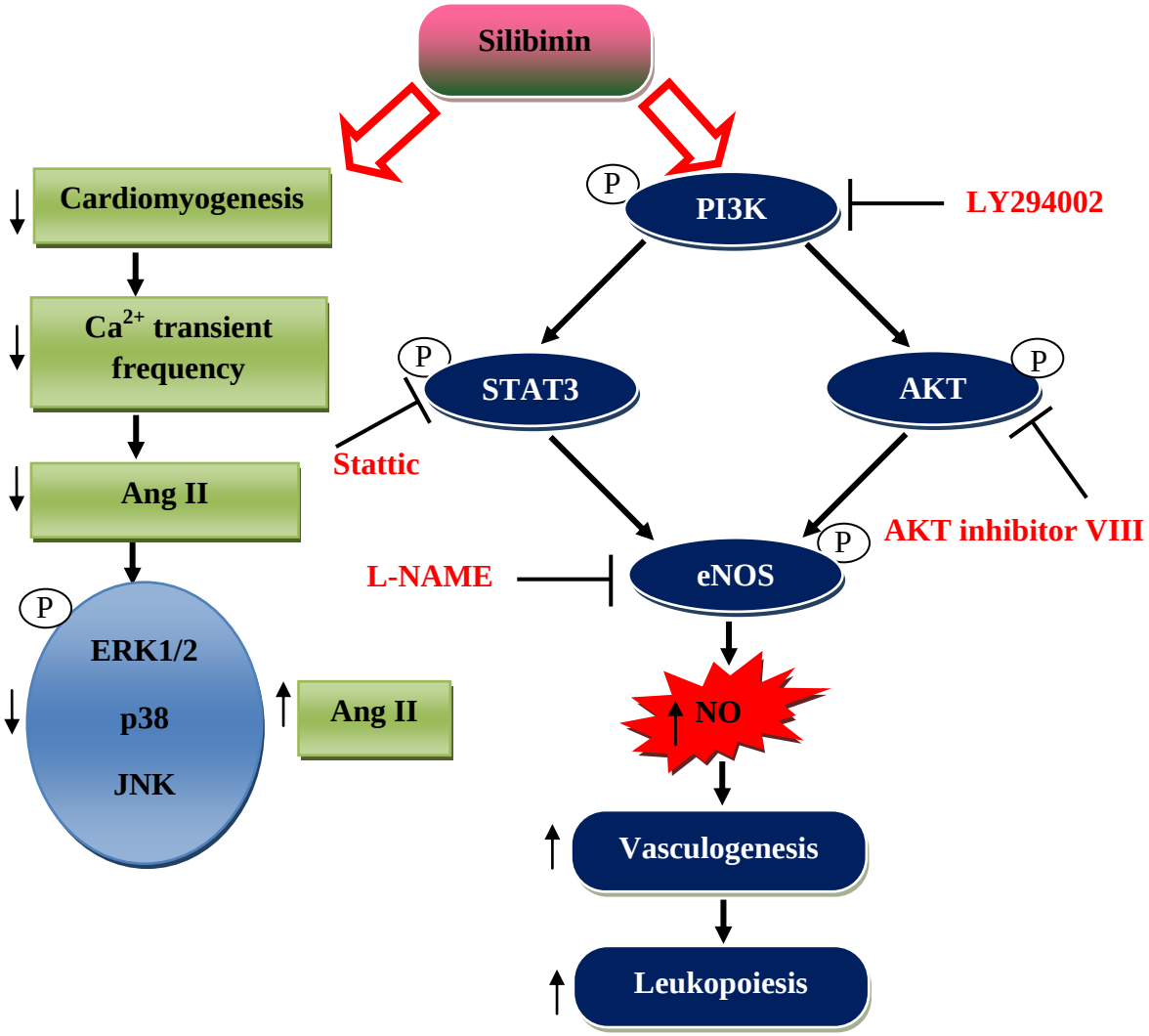

Figure 4.1: Schematic representation of Silibinin action in differentiating mouse ES cells. Silibinin downregulates cardiomyogenesis of ES cells presumably by inhibition of ERK1/2, p38 and JNK downstream of the AT1 receptor. On the other side Silibinin stimulates vasculogenesis and leukopoiesis by activating the PI3K/AKT/STAT3/eNOS signaling pathway and up-regulation of NO generation.

5. Summary

In the current study the effect of Silibinin-C-2', 3-bis (hydrogensuccinate), Disodium salt on cardiovascular differentiation and leukopoiesis of mouse ES cells was investigated. Silibinin is a bioactive substance from milk thistle (*Silybum marianum* (L.) Gaertn.), and owns cell and organ regeneration-promoting properties.

It was demonstrated that Silibinin-stimulated vasculogenesis, the expression of vasculogenic proteins (VEGFR2, HIF-1α, VE-Cadherin) and leukopoiesis ($CD45^+$-, $CD18^+$-, and $CD68^+$ -cells) of ES cells, whereas an inhibition of cardiomyogenesis was observed.

Silibinin inhibited the Ang II-mediated stimulation of cardiomyogenesis of ES cells as well as the Ang II-mediated increase in contraction frequency and frequency of Ca^{2+} spikes. However, not by blockage of the AT1 receptor itself, but by inhibition of ERK1/2, p38 and JNK signaling pathways downstream of the AT1 receptor. In adult rat cardiomyocytes Silibinin reversed the inhibition of cell contractility following Ang II treatment.

Treatment of differentiating ES cells with Silibinin resulted in NO generation and activation of eNOS within few minutes. Furthermore, activation of the PI3K/AKT and STAT3 signaling pathway was observed. Inhibition of NO generation by L-NAME, STAT3 activation by Stattic, AKT activation by AKT inhibitor VIII and PI3K activation by LY294002 abolished the stimulation of vasculogenesis and leukopoiesis by Silibinin.

Stattic inhibited the Silibinin-induced eNOS and AKT activation as well as NO generation. AKT inhibitor VIII inhibited the Silibinin-mediated NO generation and eNOS as well as STAT3 phosphorylation. The PI3K inhibitor LY294002 blunted Silibinin-mediated NO generation, eNOS activation as well as AKT and STAT3 phosphorylation.

In conclusion the data of the present study show that Silibinin stimulates vasculogenesis and leukopoiesis of ES cells through a NO-mediated and PI3K/AKT- as well as STAT3-regulated signaling pathway. On the other hand Silibinin prevents cardiomyogenesis through inhibition of the Ang II signaling pathway on the level of the ERK1/2, p38 and JNK signaling cascade.

6. Summary (German)

Zusammenfassung

In der vorliegenden Studie wurde der Effekt von Silibinin-C-2', 3-bis (Hydrogensuccinat), Dinatriumsalz auf die kardiovaskuläre Differenzierung und Leukopoiese von ES Zellen der Maus untersucht. Silibinin ist eine in der Milchdistel (*Silybum marianum* (L.) Gaertn.) vorkommende bioaktive Substanz mit Zell- und Organ-Regenerations-fördernden Eigenschaften.

Es konnte gezeigt werden, dass Silibinin die Vaskulogenese, die Expression vaskulogener Proteine (VEGFR2, HIF-1α, VE-Cadherin) und Leukopoiese von ES Zellen ($CD45^+$-, $CD18^+$-, $CD68^+$-Zellen) förderte, wogegen eine Inhibition der Kardiomyogenese beobachtet wurde.

Silibinin inhibierte die Ang II-vermittelte Stimulation der Kardiomyogenese von ES Zellen und die Ang II-induzierte Steigerung der Kontraktionsfrequenz und der Frequenz von Ca^{2+} Transienten, jedoch nicht durch Blockierung des AT1 Rezeptors, sondern durch Hemmung der ERK1/2, p38 und JNK Signalwege, die dem AT1 Rezeptor nachgeschaltet sind. In adulten Kardiomyozyten der Ratte revertierte Silibinin die durch Ang II inhibierte Zellkontraktilität.

Nach Behandlung differenzierender ES Zellen mit Silibinin konnte im Verlauf weniger Minuten eine Generierung von NO durch Aktivierung der eNOS festgestellt werden. Weiterhin wurde eine Aktivierung des PI3K/AKT und STAT3 Signalweges beobachtet. Eine Inhibition der NO Generierung durch L-NAME, der STAT3 Aktivierung durch Stattic, der AKT Aktivierung durch AKT Inhibitor VIII und der PI3K Aktivierung durch LY294002 verhinderte die Stimulation der Vaskulogenese und Leukopoiese durch Silibinin.

Stattic inhibierte die Silibinin-vermittelte eNOS und AKT Aktivierung sowie die NO-Generierung. Der AKT Inhibitor VIII inhibierte die Silibinin-induzierte NO Generierung sowie die eNOS und STAT3 Phosphorylierung. Der PI3Kinase Inhibitor LY294002

inhibierte die Silibinin-induzierte NO Generierung, eNOS Aktivierung und die AKT und STAT3 Phosphorylierung.

Die Daten der vorliegenden Studie zeigen somit, dass Silibinin die Vaskulogenese und Leukopoiese von ES Zellen über einen NO-vermittelten und PI3K/AKT und STAT3 regulierten Signalweg induziert. Auf der anderen Seite verhindert Silibinin die Kardiomyogenese durch Inhibition des Ang II Signalwegs auf der Ebene des ERK1/2, p38 und JNK Signalwegs.

7. List of abbreviations

α- and β-MHC	α- and β-myosin heavy chain
ºC	Degree Celcius
3D	Three-dimensional
ACE	An angiotensin-converting-enzyme
AKT	Protein kinase B
AKT inh. VIII	AKT inhibitor VIII
Ang II	Angiotensin II
AT1	Angiotensin II receptor 1
AT2	Angiotensin II receptor 2
BMP	Bone morphogenetic protein
Ca^{2+}	Calcium
CD31	Cluster of differentiation 31
CHO	Chinese hamster ovary
Cu	Copper
Cu_2SO_4	Copper Sulfate
DAF-FM	4-amino-5-methylamino-2',7'-difluorofluorescein diacetate
DMEM	Dulbecco's modified eagle medium
DMSO	Dimethyl sulfoxide
DOCA	Deoxycorticosterone acetate
DRAQ5	1, 5-bis{[2-(di-methylamino)ethyl]amino}-4, 8-dihydroxyanthracene-9, 10-Dione
EBs	Embryoid bodeis
EC	Endothelial cell
E-C	Excitation-contraction
EC Cells	Embryonic carcinoma Cells
ECL	Enhanced Chemi-Luminescence
EDTA	Ethylene diamine tetraacetic acid
EG cells	Embryonic germ cells
EHT	Endothelial-to-haematopoietic transition

eNOS / NOS III	Endothelial nitric oxide synthase
ERK1/2	Extracellular signal-regulated kinase 1/2
ES	Embryonic stem
ES cells	Embryonic stem cells
Esrrb	Estrogen-related receptor beta
FCS	Fetal calf serum
Fe	Iron
Flk-1	Fetal liver kinase-1
Fluo-4-AM	4-(6-Acetoxymethoxy-2,7-difluoro-3-oxo-9-xanthenyl)-4′-methyl-2,2′-(ethylenedioxy)dianiline-N,N,N′,N′-tetraacetic acid tetrakis(acetoxymethyl) ester
FoxD3	Forkhead box D3
g	Gravity 1*g* = 9,81m/s²
g	Gram
GAPDH	Glyceraldehyde-3-phosphate dehydrogenase
Gbx2	Gastrulation brain homeobox 2
G-CSF	Granulocyte colony stimulating factor
h	Hour
H_2O	Water
H_2O_2	Hydrogen peroxide
HCV	Hepatitis C Virus
HE	Haemogenic endothelium
hESCs	Human embryonic stem cells
HIF-1α	Hypoxia-inducible factor 1-alpha
HRP	Horseradish peroxidase
ICM	Inner cell mass
IGF	Insulin-like growth factor
IHC	Immunohistochemistry
IL-6	Interleukin-6
IMDM	Iscove's Modified Dulbecco's Medium
iNOS/ NOS II	Inducible nitric oxide synthase

iPS	Induced pluripotent stem
JAK	Janus kinase
JNK	c-Jun N-terminal kinase
KCl	Potassium chloride
kDa	Kilodaltons
KDR	kinase insert domain receptor
KH_2PO_4	Potassium dihydrogen phosphate
Klf2	Kruppel-like factor 2
Klf4	Kruppel-like factor 4
LIF	Leukemia inhibitory factor
L-NAME	N^G -nitro-L-argininemethyl-ester
LPS	Lipopolysaccharide
LTCC	L-type Ca^{2+} channel
MAPK	Mitogen-activated protein kinase
MEFs	Mouse embryonic fibroblasts
Mg	Magnesium
mg	Milligramm
MHC	Myosin heavy chain
min	Minute
ml	Milliliter
µm	Micrometer
µM	Micromolar
mM	Millimolar
MMPs	Matrix metalloproteinases
mTOR	Mammalian target of rapamycin
$Na_2HPO_4\,2H_2O$	Disodium hydrogen phosphate dihydrate
NaCl	Sodium chloride
Nanog	Nanog homeobox protein
NaOH	Sodium hydroxide
NEAA	Non-essential amino acids
nNOS/ NOS I	Neuronal nitric oxide synthase

NO	Nitric oxide
No.	Number
ns	Non-significant
$O_2^{\cdot-}$	Superoxide
Oct4	Octamer-binding transcription factor 4
p-AKT	Phospho AKT
PBS	Phosphate buffered saline
PBS-T	PBS-Tween/ PBS-Triton
PECAM-1	Platelet endothelial cell adhesion molecule-1
p-eNOS	Phospho eNOS
p-ERK1/2	Phospho ERK1/2
PFA	Paraformaldehyd
PI3K	Phosphatidylinositol-3-kinase
p-JNK	Phospho JNK
PKB/AKT	Protein kinase B
PLB	Phospholamban
p-p38	Phospho p38
p-PI3K	Phospho PI3K
p-STAT3	Phospho STAT3
p-VEGFR2	phosphoVEGFR2
QKI-5	Quaking isoform 5
r.p.m	Rounds per minute
RAAS	Renin-Angiotensin-Aldosteron-System
RAS	Renin-Angiotensin System
RNS	Reactive nitrogen species
ROS	Reactive oxygen species
RT	Room temperature
RyR	Ryanodine receptor
s	Second
Sall4	Sal-like protein 4
SDS	Sodium dodecyl sulfate

Ser	Serine
SERCA	Sarcoplasmic reticulum (SR) Ca^{2+} ATPase or sarco/endoplasmic reticulum Ca^{2+}-ATPase
Sil	Silibinin
SOX2	Sex determining region Y Box 2
SR	Sarcoplasmic reticulum
STAT3	Signal transducer and activator of transcription 3
TBST	Tris-buffered saline with 0.1% Tween
Tfcp2l1	Transcription Factor CP2 Like 1
Tris	Tris (hydroxymethyl) aminomethane
Tween 20	Polyoxyethylene (20) sorbitan monolaurate
VE-Cadherin	Vascular endothelial cadherin
VEGF	Vascular endothelial growth factor
VEGFR	Vascular endothelial growth factor receptor
VEGFR2	Vascular endothelial growth factor receptor 2
WB	Western blot
v/v	volume/volume
w/v	weight/volume

8. List of figures and tables

8.1. List of figures

8.2. List of tables

9. References

- Abhinand CA, Raju R, Soumya SJ, Arya PS, Perumana R. Sudhakaran PR. (2016). VEGF-A/VEGFR2 signaling network in endothelial cells relevant to angiogenesis. J Cell Commun Signal. 10(4): 347-354.
- Adegbola P, Aderibigbe I, Hammed W, Omotayo T. (2017). Antioxidant and anti-inflammatory medicinal plants have potential role in the treatment of cardiovascular disease: a review. Am J Cardiovasc Dis. 7(2): 19-32.
- Agarwal R, Agarwal C, Ichikawa H, Singh RP, Aggarwal BB. (2006). Anticancer potential of silymarin: from bench to bed side. Anticancer Res. 26(6B): 4457-4498.
- Aksoy I, Giudice V, Delahaye E, Wianny F, Aubry M, Mure M, Chen J, Jauch R, Bogu GK, Nolden T, Himmelbauer H, Xavier Doss M, Sachinidis A, Schulz H, Hummel O, Martinelli P, Hübner N, Stanton LW, Real FX, Bourillot PY, Savatier P. (2014). Klf4 and Klf5 differentially inhibit mesoderm and endoderm differentiation in embryonic stem cells. Nat Commun. 5: 3719.
- Alessi DR, Andjelkovic M, Caudwell B, Cron P, Morrice N, Cohen P, Hemmings BA. (1996). Mechanism of activation of protein kinase B by insulin and IGF-1. EMBO J. 15(23): 6541-6551.
- Ali EH, Sharifpanah F, Wartenberg M, Sauer H. (2018). Silibinin from Silybum marianum Stimulates Embryonic Stem Cell Vascular Differentiation via the STAT3/PI3-K/AKT Axis and Nitric Oxide. Planta Med. 84(11): 768-778.
- Anestopoulos I, Kavo A, Tentes I, Kortsaris A, Panayiotidis M, Lazou A, Pappa A. (2013). Silibinin protects H9c2 cardiac cells from oxidative stress and inhibits phenylephrine-induced hypertrophy: potential mechanisms. J Nutr Biochem. 24(3): 586-594.
- Angelos MG, Abrahante JE, Blum RH, Kaufman DS. (2018). Single Cell Resolution of Human Hematoendothelial Cells Defines Transcriptional Signatures of Hemogenic Endothelium. Stem Cells. 36(2): 206-217.
- Bahem R, Hoffmann A, Azonpi A, Caballero-George C, Vanderheyden P. (2015). Modulation of Calcium Signaling of Angiotensin AT1, Endothelin ETA, and ETB Receptors by Silibinin, Quercetin, Crocin, Diallyl Sulfides, and Ginsenoside Rb1. Planta Med. 81(8): 670-678.
- Bayascas JR, Alessi DR. (2005). Regulation of Akt/PKB Ser473 phosphorylation. Mol Cell. 18(2): 143-145.
- Beddington RS, Robertson EJ. (1989). An assessment of the developmental potential of embryonic stem cells in the midgestation mouse embryo. Development. 105(4): 733-737.
- Bekhite MM, Finkensieper A, Binas S, Müller J, Wetzker R, Figulla HR, Sauer H, Wartenberg M. (2011). VEGF-mediated PI3K class IA and PKC signaling in cardiomyogenesis and vasculogenesis of mouse embryonic stem cells. J Cell Sci. 124(Pt 11): 1819-1830.
- Bekhite MM, Müller V, Tröger SH, Müller JP, Figulla HR, Sauer H, Wartenberg M. (2016). Involvement of phosphoinositide 3-kinase class IA (PI3K 110α) and NADPH oxidase 1 (NOX1) in regulation of vascular differentiation induced by vascular endothelial growth factor (VEGF) in mouse embryonic stem cells. Cell Tissue Res. 364(1): 159-174.
- Bellacosa A, Kumar CC, Di Cristofano A, Testa JR. (2005). Activation of AKT kinases in cancer: implications for therapeutic targeting. Adv Cancer Res. 94: 29-86.
- Benigni A, Cassis P, Remuzzi G. (2010). Angiotensin II revisited: new roles in inflammation, immunology and aging. EMBO Mol Med. 2(7): 247-257.
- Beretta M, Bauer M, Hirsch E. (2015). PI3K signaling in the pathogenesis of obesity: The cause and the cure. Adv Biol Regul. 58: 1-15.
- Bjornson CB, Rietze RL, Reynolds BA, Magli MC, Vecovi AI. (1999). Turning brain into blood: a haematopoietic fate adopted by adult neural stem cells in vivo. Science. 283(5401): 534-537.

- Boheler KR, Czyz J, Tweedie D, Yang HT, Anisimov SV, Wobus AM. (2002). Differentiation of pluripotent embryonic stem cells into cardiomyocytes. Circ Res. 91(3): 189-201.
- Bonny O, Bochud M. (2014). Genetics of calcium homeostasis in humans: continuum between monogenic diseases and continuous phenotypes. Nephrol Dial Transplant. 29 Suppl 4: iv55-62.
- Bourillot PY, Aksoy I, Schreiber V, Wianny F, Schulz H, Hummel O, Hubner N, Savatier P. (2009). Novel STAT3 target genes exert distinct roles in the inhibition of mesoderm and endoderm differentiation in cooperation with Nanog. Stem Cells. 27(8): 1760-1771.
- Boyer LA, Lee TI, Cole MF, Johnstone SE, Levine SS, Zucker JP, Guenther MG, Kumar RM, Murray HL, Jenner RG, Gifford DK, Melton DA, Jaenisch R, Young RA. (2005). Core transcriptional regulatory circuitry in human embryonic stem cells. Cell. 122(6): 947-956.
- Bradley A, Evans M, Kaufman MH, Robertson E. (1984). Formation of germ-line chimaeras from embryo-derived teratocarcinoma cell lines. Nature. 309(5965): 255-256.
- Bratt-Leal AM, Carpenedo RL, McDevi TC (2009). Engineering the embryoid body microenvironment to direct embryonic stem cell differentiation. Biotechnol Prog. 25(1): 43-51.
- Breier G, Breviario F, Caveda L, Berthier R, Schnürch H, Gotsch U, Vestweber D, Risau W, Dejana E. (1996). Molecular cloning and expression of murine vascular endothelial-cadherin in early stage development of cardiovascular system. Blood. 87(2): 630-641.
- Brewer A, Pizzey J. (2006). GATA factors in vertebrate heart development and disease. Expert Rev Mol Med. 8(22): 1-20.
- Brychtova S, Bezdekova M, Brychta T, Tichy M. (2008). The role of vascular endothelial growth factors and their receptors in malignant melanomas. Neoplasma. 55(4): 273-279.
- Burdon T, Smith A, Savatier P. (2002). Signalling, cell cycle and pluripotency in embryonic stem cells. Trends Cell Biol. 12(9): 432-438.
- Busca A, Saxena M, Iqbal S, Angel J, Kumar A. (2014). PI3K/Akt regulates survival during differentiation of human macrophages by maintaining NF-κB-dependent expression of antiapoptotic Bcl-xL. J Leukoc Biol. 96(6): 1011-1022.
- Busche S, Gallinat S, Bohle RM, Reinecke A, Seebeck J, Franke F, Fink L, Zhu M, Sumners C, Unger T. (2000). Expression of angiotensin AT(1) and AT(2) receptors in adult rat cardiomyocytes after myocardial infarction. A single-cell reverse transcriptase-polymerase chain reaction study. Am J Pathol. 157(2): 605-611.
- Cannon RO. (1998). Role of nitric oxide in cardiovascular disease: focus on the endothelium. Clin Chem. 44(8 Pt 2): 1809-1819.
- Cantley LC. (2002). The phosphoinositide 3-kinase pathway. Science. 296(5573): 1655-1657.
- Cavas M, Beltrán D, Navarro JF. (2005). Behavioural effects of dimethyl sulfoxide (DMSO): changes in sleep architecture in rats. Toxicol Lett. 157(3): 221-32.
- Chen H, Chen SC, Zhang TH, Tian HC, Guan Y, Su DF. (1993). Protective effects of silybin and tetrandrine on the outcome of spontaneously hypertensive rats subjected to acute coronary artery occlusion. Int J Cardiol. 41(2): 103-108.
- Chen L, Zhao L, Samanta A, Mahmoudi SM, Buehler T, Cantilena A, Vincent RJ, Girgis M, Breeden J, Asante S, Xuan YT, Dawn B. (2017). STAT3 balances myocyte hypertrophy vis-a-vis autophagy in response to Angiotensin II by modulating the AMPKalpha/mTOR axis. PLoS One. 12(7): e0179835.
- Cheung CW, Gibbons N, Johnson DW, Nicol DL. (2010). Silibinin--a promising new treatment for cancer. Anticancer Agents Med Chem. 10(3): 186-195.
- Choi K, Chung YS, Zhang WJ. (2005). Hematopoietic and endothelial development of mouse embryonic stem cells in culture. Methods Mol Med. 105: 359-368.
- Choi YH, Jin GY, Guo HS, Piao HM, Li Lc, Li GZ, Lin ZH, Yan GH. (2012). Silibinin attenuates allergic airway inflammation in mice. Biochem Biophys Res Commun. 427(3): 450-455.

- Cochrane A, Kelaini S, Tsifaki M, Bojdo J, Vilà-González M, Drehmer D, Caines R, Magee C, Eleftheriadou M, Hu Y, Grieve D, Stitt AW, Zeng L, Xu Q, Margariti A. (2017). Quaking Is a Key Regulator of Endothelial Cell Differentiation, Neovascularization, and Angiogenesis. Stem Cells. 35(4): 952-966.
- Crosby CV, Fleming PA, Argraves WS, Corada M, Zanetta L, Dejana E, Drake CJ. (2005). VE-cadherin is not required for the formation of nascent blood vessels but acts to prevent their disassembly. Blood. 105 (7): 2771-2776.
- D'Amario D, Cabral-Da-Silva MC, Zheng H, Fiorini C, Goichberg P, Steadman E, Ferreira-Martins J, Sanada F, Piccoli M, Cappetta D, D'Alessandro DA, Michler RE, Hosoda T, Anastasia L, Rota M, Leri A, Anversa P, Kajstura J. (2011). Insulin-like growth factor-1 receptor identifies a pool of human cardiac stem cells with superior therapeutic potential for myocardial regeneration. Circ Res. 108(12): 1467-1481.
- Danser AHJ. (2010). Cardiac angiotensin II: does it have a function? American Journal of Physiology-Heart and Circulatory Physiology. 299(5): H1304-H1306.
- DebRoy S, Hiraga N, Imamura M, Hayes CN, Akamatsu S, Canini L, Perelson AS, Pohl RT, Persiani S, Uprichard SL, Tateno C, Dahari H, Chayama K. (2016). Hepatitis C virus dynamics and cellular gene expression in uPA-SCID chimeric mice with humanized livers during intravenous silibinin monotherapy. J Viral Hepat. 23(9): 708-717.
- Dehmlow C, Erhard J, GROOT H, DE. (1996). Inhibition of Kupffer cell functions as an explanation for the hepatoprotective properties of Silibinin. Hepatology. 23 (4): 749-754.
- Dehmlow C, Murawski N, de GH. (1996a). Scavenging of reactive oxygen species and inhibition of arachidonic acid metabolism by silibinin in human cells. Life Sci. 58(18): 1591-1600.
- Dejana E, Orsenigo F, Molendini C, Baluk P, McDonald DM. (2009). Organization and signaling of endothelial cell-to-cell junctions in various regions of the blood and lymphatic vascular trees. Cell Tissue Res. 335(1): 17-25.
- Dimmeler S, Fleming I, Fisslthaler B, Hermann C, Busse R, Zeiher AM. (1999). Activation of nitric oxide synthase in endothelial cells by Akt-dependent phosphorylation. Nature. 399(6736): 601-605.
- Dulak J, Szade K, Szade A, Nowak W, Józkowicz A. (2015). Adult stem cells: hopes and hypes of regenerative medicine. Acta Biochim Pol. 62(3): 329-337.
- Dzierzak E, Speck NA. (2008). Of lineage and legacy: the development of mammalian hematopoietic stem cells. Nat Immunol. 9(2): 129-136.
- Edgar KS, Galvin OM, Collins A, Katusic ZS, McDonald DM. (2017). BH4-Mediated Enhancement of Endothelial Nitric Oxide Synthase Activity Reduces Hyperoxia-Induced Endothelial Damage and Preserves Vascular Integrity in the Neonate. Invest Ophthalmol Vis Sci. 58(1): 230-241.
- Erdogdu O, Nathanson D, Sjöholm A, Nyström T, Zhang Q. (2010). Exendin-4 stimulates proliferation of human coronary artery endothelial cells through eNOS-, PKA- and PI3K/Akt-dependent pathways and requires GLP-1 receptor. Mol Cell Endocrinol. 325(1-2): 26-35.
- Evans MJ, Kaufman MH. (1981). Establishment in culture of pluripotential cells from mouse embryos. Nature. 292(5819): 154-156.
- Fan S, Li L, Chen S, Yu Y, Qi M, Tashiro S, Onodera S, Ikejima T. (2011). Silibinin induced-autophagic and apoptotic death is associated with an increase in reactive oxygen and nitrogen species in HeLa cells. Free Radic Res. 45(11-12): 1307-1324.
- Federico A, Dallio M, Loguercio C. (2017). Silymarin/Silybin and Chronic Liver Disease: A Marriage of Many Years. Molecules. 22(2): E191.
- Ferenci P, Scherzer TM, Kerschner H, Rutter K, Beinhardt S, Hofer H, Schöniger-Hekele M, Holzmann H, Steindl-Munda P. (2008). Silibinin is a potent antiviral agent in patients with

chronic hepatitis C not responding to pegylated interferon/ribavirin therapy. Gastroenterology. 135(5): 1561-1567.

- Fisher SC, Van Zutphen AR, Werler MM, Lin AE, Romitti PA, Druschel CM, Browne ML. (2017). Maternal Antihypertensive Medication Use and Congenital Heart Defects: Updated Results From the National Birth Defects Prevention Study. Hypertension. 69(5): 798-805.
- Fleming I, Busse R. (2003). Molecular mechanisms involved in the regulation of the endothelial nitric oxide synthase. Am J Physiol Regul Integr Comp Physiol. 284(1): R1-12.
- Förstermann U, Sessa WC. (2012). Nitric oxide synthases: regulation and function. Eur Heart J. 33(7): 829-837, 837a-837d.
- Fuh G, Li B, Crowley C, Cunningham B, Wells JA. (1998). Requirements for binding and signaling of the kinase domain receptor for vascular endothelial growth factor. Biol Chem. 273(18): 11197-11204.
- Gao J, Chao J, Parbhu KJ, Yu L, Xiao L, Gao F, Gao L. (2012). Ontogeny of angiotensin type 2 and type 1 receptor expression in mice. J Renin Angiotensin Aldosterone Syst. 13(3): 341-352.
- Gembardt F, Heringer-Walther S, van Esch JH, Sterner-Kock A, van VR, Le TH, Garrelds IM, Coffman TM, Danser AH, Schultheiss HP, Walther T. (2008). Cardiovascular phenotype of mice lacking all three subtypes of angiotensin II receptors. FASEB J. 22(8): 3068-3077.
- Gerhardt H, Golding M, Fruttiger M, Ruhrberg C, Lundkvist A, Abramsson A, Jeltsch M, Mitchell C, Alitalo K, Shima D, Betsholtz C. (2003). VEGF guides angiogenic sprouting utilizing endothelial tip cell filopodia. J Cell Biol. 161(6): 1163-1177.
- Gerri C, Marass M, Rossi A, Stainier DYR. (2018). Hif-1α and Hif-2α regulate hemogenic endothelium and hematopoietic stem cell formation in zebrafish. Blood. 131(9): 63-973.
- Geudens I, Gerhardt H. (2011). Coordinating cell behaviour during blood vessel formation. Development. 138(21): 4569-4583.
- Ghimire K, Altmann HM, Straub AC, Isenberg JS. (2017). Nitric oxide: what's new to NO? Am J Physiol Cell Physiol. 312(3): C254-C262.
- Giannotta M, Trani M, Dejana E. (2013). VE-cadherin and endothelial adherens junctions: active guardians of vascular integrity. Dev Cell. 126(5): 441-454.
- Gonzalez JM, Morgani SM, Bone RA, Bonderup K, Abelchian S, Brakebusch C, Brickman JM. (2016). Embryonic Stem Cell Culture Conditions Support Distinct States Associated with Different Developmental Stages and Potency. Stem Cell Reports. 7(2): 177-191.
- Gory-Fauré S, Prandini MH, Pointu H, Roullot V, Pignot-Paintrand I, Vernet M, Huber P. (1999). Role of vascular endothelial-cadherin in vascular morphogenesis. Development. 26(10): 2093-2102.
- Gufford BT., Graf TN., Paguigan ND, Oberlies N, H, Paine MF. (2015). Chemoenzymatic Synthesis, Characterization, and Scale-Up of Milk Thistle Flavonolignan Glucuronides. Drug Metab. and Dispos. 43(11): 1734-1743.
- Guo Y, Wang S, Wang Y, Zhu T. (2016). Silymarin improved diet-induced liver damage and insulin resistance by decreasing inflammation in mice. Pharm Biol. 54(12): 2995-3000.
- Haideri SS, McKinnon AC, Taylor AH, Kirkwood P, Starkey Lewis PJ, O'Duibhir E, Vernay B, Forbes S, Forrester LM. (2017). Injection of embryonic stem cell derived macrophages ameliorates fibrosis in a murine model of liver injury. NPJ Regen Med. 2: 14.
- Han HJ, Heo JS, Lee YJ. (2005). ANG II increases 2-deoxyglucose uptake in mouse embryonic stem cells. Life Sci. 77(15): 1916-1933.
- Hannig M, Figulla HR, Sauer H, Wartenberg M. (2010). Control of leucocyte differentiation from embryonic stem cells upon vasculogenesis and confrontation with tumour tissue. J Cell Mol Med. 14(1-2): 303-312.
- Hewitt KJ, Johnson KD, Gao X, Keles S, Bresnick EH. (2016). The Hematopoietic Stem and Progenitor Cell Cistrome: GATA Factor-Dependent cis-Regulatory Mechanisms. Curr Top Dev Biol. 118: 45-76.

- Hillmer EJ, Zhang H, Li HS, Watowich SS. (2016). STAT3 signaling in immunity. Cytokine Growth Factor Rev. 31: 1-15.
- Hooper WC, Catravas JD, Heistad DD, Sessa WC, Mensah GA. (2007). Vascular endothelium summary statement I: Health promotion and chronic disease prevention. Vascul Pharmacol. 46(5): 315-317.
- Hutterer E., Asslaber D., Caldana C., Krenn P. W., Zucchetto A., Gattei V., Hartmann T. N. (2015). CD18 (ITGB2) expression in chronic lymphocytic leukaemia is regulated by DNA methylation-dependent and -independent mechanisms. British Journal of Haematology. 169(2): 286-289.
- Ignarro LJ, Napoli C. (2004). Novel features of nitric oxide, endothelial nitric oxide synthase, and atherosclerosis. Current Atherosclerosis Reports. 6(4): 281-287.
- Isenberg JS. (2003). Inhibition of nitric oxide synthase (NOS) conversion of L-arginine to nitric oxide (NO) decreases low density mononuclear cell (LD MNC) trans-endothelial migration and cytokine output. J Surg Res. 114(1): 100-106.
- Isenović E, Walsh MF, Muniyappa R, Bard M, Diglio CA, Sowers JR. (2002). Phosphatidylinositol 3-kinase may mediate isoproterenol-induced vascular relaxation in part through nitric oxide production. Metabolism. 51(3): 380-386.
- Ishida M, El-Mounayri O, Kattman S, Zandstra P, Sakamoto H, Ogawa M, Keller G, Husain M. (2012). Regulated expression and role of c-Myb in the cardiovascular-directed differentiation of mouse embryonic stem cells. Circ Res. 110(2): 253-264.
- Israely E, Ginsberg M, Nolan D, Ding BS, James D, Elemento O, Rafii S, Rabbany SY. (2014). Akt suppression of TGFβ signaling contributes to the maintenance of vascular identity in embryonic stem cell-derived endothelial cells. Stem Cells. 32(1): 177-190.
- Itoh Y, Ma FH, Hoshi H, Oka M, Noda K, Ukai Y, Kojima H, Nagano T, Toda N. (2000). Determination and bioimaging method for nitric oxide in biological specimens by diaminofluorescein fluorometry. Anal Biochem. 287(2): 203-209.
- Jadhav GB, Upasani CD. (2011). Antihypertensive effect of Silymarin on DOCA salt induced hypertension in unilateral nephrectomized rats. Orient Pharm Exp Med. 11(2): 101-106.
- Jamali M, Rogerson PJ, Wilton S, Skerjanc IS. (2001). Nkx2-5 activity is essential for cardiomyogenesis. J Biol Chem. 276(45): 42252-42258.
- Jin S, Collin J, Zhu L, Montaner D, Armstrong L, Neganova I, Lako M. (2016). A novel role for miR-1305 in regulation of pluripotency-differntiation balace, cell cycle and apoptosis in human pluripotent stem cells. Stem Cells. 34(9): 2306-2317.
- Johnson MH, Ziomek CA. (1981). Induction of polarity in mouse 8-cell blastomeres: specificity, geometry, and stability. J Cell Biol. 91(1): 303-308.
- Johnson VJ, He Q, Osuchowski MF, Sharma RP. (2003). Physiological responses of a natural antioxidant flavonoid mixture, silymarin, in BALB/c mice: III. Silymarin inhibits T-lymphocyte function at low doses but stimulates inflammatory processes at high doses. Planta Med. 69(1): 44-49.
- Jones AM, Wilkerson DP, Campbell IT. (2004). Nitric oxide synthase inhibition with L-NAME reduces maximal oxygen uptake but not gas exchange threshold during incremental cycle exercise in man., J Physiol. 560(Pt 1): 329-338.
- Kampoli AM, Tousoulis D, Tentolouris C, Stefanadis C. (2012). Novel agents targeting nitric oxide. Curr Vasc Pharmacol. 10(1): 61-76.
- Kaser-Eichberger A., Schroedl F., Bieler L., Trost A., Bogner B., Runge C., Tempfer H., Zaunmair P., Kreutzer C., Traweger A., Reitsamer HA., Couillard-Despres S3. (2016). Expression of Lymphatic Markers in the Adult Rat Spinal Cord. Front Cell Neurosci. 10: 23.
- Kent L. (2009). Freezing and Thawing Human Embryonic Stem Cells. JoVE. (34): 1555.

- Kim DJ, Reddy K, Kim MO, Li Y, Nadas J, Cho YY, Kim JE, Shim JH, Song NR, Carper A, Lubet RA, Bode AM, Dong Z. (2011). -Chloroacetyl)-indole, a novel allosteric AKT inhibitor suppresses colon cancer growth in vitro and in vivo. Cancer Prev Res (Phila). 4(11): 1842-1851.
- Kim JL, Kang SW, Kang MK, Gong JH, Lee ES, Han SJ, Kang YH. (2012). Osteoblastogenesis and osteoprotection enhanced by flavonolignan silibinin in osteoblasts and osteoclasts. J Cell Biochem. 113(1): 247-259.
- Kim JL, Kim YH, Kang MK, Gong JH, Han SJ, Kang YH. (2013). Antiosteoclastic Activity of Milk Thistle Extract after Ovariectomy to Suppress Estrogen Deficiency-Induced Osteoporosis. Hindawi Publishing Corporation. BioMed Research International. 2013 (919374): 11.
- Kim SH, Oh DS, Oh JY, Son TG, Yuk DY, Jung YS. (2016). Silymarin Prevents Restraint Stress-Induced Acute Liver Injury by Ameliorating Oxidative Stress and Reducing Inflammatory Response. Molecules. 21(4): 443.
- Koch S, Claesson-Welsh L. (2012). Signal transduction by vascular endothelial growth factor receptors. 2(7): a006502.
- Koh TJ, DiPietro LA. (2001). Inflammation and wound healing: the role of the macrophage. Expert Rev Mol Med. 13: e23.
- Korpisalo P., Ylä-Herttuala S. (2010). Stimulation of functional vessel growth by gene therapy. Integr. Biol. 2(2-3): 102-112.
- Koyasu S. (2003). The role of PI3K in immune cells. Nat Immunol. 4(4): 313-319.
- Kroll DJ, Shaw HS, Oberlies NH. (2007). Milk thistle nomenclature: why it matters in cancer research and pharmacokinetic studies. Integr Cancer Ther. 6(2): 110-119.
- Kumar S, Singh RK, Bhardwaj TR. (2017). Therapeutic role of nitric oxide as emerging molecule. Biomed Pharmacother. 85: 182-201.
- Lee JI, Narayan M, Barrett JS. (2007). Analysis and comparison of active constituents in commercial standardized silymarin extracts by liquid chromatography-electrospray ionization mass spectrometry. J Chromatogr B Analyt Technol Biomed Life Sci. 845(1): 95-103.
- Lee JW, Bae SH, Jeong JW, Kim SH, Kim KW. (2004). Hypoxia-inducible factor (HIF-1) alpha: its protein stability and biological functions. Exp Mol Med. 36(1): 1-12.
- Lee MY, Luciano AK1, Ackah E2, Rodriguez-Vita J3, Bancroft TA4, Eichmann A2, Simons M2, Kyriakides TR4, Morales-Ruiz M5, Sessa WC6. (2014). Endothelial Akt1 mediates angiogenesis by phosphorylating multiple angiogenic substrates. Proc Natl Acad Sci U S A. 111(35): 12865-12870.
- Lee SJ, Namkoong S, Kim YM, Kim CK, Lee H, Ha KS, Chung HT, Kwon YG, Kim YM. (2006). Fractalkine stimulates angiogenesis by activating the Raf-1/MEK/ERK- and PI3K/Akt/eNOS-dependent signal pathways. Am J Physiol Heart Circ Physiol. 291(6): H2836-H2846.
- Lensch MW, Daheron L, Schlaeger TM. (2006). Pluripotent stem cells and their niches. Stem Cell Rev. 2(3): 185-201.
- Levy DE, Lee CK. (2002). What does Stat3 do? J Clin Invest. 109(9): 1143-1148.
- Li M., Ikehara S. (2013). Bone-marrow-derived mesenchymal stem cells for organ repair. Stem Cells Int. 2013(132642): 8.
- Liang HC, Holmes R, Zúñiga-Pflücker JC. (2013). Directed differentiation of embryonic stem cells to the T-lymphocyte lineage. Methods Mol Biol. 1029: 119-128.
- Lieber JG, Keller GM, Worthen GS. (2003). The in vitro differentiation of mouse embryonic stem cells into neutrophils. Methods Enzymol. 365: 129-142.
- Lin CH, Li CH, Liao PL, Tse LS, Huang WK, Cheng HW, Cheng YW. (2013). Silibinin inhibits VEGF secretion and age-related macular degeneration in a hypoxia-dependent manner through the PI-3 kinase/Akt/mTOR pathway. Br J Pharmacol. 168(4): 920-931.

- Lirussi F, Beccarello A, Zanette G, De Monte A, Donadon V, Velussi M, Crepaldi G. (2002). Silybin-beta-cyclodextrin in the treatment of patients with diabetes mellitus and alcoholic liver disease. Efficacy study of a new preparation of an anti-oxidant agent. Diabetes Nutr Metab. 15(4): 222-231.
- Liu VW, Huang PL. (2008). Cardiovascular roles of nitric oxide: a review of insights from nitric oxide synthase gene disrupted mice. Cardiovasc Res. 77(1): 19-29.
- Loguercio C, Festi D. (2011). Silybin and the liver: From basic research to clinical practice. World J Gastroenterol. 17(18): 2288-2301.
- Lohela M, Bry M, Tammela T, Alitalo K. (2009). VEGFs and receptors involved in angiogenesis versus lymphangiogenesis. Curr Opin Cell Biol. 21(2): 154-165.
- Lowry OH, Rosenbrough NJ, Farr AL, Randall RJ. (1951). Protein measurement with the Folin phenol reagent. J. Biol. Chem. 193: 265-275.
- Lu A, Wang L, Qian L. (2015). The role of eNOS in the migration and proliferation of bone-marrow derived endothelial progenitor cells and in vitro angiogenesis. Cell Biology International. 39(4): 484-490.
- Lu P, Mamiya T, Lu LL, Mouri A, Zou L, Nagai T, Hiramatsu M, Ikejima T, Nabeshima T. (2009). Silibinin prevents amyloid beta peptide-induced memory impairment and oxidative stress in mice. Br J Pharmacol. 157(7): 1270-1277.
- Luevano M, Madrigal A, Saudemont A. (2012). Generation of natural killer cells from hematopoietic stem cells in vitro for immunotherapy. Cell Mol Immunol. 9(4): 310-320.
- Lum JJ, Bui T, Gruber M, Gordan JD, DeBerardinis RJ, Covello KL, Simon MC, Thompson CB (2007). The transcription factor HIF-1alpha plays a critical role in the growth factor-dependent regulation of both aerobic and anaerobic glycolysis. Genes Dev. 21(9): 1037-1049.
- Lundberg JO, Weitzberg E. (2009). NO generation from inorganic nitrate and nitrite: Role in physiology, nutrition and therapeutics. Arch Pharm Res. 32(8): 1119-1126.
- Lv J, Sun B, Mai Z, Jiang M, Du J. (2017). STAT3 potentiates the ability of airway smooth muscle cells to promote angiogenesis by regulating VEGF signalling. Exp Physiol. 102(5): 598-606.
- Marikawa Y, Alarcón VB. (2009). Establishment of trophectoderm and inner cell mass lineages in the mouse embryo. Mol Reprod Dev. 76(11): 1019-1032.
- Martelli AM, Evangelisti C, Chiarini F, Grimaldi C, Cappellini A, Ognibene A, McCubrey JA. (2010). The emerging role of the phosphatidylinositol 3-kinase/Akt/mammalian target of rapamycin signaling network in normal myelopoiesis and leukemogenesis. Biochim Biophys Acta. 1803(9): 991-1002.
- Martin G. (1981). Isolation of a pluripotent cell line from early mouse embryos cultured in medium conditioned by teratocarcinoma cells. Proc Natl Acad Sci USA. 78(12): 7634-7638.
- Mateen S, Raina K, Agarwal R. (2013). Chemopreventive and Anti-cancer Efficacy of Silibinin against Growth and Progression of Lung Cancer. Nutr Cancer. 65(01): 3-11.
- Mengs U, Pohl RT, Mitchell T. (2012). Legalon® SIL: The Antidote of Choice in Patients with Acute Hepatotoxicity from Amatoxin Poisoning. Curr Pharm Biotechnol. 13(10): 1964-1970.
- Milosevic N, Bekhite MM, Sharifpanah F, Ruhe C, Wartenberg M, Sauer H. (2010). Redox stimulation of cardiomyogenesis versus inhibition of vasculogenesis upon treatment of mouse embryonic stem cells with thalidomide. Antioxid Redox Signal. 13(12): 1813-1827.
- Mira L, Silva M, Manso CF. (1994). Scavenging of reactive oxygen species by silibinin dihemisuccinate. Biochem Pharmacol. 48(4): 753-759.
- Mufti S, Wenzel S, Euler G, Piper HM, Schlüter KD. (2008). Angiotensin II-dependent loss of cardiac function: mechanisms and pharmacological targets attenuating this effect. J Cell Physiol. 217(1): 242-249.

- Müller AM, Hermanns MI, Skrzynski C, Nesslinger M, Müller KM, Kirkpatrick CJ. (2002). Expression of the endothelial markers PECAM-1, vWf, and CD34 *in vivo* and *in vitro*. Exp Mol Pathol. 72(3): 221-229.
- Murphy TJ, Takeuchi K, Alexander RW. (1992). Molecular cloning of AT1 angiotensin receptors. Am J Hypertens. 5(12 pt 2): 236S-242S.
- Neha, Jaggi AS, Singh N. (2016). Silymarin and Its Role in Chronic Diseases. Adv Exp Med Biol. 929: 25-44.
- Newman PJ, Berndt MC, Gorski J, White GC 2nd, Lyman S, Paddock C, Muller WA. (1990). PECAM-1 (CD31) cloning and relation to adhesion molecules of the immunoglobulin gene superfamily. Science. 247(4947): 1219-1222.
- Nicola NA, Babon JJ. (2015). Leukemia inhibitory factor (LIF). Cytokine Growth Factor Rev. 26(5): 533-544.
- Nishida M, Tanabe S, Maruyama Y, Mangmool S, Urayama K, Nagamatsu Y, Takagahara S, Turner JH, Kozasa T, Kobayashi H, Sato Y, Kawanishi T, Inoue R, Nagao T, Kurose H. (2005). G alpha 12/13- and reactive oxygen species-dependent activation of c-Jun NH2-terminal kinase and p38 mitogen-activated protein kinase by angiotensin receptor stimulation in rat neonatal cardiomyocytes. J Biol Chem. 280(18): 18434-18441.
- Niu G, Wright KL, Huang M, Song L, Haura E, Turkson J, Zhang S, Wang T, Sinibaldi D, Coppola D, Heller R, Ellis LM, Karras J, Bromberg J, Pardoll D, Jove R, Yu H. (2002). Constitutive Stat3 activity up-regulates VEGF expression and tumor angiogenesis. Oncogene. 21(13): 2000-2008.
- Ogawa M, Fraser S, Fujimoto T, Endoh M, Nishikawa S, Nishikawa SI. (2001). Origin of hematopoietic progenitors during embryogenesis. Int Rev Immunol. 20(1): 21-44.
- Özten-Kandaş N, Bosland MC. (2011). Chemoprevention of prostate cancer: Natural compounds, antiandrogens, and antioxidants - *In vivo* evidence. J Carcinog. 10: 27.
- Pan G, Thomson JA. (2007). Nanog and transcriptional networks in embryonic stem cell pluripotency. Cell Res. 17(1): 42-49.
- Panche AN, Diwan AD, Chandra SR. (2016). Flavonoids: an overview. J Nutr Sci. 29;5: e47.
- Passier R, Mummery C. (2003). Origin and use of embryonic and adult stem cells in differentiation and tissue repair. Cardiovasc. Res. 58(2): 324-335.
- Patel VB, Zhong JC1, Grant MB1, Oudit GY2. (2016). Role of the ACE2/Angiotensin 1-7 Axis of the Renin-Angiotensin System in Heart Failure. Circ Res. 118(8): 1313-1326.
- Patel-Hett S, D'Amore PA. (2011). Signal transduction in vasculogenesis and developmental angiogenesis. Int J Dev Biol. 55(4-5): 353-363.
- Payer BA, Reiberger T, Rutter K, Beinhardt S, Staettermayer AF, Peck-Radosavljevic M, Ferenci P. (2010). Successful HCV eradication and inhibition of HIV replication by intravenous silibinin in an HIV-HCV coinfected patient. J Clin Virol. 49(2): 131-133.
- Peng L, Wu TT, Tchieu JH, Feng J, Brown HJ, Feng J, Li X, Qi J, Deng H, Vivanco I, Mellinghoff IK, Jamieson C, Sun R. (2010). Inhibition of the phosphatidylinositol 3-kinase-Akt pathway enhances gamma-2 herpesvirus lytic replication and facilitates reactivation from latency. J Gen Virol. 91(Pt 2): 463-469.
- Pera MF, Reubinoff B, Trounson A. (2000). Human embryonic stem cells. J Cell Sci. 113(Pt 1): 5-10.
- Perfahl H, Hughes BD, Alarcón T, Maini PK, Lloyd MC, Reuss M, Byrne HM. (2017). 3D hybrid modelling of vascular network formation. Journal of Theoretical Biology. 414: 254-268.
- Pfeiffer S, Leopold E, Schmidt K, Brunner F, Mayer B. (1996). Inhibition of nitric oxide synthesis by NG-nitro-L-arginine methyl ester (L-NAME): requirement for bioactivation to the free acid, NG-nitro-L-arginine. Br J Pharmacol. 118(6): 1433-1440.

- Pisoschi AM, Pop A. (2015). The role of antioxidants in the chemistry of oxidative stress: A review. Eur J Med Chem. 97: 55-74.
- Polyak SJ, Ferenci p, Pawlotsky JM. (2013). Hepatoprotective and Antiviral Functions of Silymarin Components in HCV Infection. Hepatology. 57(3): 1262-1271.
- Polyak SJ, Morishima C, Shuhart MC, Wang CC, Liu Y, Lee DY. (2007). Inhibition of T-cell inflammatory cytokines, hepatocyte NF-kappaB signaling, and HCV infection by standardized Silymarin. Gastroenterology. 132(5): 1925-1936.
- Polyak SJ, Morishimaa C , Lohmannd V, Pala S, Lee YW, Liue Y, Graf TN, Oberliesf NH. (2010). Identification of hepatoprotective flavonolignans from silymarin. PNAS. 107(13): 5995-5999.
- Price RL, Carver W, Simpson DG, Fu L, Zhao J, Borg TK, Terracio L. (1997). The effects of angiotensin II and specific angiotensin receptor blockers on embryonic cardiac development and looping patterns. Dev Biol. 192(2): 572-584.
- Pucéat M, Jaconi M. (2005). Ca^{2+} signalling in cardiogenesis. Cell Calcium. 38(3-4): 383-389.
- Qiu D, Ye S, Ruiz B, Zhou X, Liu D, Zhang Q, Ying QL. (2015). Klf2 and Tfcp2l1, Two Wnt/β-Catenin Targets, Act Synergistically to induce and Maintain Naive Pluripotency. Stem Cell Reports. 5(3): 314-322.
- Rakocevic J, Orlic D, Mitrovic-Ajtic O, Tomasevic M, Dobric M, Zlatic N, Milasinovic D, Stankovic G, Ostojić M, Labudovic-Borovic M. (2017). Endothelial cell markers from clinician's perspective. Exp Mol Pathol. 102(2): 303-313.
- Ramos-Vara JA, Miller MA (2014). When tissue antigens and antibodies get along: revisiting the technical aspects of immunohistochemistry--the red, brown, and blue technique. Vet Pathol. 51(1): 42-87.
- Raskovic A, Stilinovic N, Kolarovic J, Vasovic V, Vukmirovic S, Mikov M. (2011). The protective effects of silymarin against doxorubicin-induced cardiotoxicity and hepatotoxicity in rats. Molecules. 16(10): 8601-8613.
- Reischauer S, Stone OA, Villasenor A, Chi N, Jin SW, Martin M, Lee MT, Fukuda N, Marass M, Witty A, Fiddes I, Kuo T, Chung WS, Salek S, Lerrigo R, Alsiö J, Luo S, Tworus D, Augustine SM, Mucenieks S, Nystedt B, Giraldez AJ, Schroth GP, Andersson O, Stainier DY. (2016). Cloche is a bHLH-PAS transcription factor that drives haemato-vascular specification. Nature. 535(7611): 294-298.
- Richards M, Fong CY, Chan WK, Wong PC, Bongso A. (2002). Human feeders support prolonged undifferentiated growth of human inner cell masses and embryonic stem cells. Nat Biotechnol. 20(9): 933-936.
- Risau W, Flamme I. (1995). Vasculogenesis. Annu. Rev. Cell Dev. Biol. 11: 73-91.
- Risau W. (1997). Mechanisms of angiogenesis. Nature. 386(6626): 671-674.
- Robertson E, Bradley A, Kuehn M, Evans M. (1986). Germ-line transmission of genes introduced into cultured pluripotential cells by retroviral vector. Nature 323(6087): 445-448.
- Rochette L, Lorin J, Zeller M, Guilland JC, Lorgis L, Cottin Y, Vergely C. (2013). Nitric oxide synthase inhibition and oxidative stress in cardiovascular diseases: possible therapeutic targets? Pharmacol Ther. 140(3): 239-257.
- Rui YC, Chen XS, Guan AH, Han JS. (1986). Effects of silybin on hemodynamics in anesthetized open-chest cats. Zhongguo Yao Li Xue Bao. 7(1): 34-36.
- Samanta R, Pattnaik AK, Pradhan KK, Mehta BK, Pattanayak SP, Banerjee S. (2016). Wound Healing Activity of Silibinin in Mice. Pharmacognosy Res. 8(4): 298-302.
- Sauer H, Ravindran F, Beldoch M, Sharifpanah F, Jedelska J, Strehlow B, Wartenberg M. (2013). alpha2-Macroglobulin enhances vasculogenesis/angiogenesis of mouse embryonic stem cells by stimulation of nitric oxide generation and induction of fibroblast growth factor-2 expression. Stem Cells Dev. 22(9): 1443-1454.

- Sauer H, ThebenT, Hescheler J, Lindner M, Brandt MC, Wartenberg M. (2001a). Characteristics of calcium sparks in cardiomyocytes derived from embryonic stem cells. Am. J. Physiol Heart Circ. Physiol. 281(1): H411-H421.
- Scheid MP, Woodgett JR. (2003). Unravelling the activation mechanisms of protein kinase B/Akt. FEBS Lett. 546(1): 108-112.
- Schindelin J, Arganda-Carreras I, Frise E, Kaynig V, Longair M, Pietzsch T, Preibisch S, Rueden C, Saalfeld S, Schmid B, Tinevez JY, White DJ, Hartenstein V, Eliceiri K, Tomancak P, Cardona A. (2012). Fiji: an open-source platform for biological-image analysis. Nat Methods. 9: 676–682.
- Schuppan D, Jia, JD, Brinkhau B, Hahn EG. (1999). Herbal products for liver diseases: a therapeutic challenge for the new millennium. Hepatology. 30(4): 1099-1104.
- Schutz S, Le Moullec JM, Corvol P, Gasc JM. (1996). Early expression of all the components of the renin-angiotensin-system in human development. Am J Pathol. 149(6): 2067-2079.
- Sharifpanah F, Behr S, Wartenberg M, Sauer H. (2016). Mechanical strain stimulates vasculogenesis and expression of angiogenesis guidance molecules of embryonic stem cells through elevation of intracellular calcium, reactive oxygen species and nitric oxide generation. Biochim.Biophys.Acta. 1863(12): 3096-3105.
- Sharifpanah F, De Silva S, Bekhite MM, Hurtado-Oliveros J, Preissner KT, Wartenberg M, Sauer H. (2015). Stimulation of vasculogenesis and leukopoiesis of embryonic stem cells by extracellular transfer RNA and ribosomal RNA. Free Radic Biol Med. 89: 1203-1217.
- Shaul PW. (2002). Regulation of endothelial nitric oxide synthase: location, location, location. Annu Rev Physiol. 64: 749-774.
- Shen J, Qu CK (2008). In vitro hematopoietic differentiation of murine embryonic stem cells. Methods Mol Biol. 430:103-118.
- Sheng L, Mao X, Yu Q, Yu D. (2017). Effect of the PI3K/AKT signaling pathway on hypoxia-induced proliferation and differentiation of bone marrow-derived mesenchymal stem cells. Exp Ther Med. 13(1): 55-62.
- Shinkai A, Ito M, Anazawa H, Yamaguchi S, Shitara K, Shibuya M. (1998). Mapping of the sites involved in ligand association and dissociation at the extracellular domain of the kinase insert domain-containing receptor for vascular endothelial growth factor. J Biol Chem. 273(47): 31283-31288.
- Shiojima I, Walsh K. (2002). Role of AKT Signaling in Vascular Homeostasis and Angiogenesis. Circulation Research. 90(12): 1243-1250.
- Sidorkiewicz M, Rebas E, Szymajda M, Lawnicka H, Pawlikowski M, Lachowicz A. (2009). Angiotensin receptors in hormone-independent prostate cancer cell line DU145: presence of two variants of angiotensin type 1 receptor. Med Sci Monit. 15(4): BR106-BR110.
- Siegel AB, Stebbing J. (2013). Milk thistle: early seeds of potential. Lancet Oncol. 14 (10): 929-930.
- Singh M, Suman S, Yogeshwer Shukla Y. (2014). New Enlightenment of Skin Cancer Chemoprevention through Phytochemicals: In Vitro and In Vivo Studies and the Underlying Mechanisms. BioMed Research International. 2014(243452): 18.
- Singh RP, Agarwal R. (2009). Cosmeceuticals and silibinin. Clin Dermatol. 27(5): 479-484.
- Singh RP, Deep G, Chittezhath M, Kaur M, Dwyer-Nield LD, Malkinson AM, Agarwal R. (2006). Effect of silibinin on the growth and progression of primary lung tumors in mice. J Natl Cancer Inst. 98(12): 846-855.
- Singh RP, Tyagi A, Sharma G, Mohan S, Agarwal R. (2008). Oral silibinin inhibits in vivo human bladder tumor xenograft growth involving down-regulation of survivin. Clin Cancer Res. 14(1): 300-308.

- Skwarek-Maruszewska A, Boczkowska M, Zajac AL, Kremneva E, Svitkina T, Dominguez R, Lappalainen R. (2013). Different Localizations and Cellular Behaviors of Leiomodin and Tropomodulin in Mature Cardiomyocyte Sarcomeres. Mol Biol Cell. 21(19): 3352-3361.
- Sobhani A, Khanlarkhani N, Baazm M, Mohammadzadeh F, Najafi A, Mehdinejadiani S, Sargolzaei Aval F. (2017). Multipotent Stem Cell and Current Application. Acta Med Iran. 55(1): 6-23.
- Steckelings UM, Rettig R, Unger T. (2007). Angiotensin in the kidney: a key to understanding hypertension? Cell Metab. 5(1): 7-8.
- Stewart CL, Kaspar P, Brunet LJ, Bhatt H, Gadi I, Köntgen F, Abbondanzo SJ. (1992). Blastocyst implantation depends on maternal expression of leukaemia inhibitory factor. Nature. 359(6390): 76-79.
- Subramanian A, Guo B, Marsden MD, Galic Z, Kitchen S, Kacena A, Brown HJ, Cheng G, Zack JA. (2009). Macrophage differentiation from embryoid bodies derived from human embryonic stem cells. J Stem Cells. 4(1): 29-45.
- Suga H, Rennert RC, Rodrigues M, Sorkin M, Glotzbach JP, Januszyk M, Fujiwara T, Longaker MT, Gurtner GC. (2014).Tracking the elusive fibrocyte: identification and characterization of collagen-producing hematopoietic lineage cells during murine wound healing. Stem Cells. 32(5): 1347-1360.
- Sundgren NC, Giraud GD, Stork PJ, Maylie JG, Thornburg KL. (2003). Angiotensin II stimulates hyperplasia but not hypertrophy in immature ovine cardiomyocytes. J Physiol. 548(pt 3): 881-891.
- Surai PF. (2015). Silymarin as a Natural Antioxidant: An Overview of the Current Evidence and Perspectives. Antioxidants. (Basel) 4(1): 204-247.
- Tajsharghi H. (2008). Thick and Thin Filament Gene Mutations in Striated Muscle Diseases. Int J Mol Sci. 9(7): 1259-1275.
- Tamm C, Galitó SP, Annerén C. (2013). A Comparative Study of Protocols for Mouse Embryonic Stem Cell Culturing. PLOS ONE. 8(12): e81156.
- Thomas DD, Ridnour LA, Isenberg JS, Flores-Santana W, Switzer CH, Donzelli S, Hussain P, Vecoli C, Paolocci N, Ambs S, Colton CA, Harris CC, Roberts DD, Wink DA. (2008). The chemical biology of nitric oxide: implications in cellular signaling. Free Radic Biol Med. 45(1): 18-31.
- Thomas JA, Pope C, Wojtacha D, Robson AJ, Gordon-Walker TT, Hartland S, Ramachandran P, Van Deemter M, Hume DA, Iredale JP, Forbes SJ. (2011). Macrophage therapy for murine liver fibrosis recruits host effector cells improving fibrosis, regeneration, and function. Hepatology. 53(6): 2003-2015.
- Thomson JA, Itskovitz-Eldor J, Shapiro SS, Waknitz MA, Swiergiel JJ, Marshall VS, Jones JM. (1998). Embryonic stem cell lines derived from human blastocysts. Science. 282(5391): 1145-1147.
- Toma JG, Akhavan M, Fernandes KJ, Barnabé-Heider F, Sadikot A, Kaplan DR, Miller FD. (2001). Isolation of multipotent adult stem cells from the dermis of mammalian skin. Nat Cell Biol. 3(9): 778-784.
- Tota S, Kamat PK, Shukla R, Nath C. (2011). Improvement of brain energy metabolism and cholinergic functions contributes to the beneficial effects of silibinin against streptozotocin induced memory impairment. Behav Brain Res. 221(1): 207-215.
- Tseng SY, Nishimoto KP, Silk KM, Majumdar AS, Dawes GN, Waldmann H, Fairchild PJ, Lebkowski JS, Reddy A. (2009). Generation of immunogenic dendritic cells from human embryonic stem cells without serum and feeder cells. Regen Med. 4(4): 513-526.
- Tyagi A, Agarwal C, Harrison G, Glode LM, Agarwal R. (2004). Silibinin causes cell cycle arrest and apoptosis in human bladder transitional cell carcinoma cells by regulating CDKI-CDK-cyclin cascade, and caspase 3 and PARP cleavages. Carcinogenesis. 25(9): 1711-1720.

- Ueyama T, Kasahara H, Ishiwata T, Nie Q, Izumo S. (2003). Myocardin expression is regulated by Nkx2.5, and its function is required for cardiomyogenesis. Mol Cell Biol. 23(24): 9222-9232.
- van Esch JH, Gembardt F, Sterner-Kock A, Heringer-Walther S, Le TH, Lassner D, Stijnen T, Coffman TM, Schultheiss HP, Danser AH, Walther T. (2010). Cardiac phenotype and angiotensin II levels in AT1a, AT1b, and AT2 receptor single, double, and triple knockouts. Cardiovasc Res. 86(3): 401-409.
- Varghese L, Agarwal C, Tyagi A, Singh RP, Agarwal R. (2005). Silibinin Efficacy against Human Hepatocellular Carcinoma. Clin Cancer Res. 11(23): 8441-8448.
- Vats A, Tolley NS, Bishop AE, Polak JM. (2005). Embryonic stem cells and tissue engineering: delivering stem cells to the clinic. J R Soc Med. 98(8): 346-350.
- Verma S, Thuluvath PJ. (2007). Complementary and alternative medicine in hepatology: review of the evidence of efficacy. Clin Gastroenterol Hepatol. 5(4): 408-416.
- Verweij J, Pinedo HM. (1990). Mitomycin C: mechanism of action, usefulness and limitations. Anticancer Drugs. 1(1): 5-13.
- Vestweber D. (2008). VE-cadherin: the major endothelial adhesion molecule controlling cellular junctions and blood vessel formation. Arterioscler Thromb Vasc Biol. 28(2): 223-232.
- Vongvatcharanon U, Vongvatcharanon S, Radenahmad N, Kirirat P, Intasaro P, Sobhon P, Parker T. (2004). Angiotensin II may mediate apoptosis via AT1-receptors in the rat cardiac conduction system. J Renin Angiotensin Aldosterone Syst. 5(3): 135-140.
- Voroneanu L, Nistor I, Dumea R, Apetrii M, Covic A. (2016). Silymarin in Type 2 Diabetes Mellitus: A Systematic Review and Meta-Analysis of Randomized Controlled Trials. J Diabetes Res. 2016(5147468): 10.
- Wagoner J, Morishima C, Graf TN, Oberlies NH, Teissier E, Pécheur EI, Tavis JE, Polyak SJ. (2011). Differential *in vitro* effects of intravenous versus oral formulations of Silibinin on the HCV life cycle and inflammation. PLoS One. 6(1): e16464.
- Walford G, Loscalzo J. (2003). Nitric oxide in vascular biology. J Thromb Haemost. 1(10): 2112-2118.
- Wang H, Lafdil F, Kong X, Gao B. (2011). Signal transducer and activator of transcription 3 in liver diseases: a novel therapeutic target. Int J Biol Sci. 7(5): 536-550.
- Wang HJ, Wei XF, Jiang YY, Huang H, Yang Y, Fan SM, Zang LH, Tashiro S, Onodera S, Ikejima T. (2010). Silibinin induces the generation of nitric oxide in human breast cancer MCF‐7 cells. Free Radic Res. 44(5): 577–584.
- Wang YK1, Hong YJ, Huang ZQ. (2005). Protective effects of silybin on human umbilical vein endothelial cell injury induced by H2O2 in vitro. Vascul Pharmacol. 43(4): 198-206.
- Wartenberg M, Dönmez F, Budde P, Sauer H. (2006). Embryonic stem cells: a novel tool for the study of antiangiogenesis and tumor-induced angiogenesis. Handb.Exp.Pharmacol. (174): 53-71.
- Wellington K, Jarvis B. (2001). Silymarin: a review of its clinical properties in the management of hepatic disorders. BioDrugs. 15(7): 465-489.
- Westfall MV, Pasyk KA, Yule DI, Samuelson LC, Metzger JM. (1997). Ultrastructure and cell-cell coupling of cardiac myocytes differentiating in embryonic stem cell cultures. Cell Motil Cytoskeleton. 36(1): 43-54.
- White J, Barro MV, Makarenkova HP, Sanger JW, Sanger JM. (2014). Localization of sarcomeric proteins during myofibril assembly in cultured mouse primary skeletal myotubes. Anat Rec (Hoboken). 297(9): 1571-1584.
- Wink DA, Hanbauer I, Grisham MB, Laval F, Nims RW, Laval J, Cook J, Pacelli R, Liebmann J, Krishna M, Ford PC, Mitchell JB. (1996). Chemical biology of nitric oxide: regulation and protective and toxic mechanisms. Curr Top Cell Regul. 34: 159-187.

- Wink DA, Mitchell JB. (1998). Chemical biology of nitric oxide: Insights into regulatory, cytotoxic, and cytoprotective mechanisms of nitric oxide. Free Radic Biol Med. 25(4-5): 434-456.
- Wobus AM, Boheler KR. (2005). Embryonic stem cells: prospects for developmental biology and cell therapy. Physiol Rev. 85(2): 635-678.
- Wobus AM. (2001). Potential of embryonic stem cells. Mol Aspects Med. 22: 149-164.
- Wu JW, Lin LC, Hung SC, Lin CH, Chi CW, Tsa TH. (2008). Hepatobiliary Excretion of Silibinin in Normal and Liver Cirrhotic Rats. Drug Metabolism and Disposition. 36(3): 589-596.
- Wu L, Jia Z, Yan L, Wang W, Wang J, Zhang Y, Zhou C. (2013). Angiotensin II promotes cardiac differentiation of embryonic stem cells via angiotensin type 1 receptor. Differentiation. 86(1-2): 23-29.
- Xie X, Chan KS, Cao F, Huang M, Li Z, Lee A, Weissman IL, Wu JC. (2009). Imaging of STAT3 signaling pathway during mouse embryonic stem cell differentiation. Stem Cells Dev. 18(2): 205-214.
- Xu J, Carretero OA, Liao TD, Peng H, Shesely EG, Xu J, Liu TS, Yang JJ, Reudelhuber TL, Yang XP. (2010). Local angiotensin II aggravates cardiac remodeling in hypertension. Am J Physiol Heart Circ Physiol. 299(5): H1328-H1338.
- Yin F, Liu J, Ji X, Wang Y, Zidichouski J, Zhang J. (2011). Silibinin: a novel inhibitor of Aβ aggregation. Neurochem Int. 58(3): 399-403.
- Yu S, Wong SL, Lau CW, Huang Y, Yu CM. (2011). Oxidized LDL at low concentration promotes in-vitro angiogenesis and activates nitric oxide synthase through PI3K/Akt/eNOS pathway in human coronary artery endothelial cells. Biochem Biophys Res Commun. 407(1): 44-48.
- Yu Y, Fan SM, Yuan SJ, Tashiro S, Onodera S, Ikejima T. (2012). Nitric oxide (•NO) generation but not ROS plays a major role in silibinin-induced autophagic and apoptotic death in human epidermoid carcinoma A431 cells. Free Radic Res. 46(11): 1346-1360.
- Yzaguirre AD, Howell ED, Li Y1, Liu Z, Speck NA. (2018). Runx1 is sufficient for blood cell formation from non-hemogenic endothelial cells in vivo only during early embryogenesis. Development. 145(2). pii: dev158162.
- Zeisberg EM, Ma Q, Juraszek AL, Moses K, Schwartz RJ, Izumo S, Pu WT. (2005). Morphogenesis of the right ventricle requires myocardial expression of Gata4. J Clin Invest. 115(6): 1522-1531.
- Zeng J, Sun Y, Wu K, Li L, Zhang G, Yang Z, Wang Z, Zhang D, Xue Y, Chen Y, Zhu G, Wang X, He D. (2011). Chemopreventive and chemotherapeutic effects of intravesical silibinin against bladder cancer by acting on mitochondria. Mol Cancer Ther. 10(1): 104-116.
- Zhang H, Nguyen-Jackson H, Panopoulos AD, Li HS, urray PJ, Watowich SS. (2010). STAT3 controls myeloid progenitor growth during emergency granulopoiesis. Blood 116: 2462-2471.
- Zhang T, Miyamoto S, Brown JH. (2004). Cardiomyocyte calcium and calcium/calmodulin-dependent protein kinase II: friends or foes? Recent Prog Horm Res. 59: 141-168.
- Zheng N, Liu L, Liu WW, Li F, Hayashi T, Tashiro SI, Onodera S, Ikejima T. (2017). Crosstalk of ROS/RNS and autophagy in silibinin-induced apoptosis of MCF-7 human breast cancer cells *in vitro.* Acta Pharmacologica Sinica. 38(2): 277-289.
- Zheng X, Wu Y, Zhu L, Chen Q, Zhou Y, Yan H, Chen T, Xiao Q, Zhu J, Zhang L. (2013). Angiotensin II promotes differentiation of mouse embryonic stem cells to smooth muscle cells through PI3-kinase signaling pathway and NF-kappaB. Differentiation. 85(1-2): 41-54.
- Zhou B, Wu LJ, Li LH, Tashiro S, Onodera S, Uchiumi F, Ikejima T. (2006). Silibinin protects against isoproterenol-induced rat cardiac myocyte injury through mitochondrial pathway after up-regulation of SIRT1. J Pharmacol Sci. 102(4): 387-395.

- Zhou B, Wu LJ, Tashiro S, Onodera S, Uchiumi F, Ikejima T. (2006a). Silibinin protects rat cardiac myocyte from isoproterenol-induced DNA damage independent on regulation of cell cycle. Biol Pharm Bull. 29(9): 1900-1905.
- Zhou L, Ma B, Han X. (2016). The role of autophagy in angiotensin II-induced pathological cardiac hypertrophy. J Mol Endocrinol. 57(4): R143-R152.
- Zhu YC, Zhu YZ, Lu N, Wang MJ, Wang YX, Yao T. (2003). Role of angiotensin AT1 and AT2 receptors in cardiac hypertrophy and cardiac remodelling. Clin Exp Pharmacol Physiol. 30(12): 911-918.
- Zimna A, Kurpisz M. (2015). Hypoxia-Inducible Factor-1 in Physiological and Pathophysiological Angiogenesis: Applications and Therapies. Biomed Res Int. 2015: 549412.

Publications

Parts of this thesis have been published in:

- **Ali E H,** Sharifpanah F, Wartenberg M, Sauer H. **(2018)**. Silibinin from Silybum marianum stimulates embryonic stem cell vascular differentiation via the STAT3/PI3-K/AKT axis and nitric oxide. Planta Med. 84(11): 768-778.

- **Ali E H,** Sharifpanah F, Tsang SY, Wartenberg M, Sauer H. **(2018)**. The milk thistle (*Silybum marianum)* compound silibinin inhibits cardiomyogenesis of embryonic stem cells by interfering with angiotensin II signaling. Stem Cells Int., doi: 10.1155/2018/9215792.

- Sharifpanah F, **Ali E H**, Wartenberg M, Sauer H. **(2018)**. The milk thistle (*Silybum marianum)* compound Silibinin stimulates leukopoiesis from mouse embryonic stem cells. Phytotherapy Res., doi: 10.1002/ptr.6241.

Poster Presentations

- **Enas Hussein Ali,** Fatemeh Sharifpanah, Maria Wartenberg, Heinrich Sauer. Differential Effects of Silibinin on Cardiovascular Differentiation of Mouse Embryonic Stem Cells. ECCPS Retreat 2016. Hotel Dolce Bad Nauheim 07th-08th July 2016. Germany.

- **Enas Hussein Ali,** Fatemeh Sharifpanah, Maria Wartenberg, Heinrich Sauer. Stimulation of Vasculogenesis from Embryonic Stem Cells by the Milk Thistle (*Silybum marianum)* Comound Silibinin. Joint International Meeting in Vascular Biology Sep 26, 2016 – Sep 28, 2016. Goethe University Hospital, Frankfurt. Germany.

- **Enas Hussein Ali,** Fatemeh Sharifpanah, Maria Wartenberg, Heinrich Sauer. Stimulation of vasculogenesis from embryonic stem cells by the milk thistle (*Silybum marianum)* compound silibinin via the STAT3/Akt/eNOS axis. 96th Annual Meeting of the Geman Physiology Society 16-18 March 2017. Germany.

- **Enas Hussein Ali,** Fatemeh Sharifpanah, Maria Wartenberg, Heinrich Sauer. Stimulation of vasculogenesis from embryonic stem cells by the milk thistle (*Silybum marianum)* compound silibinin via the STAT3/PI3-K/AKT axis and generation of nitric oxide. ECCPS Symposium Posterpresentation-Area Cellular Plasticity and Heterogeneity. 7th-8th Juni, 2017. Bad Nauheim. Germany.

Declaration

I hereby declare under oath, that this dissertation "**Differential Effects of Silibinin on Cardiovascular and Leukocyte Differentiation of Mouse Embryonic Stem Cells**" have produced by myself, without unpermitted help, and all the results of this dissertation have not been presented elsewhere as an examination paper.

…….

Enas Hussein Ali

Acknowledgements

Above all, I am really grateful to my God for blessings, sustenance, providence, protection, and patience during hard times.

First and foremost, I would like to extend my deepest gratitude to my supervisor **Prof. Dr. Heinrich Sauer** for giving me the opportunity to work on this research topic, he was always compassionate, knowledgeable, supportive person, and he provided me with endless guidance and help in difficult time. Thanks a lot for that!

My deep gratitude and thanks to **Prof. Dr. Maria Wartenberg** for her kindness and encouragement.

Also, I am very grateful to **Dr. Fatemeh Sharifpanah**, who taught me a lot during my research's time. She was a distinctive teacher and colleague.

My special thanks to **Barbara Arnold** for her excellent technical assistance. Special thanks also to **Prof. Dr. Klaus-Dieter Schlüter** for the assistance to perform experiments on adult rat cardiac cell function.

I would also like to specially thank to **Amer Taha** who worked with me in the lab, I spent beautiful, useful and wonderful moments with him.

Many thanks to **Dr. Mohamed Bekhite**, who kindly helped me.

I wish to thank my friends **Ammar**, **Dr. Omer, Sun, Ümmühan Büsra**, **Wasan**, **Zainab**, **Wathah, Dr. Abdulmaged** and all the others I haven't mentioned.

My special thanks to **Prof. Dr. Kadhim M. Ibrahim** and **Prof. Dr. Shehab A. Lafi.**

I would like to express my deep gratitude to my family for all their constant love and support at all times.

I would like to thank the Ministry of Higher Education & Scientific Research, Kufa University, Science College, Biology Department, Iraq.

I was very lucky to be one of PhD students in the Institute of Physiology; I am grateful to all members of this institute for everything that they had introduced me during my research's time.

Finally, I want to express my special thanks to Germany, the beautiful country in which I lived, felt with safety and gained lot of things that will help me to manage my future life.

Der Lebenslauf wurde aus der elektronischen Version der Arbeit entfernt.

The curriculum vitae was removed from the electronic version of the paper.